UNIFORMED SERVICES UNIVERSITY, SCHOOL OF MEDICINE GRADUATE PROGRAMS
Graduate Education Office (A 1045), 4301 Jones Bridge Road, Bethesda, MD 20814

DISSERTATION APPROVAL FOR THE DOCTORAL DISSERTATION IN THE NEUROSCIENCE GRADUATE PROGRAM

Title of Dissertation: "Neurogenin1 Expression and Function in the Developing Mouse Cerebellum"

Name of Candidate: Travis Lundell
Doctor of Philosophy Degree
December 13, 2011

DISSERTATION AND ABSTRACT APPROVED:

DATE:

Joseph L McCabe 12/14/11
Dr. Joseph McCabe
DEPARTMENT OF ANATOMY, PHYSIOLOGY, AND GENETICS
Committee Chairperson

12/14/11
Dr. Martin Doughty
DEPARTMENT OF ANATOMY, PHYSIOLOGY, AND GENETICS
Dissertation Advisor

12/14/11
Dr. Maria Braga
DEPARTMENT OF ANATOMY, PHYSIOLOGY, AND GENETICS
Committee Member

Sharon L Juliano 12/14/11
Dr. Sharon Juliano
DEPARTMENT OF ANATOMY, PHYSIOLOGY, AND GENETICS
Committee Member

M L Cutler 12/14/11
Dr. Mary Lou Cutler
DEPARTMENT OF PATHOLOGY
Committee Member

COPYRIGHT STATEMENT

The author hereby certifies that the use of any copyrighted material in the thesis manuscript entitled:

"Neurogenin1 Expression and Function in the Developing Mouse Cerebellum"

is appropriately acknowledged and, beyond brief excerpts, is with the permission of the copyright owner.

Travis Lundell
Neuroscience Graduate Program
Uniformed Services University
12/14/2011

ABSTRACT

Title of Thesis: Neurogenin1 Expression and Function in the Developing Mouse Cerebellum

Author: Travis G. Lundell, Doctor of Philosophy, 2011

Thesis directed by: Martin Doughty, Ph.D., Assistant Professor, Department of Anatomy, Physiology, and Genetics, Program in Neuroscience

The basic helix-loop-helix (bHLH) transcription factors Ptf1a and Math1 are necessary for the specification of gamma-aminobutyric acid (GABA)-ergic and glutamatergic cell lineages in the cerebellum, respectively. Recent evidence suggests that cascades of bHLH factor activities drive cell type specificity in Ptf1a-positive and Math1-positive lineages. Neurogenin1 (Neurog1) is a bHLH transcription factor involved in the development of several nervous system structures including the cerebral cortex, trigeminal sensory neurons, inner-ear sensory neurons, and olfactory sensory neurons. Recently, expression of Neurog1 has been reported to be co-expressed in Ptf1a-expressing cells in the ventricular zone (VZ) of the developing cerebellum, suggesting a role in subtype specification of GABAergic progenitor cells.

Using immunohistochemistry and transgenic reporter mice, we have demonstrated that Neurog1 is expressed during a prolonged period of cerebellar development that spans embryonic and postnatal phases of neurogenesis. Neurog1 is expressed in neuronal cell lineages of the cerebellar cortex, primarily by GABAergic cell lineages. However, Neurog1 is also expressed in small populations of glutamatergic unipolar brush cells and by a very limited number of granule cells.

Using inducible reporter mice, we have determined the temporal sequence of Neurog1-fated progenitors. Neurog1-fated progenitors first specify Purkinje cells in the

emerging cerebellar primordium and then all inhibitory interneuron cells types of the cortex. We demonstrate that expression of Neurog1 is sequential and overlapping in inhibitory interneuron cell type progenitors as first Golgi, Lugaro, basket and then stellate interneuron cell types are specified in an inside-out pattern in the developing cerebellar cortex. Interestingly, the specification of the earliest inhibitory interneuron cell types, Golgi cells, overlaps with later generated Purkinje cells, suggesting that these two cell types are not generated sequentially as previously reported.

Finally, we analyzed the effect of Neurog1 on cell fate and cell cycle parameters. We report that loss of function of Neurog1 results in deficits in Purkinje cell progenitors and GABAergic interneuron progenitors. However, analysis of cell cycle exit and G2-M phase length reveals no significant findings. Therefore, our investigation into the specific cause of these deficits remains unknown. The data suggest Neurog1 is a component of the bHLH factor code regulating cell type specification in the cerebellar cortex.

NEUROGENIN1 EXPRESSION AND FUNCTION IN THE DEVELOPING MOUSE CEREBELLUM

By

TRAVIS GRAY LUNDELL

Doctoral dissertation submitted to the faculty of the Neuroscience
Graduate Program of the Uniformed Services University
of the Health Sciences in partial fulfillment of
the requirements for the degree of
Doctor of Philosophy

Uniformed Services University of the Health Sciences

2011

ACKNOWLEDGEMENTS

First and foremost I would like to acknowledge my advisor Dr. Martin Doughty. When I was a first-year student he approached me about rotating in his lab. I happily accepted his offer and quickly became intrigued with neurohistology and development of the cerebellum. I am endebted to him for taking a chance on me. Under his mentorship I have acquired skills that will serve me throughout my academic and professional career. I feel honored to be his first graduate student. Having children of my own, he has been a great example of balancing work and family and has been exceptionally understanding when I've had to leave the lab early to attend to my family's needs. He also has a good choice in wardrobe. On a number of occasions we have come to the lab wearing the same or very similar outfits. Even when I tried to avoid it, somehow it still happened.

I am also thankful to the members of our lab, Qiong Zhou and Dr. Kryslaine Radomski. Each of our personalities meshed well together and without their help, friendship, and counseling sessions I would not have enjoyed, much less survived the numerous hours spent in the lab. I'll remember Qiong for her hard work and persistence. I've never seen anyone resist their boss's instructions more than Qiong, which provided a little comic relief to everyone excluding perhaps Dr. Doughty. Krys provided an enormous amount of support and I thank her for playing a dual role as my lab partner and therapist. I could complain to her about anything and she would, at the very least provide a listening ear. The summer interns, although temporary members of our lab, also assisted with my projects they include Herman Kamboj, Lucy (Xinyue) Liu, and Kevin Yi

I am also indebted to Dr. Sharon Juliano as a mentor and for the use of her lab resources. I am especially grateful for the access I have had to the cryostat and vibratome.

I made good use out of both instruments but primarily the cryostat which I claim as my second home.

I thank the USUHS Biomedical Instrumentation Center for the training and use of their equipment. I probably had too much fun taking images on the confocal microsope; however, the fun was balanced out by spending long boring hours on the stereology equipment. I thank Tom Baginski, who made himself available to provide support on the confocal microscope whenever I needed it. He frequently checked in to see if everything was working properly, and I appreciated his concern and initiative. I give a special thanks to Dennis McDaniels for his help with the stereology equipment and the nanozoomer. I was the first person to use the stereology equipment for a complete experiment, so we went through a lot of trials just to get the equipment to work the way we wanted it to. Whenever we thought we had all the bugs sorted out, a new one appeared. We spent many hours watching, waiting, and hoping the equipment didn't fail, so there was ample opportunity to talk about other things on our minds like our vacation plans and how we handle the tantrum-phase of our children.

I thank my committee members Doctors Martin Doughty, Joseph McCabe, Sharon Juliano, Maria Braga, and MaryLou Cutler for their cooperation, patience, and guidance as I worked through my thesis. They have been a pleasure to work with. Coincidentally, Dr. McCabe was the first person I met when I was visiting for my interviews. He is one of the most approachable people I know and I'm thankful for the help he has given me as my Committee Chair.

Before I began my graduate studies I had very little research experience but there were several educators along the way that encouraged me and picked me up when I was

down who need to be recognized. My first rotation as a graduate student was in Dr. Ying Hong Feng's lab. I only had a few months of experience in his lab when it was time for the Neuroscience Open House. Although the deadline for entry had passed he insisted I present a poster. I was terrified and panicked but his persistence and guidance helped me get through it and gave me the confidence I needed for future presentations. Dr. Diane Borst was my temporary advisor, and her lab was my last rotation. Her kindness was exactly what I needed at that point in my education and life. She showed interest in my personal life yet maintained a professional relationship. She still remembers my birthday and my kids' birthdays even though it has been more than three years since I was in her lab. Beyond her friendly attributes she is an excellent instructor and has a knack for explaining difficult concepts. Dr. Regina Armstrong was the Neuroscience Program Director when I interviewed and for the first few years of my education at USUHS. She has been a great example of discipline and hard work. She once suggested to me that being a graduate student should be listed as an "extreme sport" because of the endurance required to run the course, the many skills needed to complete the tasks, and the need to balance all other aspects of life simultaneously. I also respect her for her straightforward personality. She corrected me when I needed correction and I am a better individual because of it. Dr. Regina Day was the director of the Cell Biology course and went above and beyond what can be expected of someone with so many responsibilities. More than anything she was genuinely interested in my success as a student. Dr. Gregory Mueller was also one of those to whom I could turn for assistance regardless of the problem. I once told him that my psoas muscle was hurting. Previous to the injury I had no idea what the psoas was. He told me he knew some stretches that would help me out so he

lent me a disc that taught me how to stretch the psoas. I didn't know anyone knew what or where the psoas muscle was.

Outside of school I received a lot of support from friends. When I started school I was fortunate to attend the same church as Brian Brewer who was starting his first year of medical school at USUHS. We made it through the head and neck neuroanatomy and physiology course together. He was also there to listen to my frustrations and act as my career counselor when I needed direction. I thank him for his listening ear and words of wisdom that he has continued to share despite his busy schedule as an anesthesiologist resident. I would also like to thank Jeff Burnett who is also a friend I met at church and happened to be a post-bac fellow at NIH. We had a lot of opportunity to talk as we carpooled together to and from school/work. It seemed like most of our conversations on the way to school were about what experiment we were going to do that day and on the way home sharing our disappointment on how they didn't go as planned. Despite our frustrations we enjoyed sharing ideas on how to proceed with problems we were having in the lab. When we didn't want to talk science, we always ended up talking about Boy Scouts or politics. I would also like to thank Carl and Callie Brewer who are, again, friends my wife and I met at church. They have helped me remember to have fun even during the stress and demands of graduate school. I remember when we first met them I was impressed that Callie was genuinely interested in learning about my research. If it weren't for Carl and Callie I never would have gone fencing, gone to the Washington Wizards vs. Utah Jazz game every year, had a go-to BYU football friend, and I likely would have gone insane.

Finally, I would like to thank my family, especially my parents Mike and Michele and my siblings Christina, Tim, Kathryn, Charlotte, Eric, and Ryan. They have given me words of encouragement in the hours of doubt and celebrated with me in my successes. My sister Kathryn has been my number one cheerleader and I am grateful for her genuine interst and encouragement. My mom's enthusiasm for all things neuroscience has always motivated me, even in my undergraduate studies, to learn more about the brain and related diseases. She even wanted to visit my Developmental Neuroscince class and took copious notes during her visit. I'm grateful to my grandmothers Chuckie Gray and the late Betty Lundell. If it were up to both of them they would like to have had me closer to home, but I enjoyed visting with them when I was able and talking about when I would finish my PhD and if I would ever move back to Utah. I am also very grateful to have such wonderful in-laws. My wife's parents Arvid and Kelly Carlson and her grandma Peggy Lilly have been incredibly supportive and understanding in my efforts to persue a career. I thank them for their unconditional love and especially for raising my wonderful wife Krista. It goes without saying that I couldn't have done this without her. I remember when I got my grade for the head and neck anatomy course I came home and told her "We got an A!" Without her I am truly a ship without a sail and probably without milk, cereal, and ice cream on board. I am grateful for our children Kate, Brooklyn, and Troy and all good-bye and hello kisses and hugs before and after a long day in the lab. Many people have asked how I am able to manage graduate school while raising a family. Beyond cloning myself and teaching my kids to count cells for me I have been blessed with an incredible support system both at school and at home and I am incredibly grateful

to all of them. I have an amazing family and I look forward to our next adventure together in Missouri in persuit of a career in anesthesia.

DEDICATION

One of life's greatest gifts is the opportunity to freely pursue personal ambitions and find satisfaction in the achievement of them. I feel privileged to have had this opportunity to earn an advanced degree in neuroscience while exploring the mysteries of the brain and its development. My gratitude is deepened and my resolve to make the most out of life strengthened when I reflect upon the shortened lives of several fellow classmates from my hometown of Spanish Fork, Utah. Although they did not live long enough to fully persue their hopes and dreams their memory remains in those who knew them. And if nothing else that memory inspires us to seize every moment. This dissertation is dedicated to them, their parents, and family members.

Andy Cook

Michael Curzon

Kiplyn Davis

Michael Murphey

Nicole Gray

Quinn Steadman

Michael Huff

Paul Johnson

TABLE OF CONTENTS

LIST OF FIGURES

CHAPTER 1: INTRODUCTION

Historical Perspective

The brain has not always been considered the control center for the body, indeed interest toward scientific investigation of the nervous system developed quite slowly. The first recorded observations that touch on the study of the nervous system are found in the Edwin Smith Surgical Papyrus, a document transcribed around 1700 B.C. but first written in the 35th Century B.C. (McHenry Jr., 1969). During this early period in history, the knowledge of the anatomy and function of the brain consisted of generalizations based on observations made from victims of severe head trauma. Diseases of the brain were usually written off as a consequence of evil spirits (McHenry Jr., 1969). It wasn't until the 5th Century B.C. when Hippocrates recognized that certain abnormal behaviors were in fact the effect of a diseased brain. As a result of this change in thinking, attempts to understand the brain and its associated disorders moved from mystical concepts to medically based theory (McHenry Jr., 1969).

Centuries following Hippocrates, little progress was made toward understanding the structure and function of the brain. The only major contribution of note is that of Galen in the 2nd Century A.D. whose ligation experiments on animals demonstrated that the brain controls movement (Frampton, 2008). For well over a millennium Galen's anatomical descriptions of the nervous system remained the authority in neuroanatomy. His interpretations were not disputed and corrected until much later in 16th Century by prominent neuroanatomists such as Andreas Vesalius and Costanzo Varolio (Glickstein et al., 2009). These changes brought down barriers of tradition and opened the door for new ways of thinking about the nervous system.

While the 16th century remained relatively quiet in terms of the advancement of neuroscience there was one important work developing in the workshop of two Dutch eye glass makers that would prove to be pivotal for the advancement of cell biology, including our understanding of brain structure and function. Zaccharias Janssen and his father Hans engineered the first rudimentary microscope using tubes and two lenses (Amos, 2000). Though their microscope was not used extensively for research purposes it was a critical step towards development of the modern microscope. It wasn't until one century later that Robert Hooke (England, 1635-1703) used the microscope to observe an array of materials, mostly biological specimens, that led him to identify the cell as the basic unit of living organisms, which he published along with many other observations in his book, *Micrographia* (Wolpert, 1995, Gest, 2005, Uluc et al., 2009).

Hooke's publication sparked the beginning of a new field in research now known as histology, or the study of the microscopic structure of tissue. Two pioneers in this field were Marcello Malpighi (Italy, 1628-1694) and Antonie van Leeuwenhoek (Netherlands, 1632-1723) both can be considered responsible for popularizing the use of the microscope for biological investigation. Using primitive histological methods Malpighi made significant contributions to our understanding of the kidneys, liver, lungs, skin, and circulatory system (Martins e Silva, 2009). Van Leeuwenhoek, a cloth merchant by training, improved upon the quality of the microscope enabling him to view material that was invisible to the naked eye such as bacteria and parasites (Martins e Silva, 2009). Their contributions accelerated the advancement of many fields of biological research including the eventual dawning of developmental neuroscience.

Two years prior to the establishment of the cell doctrine in 1839, Jan Evangelista Purkinje observed unstained brain sections under a microscope and became the first person to accurately describe cells of the human brain, in particular he described one of the major cell types of the cerebellum, which now bears his name, the Purkinje cell (Glickstein et al., 2009). Later, Camillo Golgi (Italy, 1843-1926) developed an effective method for staining neural tissue, which he termed the "black reaction" due to the black crystals that formed within a random population of cells (De Carlos and Borrell, 2007). This random staining of neurons and glia allowed neuronal morphology to be visualized without obstruction from neighboring cells. Santiago Ramon y Cajal (Spain, 1852-1934) used the Golgi method to make an extensive histological analysis of the brain and was the first to publish such detailed reports on the morphology of neural tissue (Mason, 2009). His work supported the neuron doctrine later presented by Heinrich Wilhelm Gottfried von Waldeyer-Hartz (Bullock et al., 2005).

Having established the cell doctrine and the neuron doctrine, the stage was set for the study of how cells, particularly neurons, develop into their mature state in the brain. Cajal was one of the first to make observations of brain development when he described growth cones and formulated theories about cell migration (de Castro et al., 2007). Beginning with Cajal, developmental neuroscience has been interested in understanding the processes and mechanisms by which a newly born cell becomes a functionally distinct neuron. As techniques and tools have become more advanced our understanding of this fundamental question has also become clearer.

Structure and Function of the Cerebellum

The cerebellum was the primary structure studied by early neurohistologists, including Malpghi and Cajal (Meyer, 1967), and continues to be an ideal system for investigating mechanisms involved in neurodevelopment. This is primarily due to its relatively simple structure (Fig. 1, p. 5). Although the cerebellum accounts for more than half of the total neuronal population of the brain it is composed of relatively few neuronal cell types. Unlike the cerebral cortex, which is composed of six layers, the cerebellum contains only three cortical layers which includes the central Purkinje cell layer (PCL) flanked by the outer molecular layer (ML) and the internal granular layer (IGL).

A monolayer of Purkinje cells interspersed with candelabrum cells comprise the PCL. Purkinje cells are inhibitory or γ-aminobutyric acid (GABA)ergic and are the only projection neurons of the cerebellar cortex, therefore, all other cell types of the cerebellar cortex modulate Purkinje cell activity either directly or indirectly (Sotelo, 2004).

The dendritic processes of Purkinje cells project into the ML as they branch out along the sagittal plane toward the pial surface. Basket and stellate cells in this upper layer form GABAergic synapses on the cell soma and dendrites of Purkinje cells, respectively (Ito, 2006). Recently, studies suggest that Candelabrum cells are also GABAergic (Crook et al., 2006)and send their dendrites vertically through the ML toward the pial surface while their axons travel horizontally through the ML (Laine and Axelrad, 1994).

Purkinje cell axons project inward through the IGL and form the white matter tracts (WM) that make up the medullary substance. Most of their axons terminate onto neurons of the deep cerebellar nuclei (DCN) located within the medullary substance or

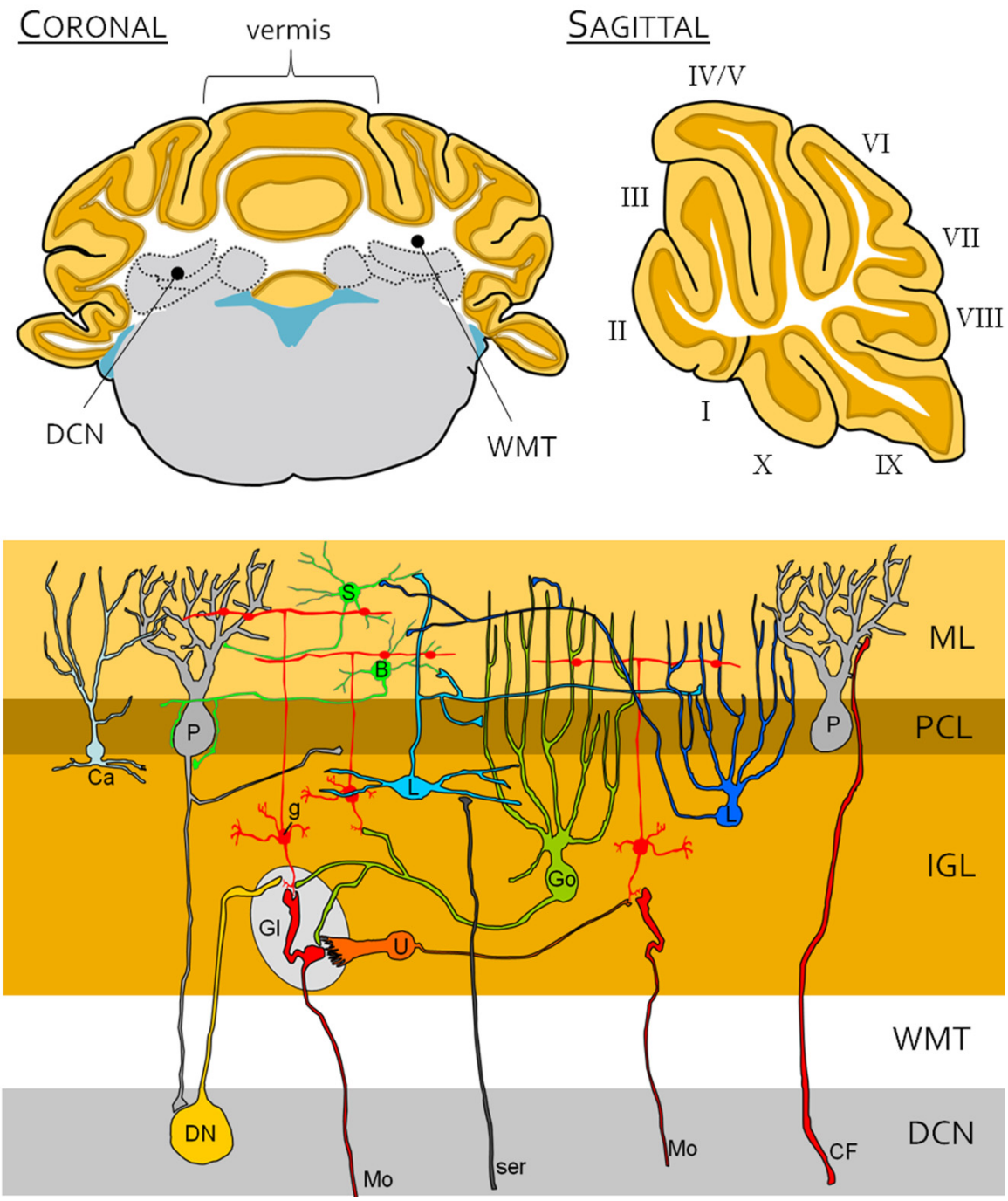

Figure 1: A simplified schematic of the structure and cellular organization of the mouse cerebellum. The coronal image demonstrates the three cortical layers divided into two hemispheres on either side of the vermis. Deep to the cortex are the white matter tracts (WMT) and 4 pair of deep cerebellar nuclei (DCN). The sagittal image shows the 10 lobules of the cerebellar vermis. The lower image demonstrates the cellular organization. Purkinje cells (*P*) are the only projection neurons of the cerebellar cortex and are inhibitory. Inhibitory Golgi (*Go*), basket (*B*), and stellate (*S*) cells are shown in *green*; inhibitory Lugaro cells (*L*) are shown in *light* (classical Lugaro cells) or *dark blue* (globular type). Excitatory granule cells (g) are in *red*, and excitatory unipolar brush cells (*U*) are marked *orange*. Climbing (*CF*) and mossy fibers (*Mo*) shown in red are also excitatory. The glomerulus (*Gl*) is the integrative unit in the granular layer. The transmitter and wiring of candelabrum cells (*Ca*) is not yet known, though their axons project into the molecular layer. Diffuse serotoninergic afferents (*ser)* project into the cerebellar cortex (image and text adapted by permission of Dr. Karl Schilling).

white matter tracts (WMT), while some bypass the nuclei to make direct connections with extracerebellar vestibular nuclei (Sotelo, 2004).

Lugaro cells and Golgi cells are the primary GABAergic interneurons of the IGL. Lugaro cells have both globular and fusiform cell bodies and extend their dendritic processes laterally along the bottom surface of the PCL and their axonal projections extend upward into the ML (Aoki et al., 1986, Sahin and Hockfield, 1990, Laine and Axelrad, 2002). Golgi cells often have a characteristically large globular cell body and extend their dendritic processes into the ML with their axons projecting to granule cells and unipolar brush cells (UBCs) through contacts made in the cerebellar glomerulus, a structure of the IGL that consists of synaptic contacts from multiple cell types ensheathed by glial cells (Sillitoe and Joyner, 2007, Schilling et al., 2008).

Granule cells are the primary glutamatergic cell type of the IGL and the most numerous cell type in the entire nervous system (Sillitoe and Joyner, 2007). They have short dendritic processes that receive synaptic input at the glomerulus. They extend their axons vertically toward the ML where they bifurcate to form two branches called parallel fibers that run perpendicular to the plane of Purkinje cell dendrites .

UBCs are the only other glutamatergic cell type of the cerebellar cortex and are also found in the IGL. They are found preferentially in lobule X but are also sparsely scattered throughout the other nine lobules (Mugnaini et al., 1997). UBCs have a thick dendritic trunk that abruptly branches into dendrioles giving it a stocky brush-like appearance. The axon projects through the IGL over both long and short distances and terminates in a small network of branches that appear as rosettes. Both dendritic and

axonal ends of UBCs form part of separate glomeruli (Nunzi et al., 2001, Schilling et al., 2008).

There are two major categories of afferents that terminate in the cerebellum, mossy fibers and climbing fibers. Mossy fibers originate from many different areas in the brain and spinal cord all of which terminate in a rosette-like structure forming the central component of the glomerulus. Climbing fibers project from the inferior olivary nucleus in the medulla and project to the ML of the cerebellar cortex where they synapse with the dendritic branches of Purkinje cells. Both types of fibers are excitatory. Other fibers, which are not classified as either mossy or climbing fibers, project from diffuse regions of the brain stem and make serotonergic, adrenergic, and cholinergic synapses in the cerebellum (Sillitoe and Joyner, 2007).

Traditionally the cerebellum has been ascribed to functions such as muscle coordination and balance (Glickstein et al., 2009). Recently, the cerebellum has also been implicated in non-motor functions such as language, emotion, and cognition (De Smet et al., 2007, Strick et al., 2009, Ten Donkelaar and Lammens, 2009).

Development of the Cerebellum

Glutamatergic and GABAergic neurons are generated from two distinct germinative zones in the cerebellar primordium: a ventricular zone (VZ) lying dorsal to the fourth ventricle; and from the rhombic lip (RL), a specialized region lying between the fourth ventricle and the roof plate (Fig. 2, p. 8). The VZ gives rise to all GABAergic cell types in the cerebellum (Carletti and Rossi, 2008) whereas RL progenitors generate glutamatergic cell lineages in the cerebellum as well as hindbrain precerebellar nuclei

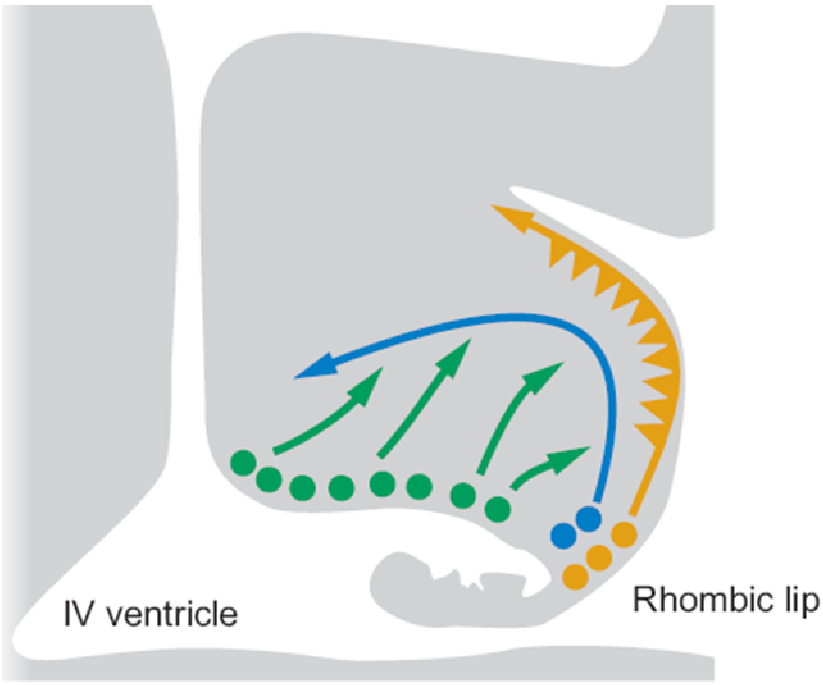

Figure 2: Schematic diagram of a sagittal view of the developing mouse cerebellum. The ventricular zone (green dots) is the site of GABAergic neurogenesis. The rhombic lip (orange and blue dots) is the site of glutamatergic neurogenesis. Arrows indicate the migration pathways of cells originating from their respective regions. The top of the figure is dorsal aspect of the cerebellum, the right is the caudal aspect. Figure adapted from Gilbertson and Ellison, 2008.

(Lin et al., 2001, Machold and Fishell, 2005, Wang et al., 2005, Englund et al., 2006, Fink et al., 2006).

Glutamatergic projection neurons of the deep cerebellar nuclei are the first neurons to be generated in the cerebellar primordium of embryonic day (E) 10.5 mice. These neurons arise from progenitors in the RL (Fink et al., 2006) and migrate to the nuclear transitory zone (NTZ) before eventually descending to the subcortical parenchyma to form the DCN. DCN projection neurons are shortly followed by GABAergic Purkinje cells arising from VZ progenitors (E11–E13.5) that migrate to an intermediate zone (IMZ) or differentiating zone in the caudal cerebellar anlage. Beginning at E13, progenitor cells from the RL migrate over the dorsal surface of the cerebellum to form the external germinal layer (EGL), a secondary proliferative zone that gives rise to glutamatergic granule cell interneurons as well as hindbrain precerebellar nuclei (Lin et al., 2001, Machold and Fishell, 2005, Wang et al., 2005). RL progenitors also give rise to UBCs during late embryogenesis (Englund et al., 2006): UBCs migrate by means of the cerebellar WM to their final destinations in the cerebellar cortex and dorsal cochlear nucleus. In the VZ, a second, prolonged wave of neurogenesis gives rise to GABAergic interneuron cell types of the DCN and cerebellar cortex (Maricich and Herrup, 1999, Leto et al., 2006, Carletti and Rossi, 2008). GABAergic interneurons are generated in defined but overlapping stages and interneuron cell types become specified in an overlapping, inside-out sequence: DCN interneurons are the first to differentiate (beginning E14.5), followed by those of the overlying cortex (E16.5 onward) that differentiate in a progression from those of the inner granule cell layer to the outer-most molecular layer (Leto et al., 2006, Leto et al., 2009). During development, mitotic

interneuron progenitors migrate to the WM as the VZ disappears. Thus neurogenesis shifts from VZ/RL to WM/EGL sites in the postnatal cerebellum as interneuron cell populations rapidly expand.

Basic Helix-loop-helix Transcription Factors and Neuronal Specification

Neuronal specification in the cerebellum requires the actions of genes encoding basic helix–loop–helix (bHLH) transcription factors. They mediate neuron specification through several proposed mechanisms, namely notch signaling, positive-feedback loops, activation of cascades of neuronal differentiation genes, inhibition of glial fates, and cell cycle regulation (Bertrand et al., 2002).

The bHLH transcription factors NeuroD and Math1 are necessary for the specification of glutamatergic granule cells from the RL (Ben-Arie et al., 1997, Miyata et al., 1999), whereas the development of all GABAergic cerebellar cell types from the VZ requires the action of Ptf1a (pancreatic transcription factor 1a) (Sellick et al., 2004, Hoshino et al., 2005a, Pascual et al., 2007). The process of GABAergic cell type specification is in part achieved by the suppression of alternate glutamatergic cell fates in VZ progenitor cells by Ptf1a (Pascual et al., 2007) but the mechanisms by which Purkinje cell and inhibitory interneuron cell populations diverge from Ptf1a-positive sources is not clear. A common theory is that co-expression of a mosaic of bHLH factors drives subtype specificity in Ptf1a-positive progenitors.

Indeed, *in situ* hybridization (ISH) reveals that Ptf1a is co-expressed with additional bHLH factors in the VZ including neurogenin1 (Neurog1) (Zordan et al., 2008), a neuronal cell fate determination factor that regulates neuronal differentiation and

sub-type specification in multiple cell lineages (Ma et al., 1998, Ota and Ito, 2003, Fukuda and Taga, 2005, Sarrazin et al., 2006).

Based on these findings my hypothesis is that Neurog1 determines neuronal sub-types from VZ progenitors in the cerebellum of mice. In this thesis I test my hypothesis using a variety of knockout and transgenic approaches. My data reveal that Neurog1 is expressed in VZ progenitors that give rise to Purkinje cells, inhibitory interneurons, and UBCs in the cerebellar cortex. These findings have been published (Lundell et al., 2009) and are supported by published data from the laboratory of Dr. Jane E Johnson (Kim et al., 2011). In addition, I have investigated the role of Neurog1 in the development of these cerebellar neuronal cell types. I used conventional *Neurog1* knockout mice to study *Neurog1* loss-of-function effects in progenitor cell proliferation, cell cycle progression, and survival.

CHAPTER 2: METHODS

Animal Management

Mice were housed in the Uniformed Services University's Center for Laboratory Animal Medicine. Animals were handled in accordance with procedures approved by the Uniformed Services University of the Health Sciences Institutional Animal Care and Use Committee (IACUC). All research complied with DoD regulations as published in DoD Directive 3216.1. The University's Center for Laboratory Animal Medicine (LAM) is a fully accredited institution with the Association for Assessment and Accreditation of Laboratory Animal Care (AAALAC).

Breeding was performed for maintaining colony numbers and providing specific developmental time-points for study. For timed-mating two females were paired with one male in the late afternoon. The following morning females were checked for vaginal plugs. If a plug was found the date was recorded and her gestational date was considered to be embryonic day 0.5.

Mice that remained in the animal facility past weaning were tattooed with an AIMS® Veterinary Tattoo Machine provided by the LAM facility. Tails were labeled with a predetermined alphanumerical code. Tail samples were collected from each mouse for genotyping and stored in a 1.5 mL centrifuge tube labeled with its respective code. Tails were either immediately processed for genotyping or stored at -20°C. For mice that were harvested at embryonic ages, tail and hind limb buds were collected for genotyping.

Tissue samples were processed using DNeasy® Blood & Tissue Kit (Qiagen) according to the manufacturer's instructions. For best results we included an extra spin

after the last wash at top speed for 1 minute in a new collection tube. This step ensured that all ethanol was cleared from the spin-column and would not contaminate the sample in the elution step.

Mouse models and genotyping

Bacterial artificial chromosome (BAC) enhanced green fluorescent protein (EGFP) reporter (*Neurog1*$^{EGFP/+}$) mice were imported from the NIH GENSAT project, Rockefeller University, New York (Gong et al., 2003). Constitutive Cre (*Neurog1*$^{Cre/+}$) and inducible CreER (*Neurog1*$^{CrER/+}$) transgenic mice (Raft et al., 2007) were generously provided by Dr. Jane Johnson, Department of Neuroscience, UT Southwestern Medical Center, Dallas, TX 75390. The Z/EG reporter strain mice (Novak et al., 2000) were purchased from The Jackson Laboratory, Bar Harbor ME (STOCK Tg(ACTB-Bgeo/GFP)21Lbe/J).

Neurog1$^{EGFP/+}$ were outbred to Swiss Webster mice (Taconic) and transgenic progeny identified by PCR using oligos: 5'-CCT ACG GCG TGC AGT GCT TCA GC-3' and 5'-CGG CGA GCT GCA CGC TGC GTC CTC-3'. *Neurog1*$^{Cre/+}$ and *Neurog1*$^{CrER/+}$ females were mated to Z/EG males to obtain double transgenic progeny. *Neurog1*$^{Cre/+}$:*Z/EG* and *Neurog1*$^{CreER/+}$:*Z/EG* progeny were identified using a β-galactosidase staining kit (Mirus Bio, LLC) for identifying the presence of the Z/EG gene, and through PCR using *Cre*-specific oligos: 5'-ACT CCC TGA GCC CCT GCG ATC TT-3' and 5'-CGC CTG GCG ATC CCT GAA CAT G-3'.

Neurogenin1 heterozygous mice (*Neurog1*$^{neo/+}$) (Ma et al., 1998) were also generously given by Dr. Jane Johnson. In these mice the single exon of *Neurog1* is replaced by the *neo* selection cassette. Two heterozygotes were crossed with each other to

obtain wild-type (WT), heterozygous (HT), and knockout (KO) littermates. Mice were identified by PCR using two primer pairs: The *Neurog1* primers, 5'-GGA GCG CCT CCT GCC TCC GCA GTG TGT CCC C-3'and 5'-GCC AGG AAA GGA GAA AGG AGA AAA GGG GAT CG-3' and the *neo* primers 5'-GCG CAG CTG TGC TCG ACG TT-3' and 5'-GCC ATG GGT CAC GAC GAG AT-3'.

BrdU injections

BromodeoxyUridine (BrdU, Sigma) was given by intraperitoneal (IP) injection at either a single dose of 100mg/kg or three doses of 50mg/kg body weight in bacteriostatic 0.9% sodium chloride solution (Hospira, Inc). Two hours after the single dose, animals were sacrificed. In the multiple-dose experiments a total of three doses were administered to a timed-pregnant mouse. Each dose was spaced by two hours and the animals were sacrificed at either three or six hours after the final dose.

Tamoxifen injections

A 1mg/100µl stock solution of tamoxifen (Sigma) in ethanol was prepared and stored at -20°C. One part stock solution to one part sunflower seed oil (Sigma) was vortexed and spun down in a vacuum centrifuge to drive off ethanol. At the time of first injection, mice were weighed and given 50mg/kg tamoxifen via IP injection. Six time-points were selected for injection: E11.5 (n = 2), E14.5 (n = 1), E16.5 (n = 1), P0 (n = 1), P7 (n = 1), and P40 (n = 2).

Tissue preparation

Mice were placed under anesthesia in an induction chamber containing a mixture of O_2 and isoflurane (2 – 4%) delivered by a vaporizer. Anesthesia was maintained

during procedures by a mixture of 1 liter per minute O_2 and 0.25 – 3% isoflurane using a nosecone. For transcardial perfusion (all mice P7 and older), mice were de-sanguinated with ice-cold PBS and perfused (Ismatec CP 78017-00) with either: 4% paraformaldehyde (PFA) in PBS (for all histological analysis unless otherwise stated); or 1% PFA 1% glutaraldehyde in PBS (dual anti-GFP, anti-GABA immunohistochemistry only). The flow-rate for perfusion was set at 3.70 mL/minute for adult mice and 1.75 mL/minute for juvenile mice. Late-stage embryonic (E17 – E20) and neonatal mice were decapitated under anesthesia. The anterior head (skull) was removed to allow adequate flow of solution over the cerebellum and avoid caving of the posterior skull during dehydration in sucrose solution. All fixed tissue was left to incubate overnight in fresh 4% PFA at 4°C.

Tissue for cryostat sectioning was then washed in PBS and transferred to 5% sucrose in PBS for 1 hour followed by consecutive treatments in 15% and 30% sucrose in PBS each until tissue sank. Tissue was then suspended in embedding medium (NEG50, Thermo Scientific), frozen over dry ice, and stored at -80°C. Tissue for vibratome sectioning was washed once in PBS and stored in PBS at 4°C.

Prior to cutting frozen sections, tissue blocks were allowed to thaw to -20°C. Blocks were placed in either coronal or sagittal plane and thickness was set to 10 – 40µm. Sections were placed sequentially across 4-5 slides forming four rows in each set of slides. Slides were stored in slide boxes at -20°C until use. Free-floating sections were cut at 50 – 100µm and stored in 0.5% PFA in PBS in 96-well plates and stored at 4°C.

Antigen retrieval

For Ki67, PHH3, and Lhx1/5 antibodies, antigen retrieval was necessary for optimal antigen detection. This step also enhanced the BrdU signal in some cases. After slides were dried they were then washed for 5 minutes in PBS and boiled in 10 mM sodium citrate (Sigma), 0.05% Tween-20 (Sigma), pH 6.0 for 15 minutes (time did not start until thermometer reached 95°C). Slides were immediately transferred to PBS at room temperature (RT) and washed 3 times in PBS.

Immunohistochemistry

Cryostat sections were air-dried at RT for 10 minutes and washed in PBS. All sections were blocked in 10% normal goat serum (NGS) in PBS for 30 minutes at RT and incubated in primary antibodies overnight at 4°C. All primary antibodies were diluted in PBS containing 1% NGS, 0.2% Triton X-100. The following day sections were washed in PBS and incubated with Alexa Fluor ® 488, 555 or 647 dye-labeled secondary antibodies (Invitrogen) at 1:1,000 dilution in PBS for 30-60 minutes at RT, washed and mounted under mowiol or glycerol in PBS. For bright-field microscopy (anti-GFP and anti-Cre immunohistochemistry only), sections were incubated with biotinylated goat anti-rabbit IgG antibodies for 1 hour at RT, followed by Vectastain ABC reagent for 30 minutes (both Vector laboratories) and immunolabeling revealed with diaminobenzidine tetrahydrochloride (DAB). Sections were then dehydrated and mounted under permount. Epifluorescent, immunofluorescent and immunohistochemical sections were viewed on a Zeiss A1 imager microscope and images captured with Axiocam digital cameras (Zeiss, Thornwood, NY). Confocal images were captured on a Zeiss Pascal laser scanning confocal microscope. Images were optimized for brightness and contrast.

Details of the primary antibodies used for immunohistochemistry are as follows. (1) 1:1,000 dilution of mouse monoclonal anti-BrdU (Clone BU 33, Sigma, product P2531, lot 027K4768). Anti-BrdU was raised against BromodeoxyUridine conjugated to KLH antigen. The antibody does not label BrdU-negative sections and BrdU-positive immunolabeling is eliminated by pre-adsorbtion with biotinylated goat anti-mouse Fab (manufacturer's technical information). (2) 1:500 dilution of rat polyclonal anti-BrdU (Clone BU1/75 (ICR1)Accurate Chemical & Scientific Corporation, product No. OBT0030). This antibody reacts with BrdU in single stranded DNA, BrdU attached to a protein carrier, or free BrdU. Also reacts with chlorodeoxyuridine with reduced intensity but does not cross react with thymidine. (3) 1:1,000 dilution of mouse monoclonal anti-Calbindin D_{28K} (anti-Calb1, Swant, Bellinzona, Switzerland, product No. 300, lot 18(F)). Anti-Calb1 was raised against Calb1 purified from chicken gut. The antibody does not cross-react with calretinin (Calb2) and specifically stains the ^{45}Ca-binding spot of Calbindin D_{28K} (MW 28,000kDa, IEP 4.8) in a two-dimensional "immunoblot" (manufacturer's technical information). (4) 1:2,500 dilution of mouse monoclonal anti-calretinin (anti-Calb2, Swant, Bellinzona, Switerland, product No. 6B3, lot 010399). This antibody is produced in mice by immunization with recombinant human calretinin-22k. It does not cross-react with other known calcium binding-proteins. (5) 1:200 dilution of rabbit monoclonal anti-cleaved caspase-3 (anti-Casp3, Cell Signaling, product No. 9664). Anti-Casp3 was raised against a synthetic peptide corresponding to amino-terminal residues adjacent to Asp175 of human caspase-3. This antibody is specific to the large fragment of activated caspase-3 resulting from cleavage adjacent to Asp175. It does not recognize full length caspase-3 or other cleaved caspases. (6) 1:500 dilution of mouse

monoclonal anti-Cre recombinase (Millipore, product No. MAB3120, lot LV1583458). The antibody was raised against Cre recombinase fusion protein containing Cre amino acid residues 77 – 343. The antibody detects natural Cre recombinase from Bacteriophage P1 at the predicted 38.5 kDa size by SDS-PAGE Western blot (manufacturer's technical information). (7) 1:2,000 dilution of mouse monoclonal anti-GABA (Sigma, product No. A0310, lot 076K4809). Anti-GABA was raised against BSA-conjugated GABA and specificity confirmed by dot blot immunoassay. The antibody does not cross-react with BSA, L-α-aminobutyric acid, L-glutamic acid, L-aspartic acid, glycine, L-glutamine, taurine, putrescine, L-alanine, and carnosine. The antibody has weak cross reactivity to β-alanine and ε-aminocaproic acid (all manufacturer's technical information). (8) 1:2,000 dilution of rabbit polyclonal anti-green fluorescent protein (anti-GFP, Invitrogen, product No. A11122, lot 51527A). The antibody was raised against GFP purified from *Aequorea Victoria* and does not immunolabel non-GFP control sections. (9) 1:1,500 dilution of mouse monoclonal anti-metabotropic glutamate receptor 2 (Grm2) (AbCam, Cambridge, MA, product No. ab15672, lot 303812). Anti-Grm2 was raised against a fusion protein antigen containing C-terminal amino acid residues 87 – 134 of mouse Grm2. The antibody recognizes Grm2 (104kDa) but not Grm3 (manufacturer's technical information). (10) 1:200 dilution of rabbit monoclonal anti-Ki67 (Thermo Scientific, clone SP6). Anti-Ki67 was raised against a synthetic peptide derived from human Ki-67 protein. (11) 1:200 dilution of mouse monoclonal 4F2 anti-Lim1/2 (Lhx1/5) (Developmental Studies Hybridoma Bank, Iowa City, IA). Anti-Lim1/2 was raised against residues 1 – 360 of rat Lim-2 expressed in *E. coli*. Antibody specificity was determined by comparison of the labeling patterns

obtained by immunohistochemistry and by in situ hybridization (Tsuchida et al., 1994). (12) 1:200 dilution of rabbit polyclonal anti-Neurog1 (gift of Jane Johnson). Anti-Neurog1 was raised against *E. coli*-derived recombinant Neurog1 protein antigen containing mouse residues 1 – 106 and does not immunolabel brain sections from *Neurog1* knockout mice (Gowan et al., 2001). (13) 1:500 dilution of mouse monoclonal anti-neuronal nuclei (NeuN) (Millipore, Clone A60, product No. MAB377, lot LV1573084). Anti-NeuN was raised against purified cell nuclei from mouse brain. (14) 1:1,000 dilution of rabbit polyclonal anti-Olig2 (Millipore, product No. AB9610, lot LV1538805). Anti-Olig2 was raised against full-length recombinant mouse Olig2 peptide and recognizes the ≈ 32 kDa Olig2 protein by Western blot (manufacturer's technical information). (15) 1:2,500 dilution of mouse monoclonal anti-parvalbumin (anti-Pvlb, Swant, Bellinzona, Switzerland, product No. 235, lot 10 – 11(F)). Anti-Pvlb was raised against parvalbumin purified from carp muscle and specifically stains the ^{45}Ca-binding spot of parvalbumin (MW 12,000kDa, IEP 4.8) in a two-dimensional "immunoblot" (manufacturer's technical information). (16) 1: 200 dilution of rabbit polyclonal anti-Pax2 (AbCam, Cambridge, MA, product No. ab37129, lots 311221 and 332813). Anti-Pax2 was raised against a recombinant protein antigen containing mouse Pax2 amino acid residues 188 – 385. The antibody recognizes Pax-2A and Pax-2B and detects two bands of approximately 34 and 41 kDa (predicted Pax2 molecular weight: 42 – 44 kDa) on western blots (manufacturer's technical information). (17) 1:200 dilution of mouse monoclonal anti-Pax6 (Developmental Studies Hybridoma Bank, Iowa City, IA). Anti-Pax6 was raised against *E. coli*-derived Pax6 recombinant protein corresponding to chicken residues 1 – 223 . Antibody specificity was determined by comparison of the

labeling patterns obtained by immunohistochemistry and by in situ hybridization (Ericson et al., 1997). (18) 1:200 dilution of guinea pig polyclonal anti-Ptf1a (gift of Jane Johnson). Anti-Ptf1a was raised against recombinant Ptf1a peptide of mouse residues 11 – 235. The specificity of the antisera was confirmed by staining E10.5 neural tube sections from wild-type and *Ptf1a*-null embryos (Hori et al., 2008). (19) 1:400 dilution of rabbit polyclonal anti-phospho-histone H3 (PHH3) (Millipore, product No. 06-570, Lot DAM1535118). Anti-PHH3 was raised against KLH-conjugated peptide corresponding to amino acids 7 – 20 of human histone H3. (20) 1:200 dilution of rabbit polyclonal anti-Tbr1 (Millipore, product No. AB9616, lot LV1504425). Anti-Tbr1 was raised against synthetic peptide antigen of mouse Tbr1 residues 662 – 681. The antibody recognizes the 68kDa Tbr1 protein on western blots (manufacturer's technical information). (21) 1:500 dilution of rabbit polyclonal anti-Tbr2 (AbCam, Cambridge, MA, product No. ab23345, lot 349210). Anti-Tbr2 was raised against a synthetic Tbr2 peptide containing mouse residues 650 – 688 conjugated to KLH. The antibody detects a single 72 kDa band corresponding to recombinant Tbr2 in western blots of transfected cell lysates. No band is detected in untransfected cells or in cells transfected with empty expression vector (manufacturer's technical information).

For dual immunofluorescence labeling with BrdU as one of the primary antibodies, sections were labeled sequentially. Sections were immunolabeled first with the non-BrdU antibody overnight. Following the first primary incubation sections were washed in PBS and incubated with 2N HCL for 1 hour at RT. Sections were then washed twice in 0.1M borate buffer (pH8.5) for at least 20 minutes each wash, followed by PBS

and incubated with mouse anti-BrdU antisera overnight at 4°C as described. Labeling was revealed using secondary antibodies as described previously.

For single immunofluorescence, the primary antibody was omitted to control for non-specific labeling of secondary antisera. For dual-immunofluorescence, each primary antibody was omitted in turn to control for cross reactivity and non-specific labeling of secondary antisera. BrdU-immunolabeled controls additionally included tissue sections from age-matched mice that did not receive a BrdU pulse. For anti-GFP immunohistochemical labeling, tissue sections from non-GFP-expressing *Neurog1*$^{Cre/+}$:+/+ and *Neurog1*$^{+/+}$:Z/EG age-matched mice were simultaneously processed to control for non-specific labeling.

Beta-galactosidase staining was performed by overnight incubation of sections in X-Gal reagent cell staining solution (Mirus Bio LLC) at 37°C according to the manufacturer's instructions.

Cell quantification using non-stereological methods

Numbers of cells co-immunoreactive for rabbit anti-Neurog1 and mouse anti-BrdU (Sigma) were recorded from serial confocal image stacks (1µm optical thickness) spanning the entire section thickness. Counts were recorded from optical sections containing Neurog1-immunoreactive profiles within image stacks. For each animal (n = 3), cell counts were recorded from the cerebellar anlage in two sets of three serial sagittal sections processed for immunocytochemistry (one medial and one lateral set, each chosen by a "blind" observer). Dual immunofluorescence was judged by a complete overlay of the immunopositive signals in the merged image and by matching coordinates of immunopositive profiles in the single channel fields. Neurog1-positive, BrdU-positive

and dual Neurog1-positive/BrdU-positive were recorded by a "blinded" observer and each counting area was ≈ $2x10^5\mu m^2$.

Numbers of cells co-immunoreactive for rabbit anti-Neurog1 and guinea-pig anti-Ptf1a were recorded from serial coronal cerebellar sections of mice processed for dual immunofluorescence (n=3). For each animal, numbers of anti-Neurog1, anti-Ptf1a and dual immunoreactive cells were recorded from the left cerebellar vermis in 3 serial vermal sections chosen by a "blind" observer. Counting was conducted by a second "blind" observer. Each counting area was ≈ $1.5x10^6\mu m^2$.

Numbers of cells immunoreactive for mouse anti-Lhx1/5 were recorded from serial sagittal sections of E13.5 *Neurog1* KO and WT littermate pairs (n=3). For each mouse, confocal images of two lateral and two medial sections in topographically matched regions were captured by a "blind" observer. Counting was conducted by a second "blind observer. Each counting area included the entire cerebellum of that section.

Cell quantification using stereological methods

Numbers of cells immunoreactive for anti-Pax2 in P0 *Neurog1* WT and KO mice (n=3) were recorded according to the following stereological methods. Every fifth section was included in the analysis beginning with a randomly chosen starting section from 1 to 5. Images were taken with a Zeiss AxioImager.M2 upright microscope and MicroBrightField's Stereo Investigator software. The parameters set for the optical fractionator probe were the same for all trials in the same experiment: Sampling grid 300 µm x 300 µm, counting frame 40 µm x 40 µm, guard zone 3 µm, dissector height 15 µm. The cut thickness was set at 40 µm but expansion of tissue occurred with the use of Mowiol® as the mounting agent, thus the mounted thickness varied between 40 µm and

50 µm. Setting the cut thickness at 40 µm limited the maximum range that the mounted thickness could be set to 40 µm, despite the mounted section actually being thicker. All sections were counterstained with DAPI to allow the region of interest (ROI) to be traced, which was done using a 5x objective. The ROI included all cerebellar tissue but excluded the EGL, therefore the line was traced just inside of the EGL. The images were taken using a 40x objective without oil. Counting was performed under "blinded" conditions using the optical fractionators probe (MBF).

Numbers of cells co-immunoreactive for rat anti-BrdU and rabbit anti-Ki67 (n=3) or numbers of cells co-immunoreactive for rat anti-BrdU and rabbit anti-PHH3 (n=3) in E12.5 *Neurog1* WT and KO mice were recorded according to the following methods. Every fourth section was included in the analysis beginning with a randomly chosen starting section from 1 to 4. Images were captured with a Zeiss Pascal confocal microscope at an optical thickness of 3-5 µm and an objective lens of 40x. For each tissue section, three images, each adjacent to the other, were taken beginning from the caudal end and moving toward the rostral end of the cerebellum in the sagittal plane. Using Adobe® Photoshop® CS4 software, a 9 x 9 grid was laid over each image. Two columns along the ventricular zone were randomly selected for counting. Counting was performed by a "blind" observer. The counter used three different markers: Blue for total BrdU-positive, yellow for BrdU-positive Ki67-negative (or PHH3-negative), and white for Ki67-positive (or PHH3-negative) BrdU-negative.

Numbers of cells co-immunoreactive for rat anti-BrdU and rabbit anti-Ki67 (n=3) or numbers of cells co-immunoreactive for rat anti-BrdU and rabbit anti-PHH3 (n=3) in E18.5 *Neurog1* WT and KO mice (n=3) were recorded according to the following

stereological methods. Every fourth section was included in the analysis beginning with a randomly chosen starting section from 1 to 4. Images were taken as described previously with modifications to the parameters of the optical fractionator probe described here: Sampling grid 270 µm x 486 µm, counting frame 60 µm x 60 µm, guard zone 5 µm, dissector height 30 µm. The cut thickness was set to 50 µm even though the actual cut thickness was 40 µm. This allowed for the mounted thickness to be set at the 50 µm, which was the average final thickness after mounting in Mowiol®. Sections were counterstained with DAPI and the ROI was traced to exclude the EGL, as described previously. Images were taken using 63x oil immersion objective. Counting was performed by a "blind" observer. The counter used three different markers in the optical dissector probe: a dot (Marker 1) for BrdU-positive, an "X" (Marker 7) for total Ki67-positive (or PHH3-positive/BrdU-negative), and a circle for BrdU-postive/Ki67-negative (or PHH3-negative).

Flow Cytometry

Cells were prepared for flow cytometry from postnatal day 6-8 (n=3) mice. On average, 3-4 *Neurog1*$^{EGFP/+}$ and 1-2 wild-type littermates (used as cell size distribution control) were harvested for each age. Mice were decapitated and the whole cerebella isolated and pooled by *Neurog1*$^{EGFP/+}$ or wild-type genotype. Cerebella were minced in Dulbecco's Ca^{2+} and Mg^{2+}-free PBS with antibiotic and anti-mycotic (Invitrogen) and digested for 30 minutes at 37°C with papain (5 U/ml) in Ca^{2+} and Mg^{2+}-free PBS supplemented with glucose (25mM), 0.5mM Mg^{2+}, cysteine (200µg/ml) and DNAse I (100 U/ml) (all Sigma). Digestion was blocked by a 5 minute incubation at 37°C in soybean trypsin inhibitor (1 mg/ml) in Ca^{2+} and Mg^{2+}-free PBS supplemented with

glucose (25 mM) and Bovine serum albumin BSA (8 mg/ml) (all Sigma). Cells were dissociated by trituration with fire-polished Pasteur pipettes of decreasing bore size and passed through 35 μm nylon mesh caps into collection tubes. Cell counts were performed and cells suspended at a density of 1 x 10^6 to 1x 10^8 cells/ml in Neurobasal-A medium, supplemented with B27 nutrients, L-glutamine (100X, 200mM) and basic fibroblast growth factor (bFGF, 5 ng/ml) (all Invitrogen). Cells were sorted for EGFP epifluorescence using a BD Biosciences FACSAria Cell-Sorting System. The cell excitation and emission settings were a 488nm laser and a 530/30 band pass filter. On average 1 x 10^7 cells were sorted and 5 x 10^5 GFP-fluorescent cells obtained (≈ 5% of the total cell population).

Quantitative real-time RT-PCR (qRT-PCR)

Total RNA was extracted from dissociated postnatal day 6 – 8 mouse cerebellar cells separated by flow cytometry. Cells were treated with TRIzol (Invitrogen) followed by chloroform-extraction and precipitation with isopropyl alcohol (0.5 ml per 1.0ml TRIzol). Qiagen RNeasy Mini columns were used to isolate total RNA and genomic DNA contaminant was removed by treating 0.5 – 10μg total RNA with 2U DNAse for 30 minutes at 37°C (TURBO DNA-free, Ambion). RNA concentration and purity were evaluated by spectrophotometer (A_{260}: $A_{280} \geq 2.0$) and first-strand cDNA synthesized from 1μg of total RNA using random primer/oligo (dT) primer according to the manufacturer's instructions (SABiosciences). Synthesized cDNA was diluted to final concentration of 10ng/μl for PCR.

Optimum primers were designed using Primer design software (Invitrogen). Primer sequence pairs were: GGCTGTATTCCCCTCCATCG and

CCAGTTGGTAACAATGCCATGT (*Actb*); GACCTGCATCTCTGATCTCG and TGTAGCCTGGCACAGTCCTC (*Neurog1*); GGAATGAATACTCTCTCCCAGC and GGTACGTCTGTGTGCCTGAC (Pax2); TCCTCTCTCGCGCTCTCTG and ATATGCTACTGGCAGGATCAAC (*18S*). Primer specificity was confirmed by verifying a single PCR product had been generated by UV gel electrophoresis, as well as by confirming the melting temperature of the product had a single value on dissociation plots. Each qRT-PCR reaction was carried out in triplicate in a 25µl volume using SYBR Green Master Mix (SABiosciences) for 15min at 95°C for initial denaturing, followed by 40 cycles of 95°C for 30 seconds and 60°C for 30 seconds in the ABI 7500 Real-Time PCR System. Mean triplicate gene of interest (GOI) C_t values were normalized to Actb C_t ($\Delta C_t = C_t$ GOI - C_t Actb) to generate ΔC_t for comparison. Controls for each independent PCR experiment were as follows: 1) 10 pg hrEGFP plasmid DNA and complimentary primers as positive PCR control; 2) RNA samples without reverse transcription (RT) to test for genomic DNA contamination; 3) PCR reaction without RNA-DNA template as a control for general contamination in the PCR reagents/set-up. Data was rejected if the following control data was obtained: PCR positive control hrEGFP ΔC_t values indicated high variability between trials (hrEGFP $\Delta\Delta C_t \geq 0.5$); or no RT control Actb $C_t \leq 10$ cycles lower than RT test samples indicated genomic DNA contamination; or no template control $C_t \leq 35$ indicated general PCR reagent contamination; as well as if the standard deviation of C_t triplicate values > 0.3 indicating significant experimental variability.

CHAPTER 3: NEUROGENIN1 EXPRESSION IN THE DEVELOPING CEREBELLUM

Neurog1 is expressed in two territories in the cerebellar primordium

We investigated the cellular identity of Neurog1 expression in the cerebellum by immunohistochemistry using a rabbit polyclonal anti-Neurog1 antisera (Gowan et al., 2001) (gift of J.Johnson, UT SW Med. Ctr.). The specificity of this antisera has been confirmed by comparison of immunohistochemistry and in situ hybridization (ISH)-labeling patterns in normal mice and by the lack of immunolabeling of *Neurog1 null* mutant embryo sections (Gowan et al., 2001). Our results are consistent with published ISH data (Salsano et al., 2007, Zordan et al., 2008) that first detect Neurog1 expression in the rostral cerebellum at E11.5 and within caudal VZ and IMZ at E12.5 and E13.5 (Salsano et al., 2007, Zordan et al., 2008). Anti-Neurog1 immunolabeling of E11 embryos reveals a continuous band of Neurog1 expression within the ventricular neuroepithelium of the isthmus and anterior pons that extends into rostral portions of the cerebellar primordium (Fig. 3, p. 28). At E13, two distinct Neurog1-immunoreactive territories are present within the cerebellum: a rostral, isthmic territory that is continuous with Neurog1-immunoreactivity in the ventricular neuroepithelium of the pons; and a non-continuous territory in the caudal VZ and IMZ of the cerebellar anlage proper that is rostral of the RL (Fig. 4, p. 29). Within the caudal Neurog1 territory there is a medial-lateral shift in the distribution of Neurog1-immunoreactive neurons in the VZ and IMZ, with the proportion of Neurog1-immunoreactive cells in the IMZ increasing and those in the VZ decreasing in the more lateral cerebellum (Fig. 4). Co-immunolabeling with

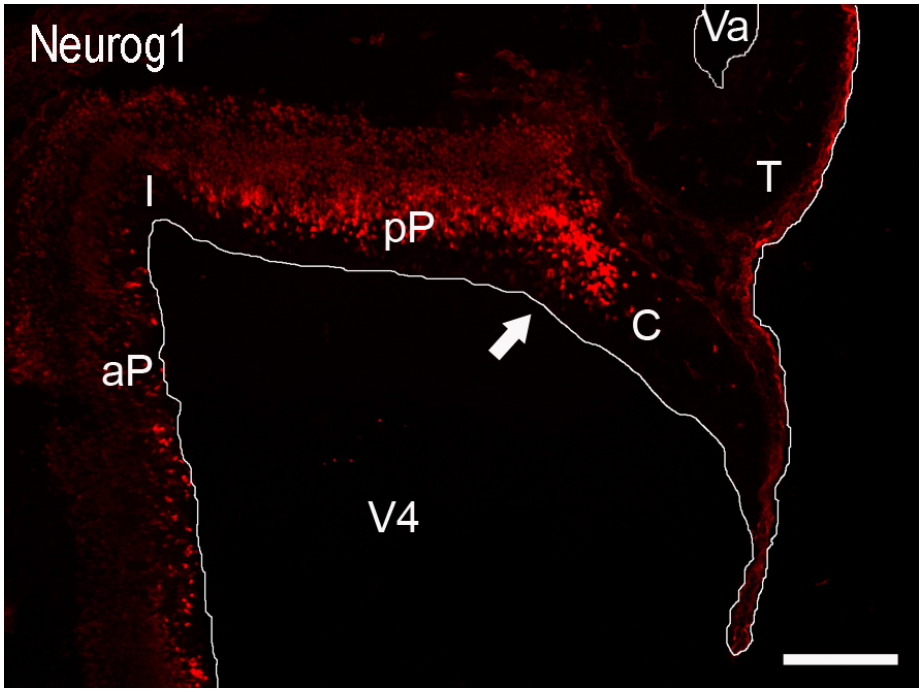

Figure 3: Neurog1 is expressed in the rostral cerebellar primordium of embryonic day (E) 11 mice. Immunolabeling reveals a continous Neurog1 expression territory that spans the neuroepithelium of the isthmus (I), posterior pons (pP), and rostral portions (arrow) of the cerebellar primordium (C). aP, anterior pontine neurospithelium; C, cerebellar primordium; I, isthmus; pP, posterior pontine neuroepithelium; T, tectum; Va, ventricular aqueduct; V4, fourth ventricle. Lines delineate significant ventral-dorsal boundaries of the mesencephalon and metencephalon for orientation. Scale bar = 100 μm.

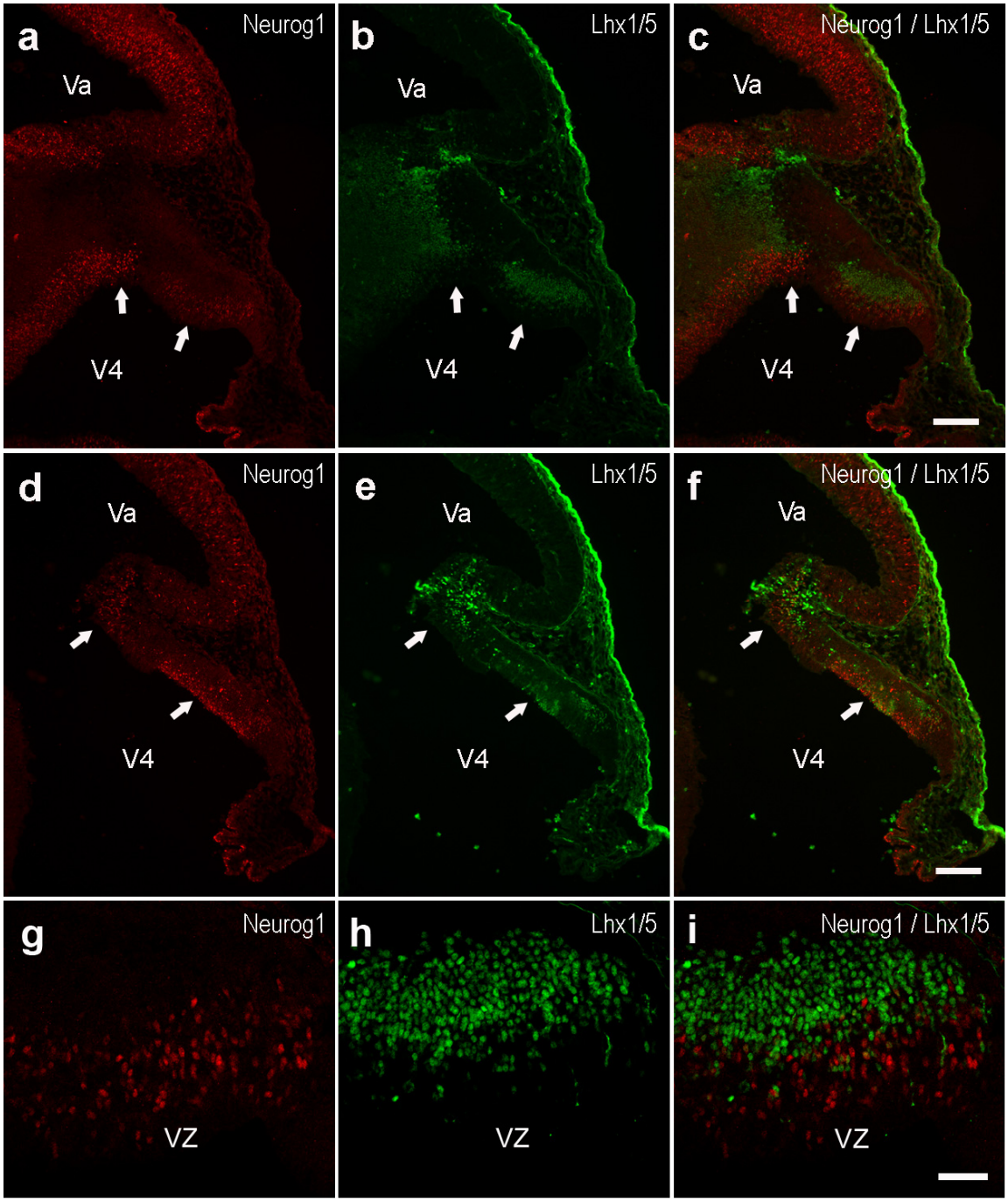

Figure 4: Neurog1 is expressed in two territories in the cerebellar primordium of embryonic (E) 13 mice. Anti-Neurog1/anti-Lhx1/5 immunofluorescence labeling of lateral (a) and medial (b) sagittal sections of the embryo: (a,d,g) anti-Neurog1; (b,e,h) anti-Lhx1/5 Captured on a confocal microscope and oriented rostral-caudal top to bottom and ventral-dorsal left to right. Arrows indicate two distinct anti-Neurog1 immunoreactive territories in the cerebellar primordium: a rostral, isthmic territory; and a caudal territory in the cerebellar anlage proper. Va, ventricular aqueduct; V4, fourth ventricle; VZ, ventricular zone (of the fourth ventricle). Scale bars = 100 μm

antisera to the LIM- homeodomain proteins Lhx1 and Lhx5 (Lhx1/5) similarly detect two discrete immunopositive territories in the E13 cerebellum that closely align with Neurog1-immunoreactivity (Fig. 4a – f). Lhx1 and Lhx5 are expressed in post-mitotic, early differentiating Purkinje cells (Zhao et al., 2007) and Lhx1 and Lhx5 ISH territories partially overlap with Neurog1 in the caudal cerebellar anlage of E12.5 mice (Zordan et al., 2008). However, high magnification confocal microscopy unexpectedly reveals that Neurog1- and Lhx1/5-immunolabeled cells are distinct in both the rostral and caudal immunoreactive territories of the E13 cerebellum. In the cerebellar anlage, dorsal Lhx1/5-positive cells are closely apposed to Neurog1-immunoreactive cells in the VZ and lower IMZ (Fig. 4g – i). Although mutually exclusive, Neurog1/Lhx1/5 expression does not confirm Neurog1 expression in Purkinje cell lineages, we nevertheless speculate that the close apposition of Neurog1-positive and Lhx1/5-positive immunoprofiles in the cerebellar anlage reflects the sequential expression of these transcription factors in Purkinje cells as they transition from proliferation to differentiation zones.

Neurog1 expression in VZ progenitors transitioning to committed neuronal lineages in the caudal cerebellum would be expected to result in a mixture of mitotic Neurog1-positive progenitor cells and post-mitotic Neurog1-positive committed neurons. We examined the mitotic status of Neurog1-positive cells using short (2 hr) BrdU pulse-labeling of E13 mice. These experiments revealed that a small fraction of Neurog1-immunoreactive cells in the VZ/IMZ are mitotic (Fig. 5, p. 30) with 4.5 ± 0.6% of Neurog1-positive cells co-immunoreactive to BrdU antisera in the cerebellar anlage. Dual Neurog1/BrdU-positive cells were found in the dorsal VZ and adjacent ventral IMZ but

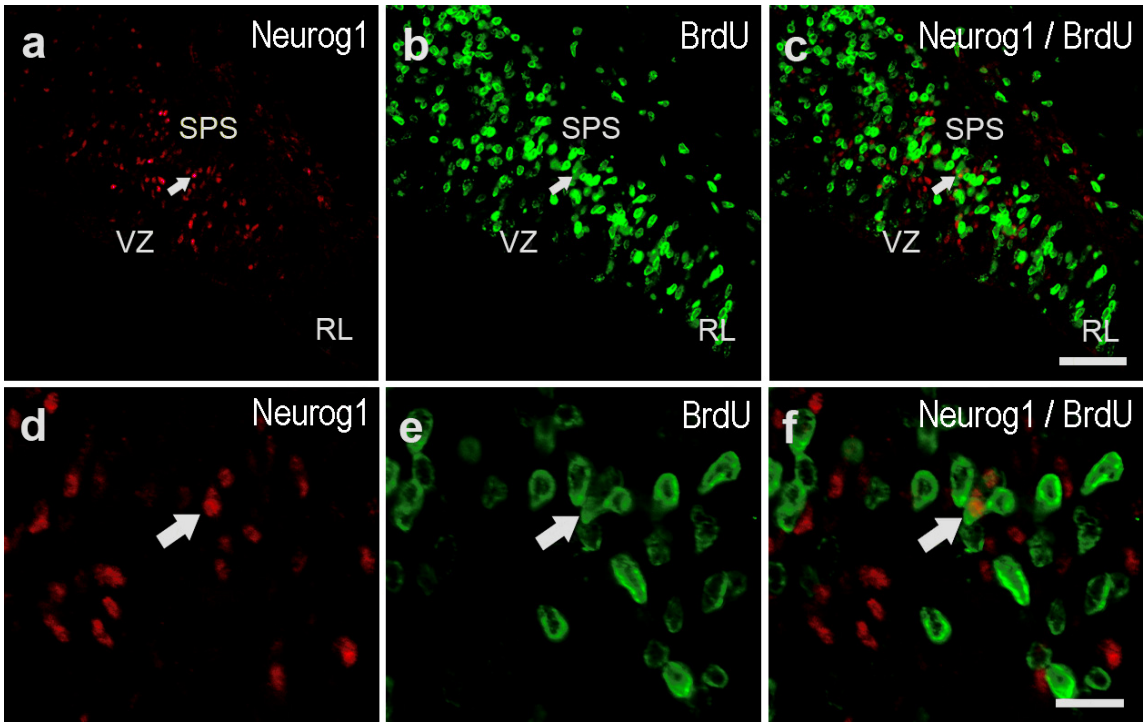

Figure 5. Neurog1 is expressed in a fraction of mitotic progenitor cells in the caudal cerebellum of embryonic day (E) 13 mice. a – f: Dual anti-Ngn1/anti-BrdU immunofluorescence labeling of sagittal sections of the embryo: anti-Ngn1 (a,d); anti-BrdU (b,e); and overlay (c,f). The figure panels are captured on a confocal microscope and are orientated rostral – caudal top-to-bottom and ventral – dorsal left-to-right, respectively. Images in d – f are taken from the caudal cerebellum shown at lower magnification in a – c. The arrow indicates a rare Neurog1/BrdU dual positive immunoreactive profile. RL, rhombic lip; SPS, subpial stream; VZ, ventricular zone; Scale bars = 50 μm in a – c, 10 μm in d – f.

not in more ventral VZ locations, suggesting that Neurog1 was expressed in mitotic progenitors undergoing late cell divisions.

In their ISH study, Zordan et al. (2008) reveal that Neurog1 expression is caudal to an anterior Pax2 ISH territory in the E12.5 – E13.5 cerebellum. Unfortunately, the identical rabbit host species of anti-Neurog1 and anti-Pax2 antisera prevent dual immunolabeling. As an alternative approach, we examined the topographical expression relationship of the two transcription factors by single-channel immunolabeling of adjacent sections. Our data confirm the presence of a distinct Pax2-positive territory in the rostral VZ and IMZ of the E13 cerebellar anlage. Comparison of adjacent immunolabeled sections indicate that this rostral Pax2-positive territory does not overlap with Neurog1-positive cells in the caudal cerebellar anlage (Fig. 6, p. 33), suggesting distinct cell lineages are derived from Neurog1-positive and Pax2-positive precursors in the E13 cerebellum. Combined, the E11.5 – 13.5 data indicate neuroepithelial Neurog1-positive progenitors develop into two distinct territories in the cerebellar primordium: a rostral, isthmic territory of unknown fate; and a caudal cerebellar territory of VZ progenitors and early-committed cell lineages that includes Purkinje cells (Fig 7, p. 34).

Low level Neurog1 expression in the VZ/IMZ of the cerebellum of E14 – E20 mice

Neurog1 ISH levels are reported to be down-regulated from E12.5 to E13.5 in the mouse cerebellum (Zordan et al., 2008). Consistent with this, we see a reduction in Neurog1-immunoreactivity in the E14 cerebellum. Neurog1-immunoreactive cells are scattered in a mid rostral-caudal band of the VZ and IMZ of the cerebellar anlage but are absent from the isthmic region (in contrast to the intense anti-Neurog1 immunoreactivity in the adjacent inferior colliculus). Neurog1-immunolabeled cells remain concentrated in

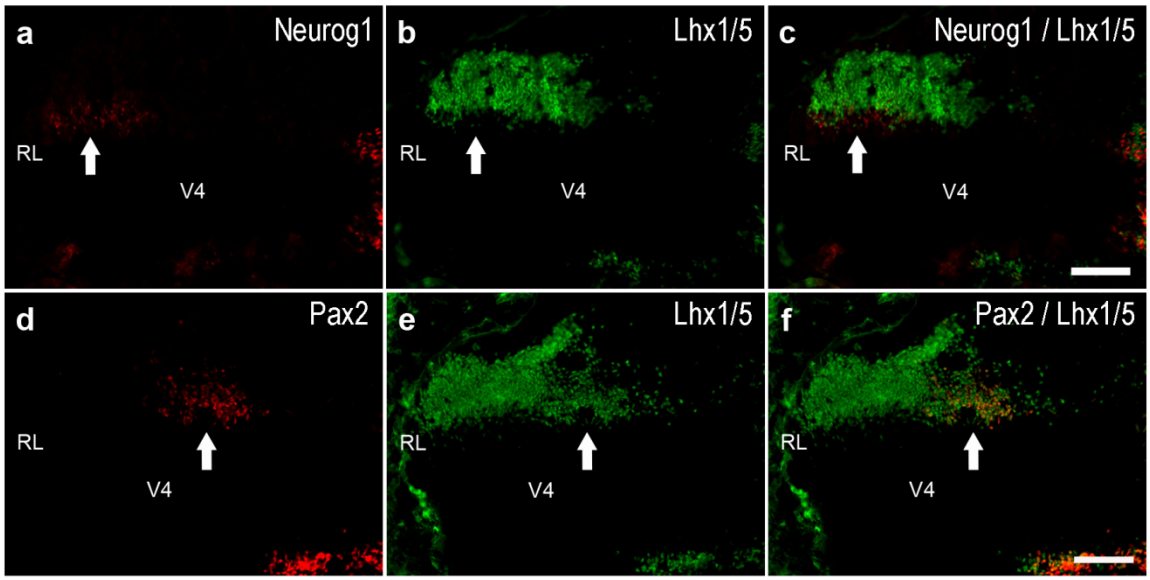

Figure 6: Distinct Neurog1 and Pax2 expression territories in the embryonic day (E) 13 cerebellar anlage. a – f: Dual anti-Neurog1/anti-Lhx1/5 (a – c) and anti-Pax2/anti-Lhx1/5 (d – f) immunofluorescence labeling of adjacent sagittal sections of the E13 embryo. Images are captured from a fluorescence microscope and are orientated rostral-caudal right-to-left and dorsal-ventral top-to-bottom. The location of the caudal Neurog1-positive cerebellar territory is highlighted by the arrow in a – c. The rostral cerebellar Pax2-positive territory is similarly highlighted in the adjacent section in d – f below. The relative positions of the two immunoreactive territories within the cerebellar anlage and their relationship to dorsal Lhx1/5-positive neurons suggests Neurog1 and Pax2 expression territories are distinct in the E13 cerebellum. RL, rhombic lip, V4, fourth ventricle. Scale bars = 100 μm.

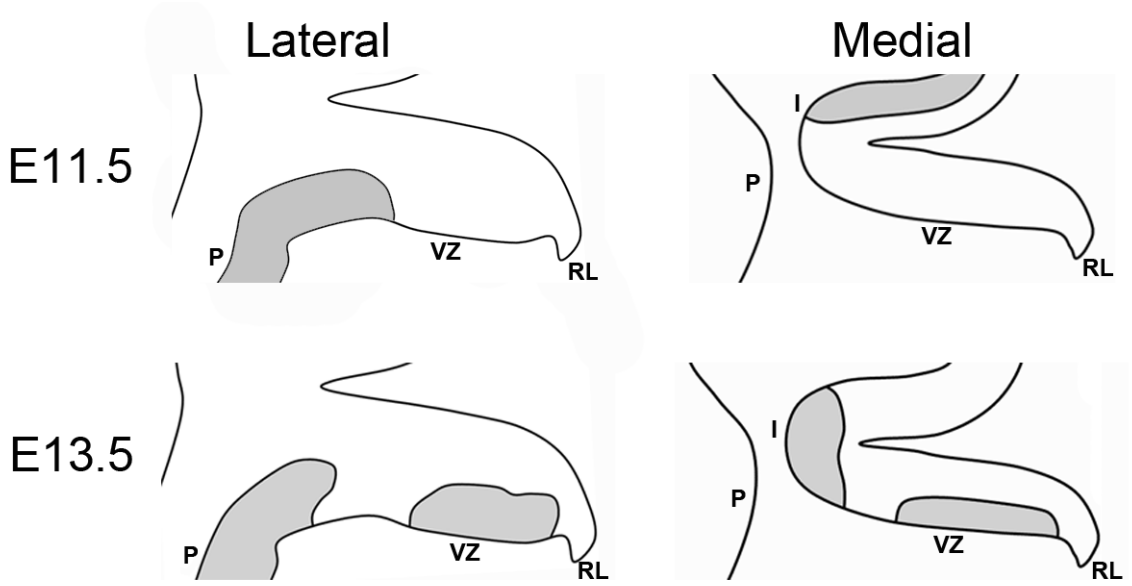

Figure 7: Schematic illustration of the development of Neurog1-positive cerebellar territory in embryonic day (E) 11.5 – E13.5 mice. Neurog1-positive cerebellar territories are shaded in gray. Neuroepithelial Neurog1-positive progenitors develop into two distinct territories in the nascent cerebellar primordium: a rostral, isthmic territory of unknown fate; and in VZ progenitors and early-committed cell lineages of the caudal cerebellar anlage that likely include Purkinje cells. I, isthmus; P, pons; RL, rhombic lip; VZ, ventricular zone.

the ventral half of the cerebellar anlage, adjacent to the VZ and are absent from the nascent external germinal layer (EGL). The density of anti-Neurog1 immunolabeling in the cerebellar VZ/IMZ remains relatively constant throughout the latter period of embryonic development, with increases primarily in the dispersal of immunopositive cells. Neurog1-immunoreactive cells can be seen extending into the dorsal half of the cerebellar anlage at E17, in proximity to the strongly immunoreactive neuroepithelium lining the ventricular aqueduct (not shown). At E20, anti-Neurog1 immunoreactive cells span the entire ventral-dorsal extent of the cerebellum, although the frequency of immunoreactive cells remains greater in the ventral cerebellum (Fig. 8a – c, p. 36). Within the medio-lateral extent of the IMZ, Neurog1-immunoreactive cells are clustered in greatest density at the lateral margins of the cerebellum (Fig. 8a – c). Neurog1-immunopositive cells at the lateral/dorsal margins of the cerebellum do not extend into the RL or into the developing EGL (Fig. 8d – i). The distribution of Neurog1-immunoreactive cells within the VZ and IMZ but not the RL/EGL is consistent with Neurog1 expression in GABAergic rather than glutamatergic cell-lineages. This assumption is supported by dual immunofluorescence labeling with antibodies to the glutamatergic cerebellar cell-lineage marker Pax6 (Engelkamp et al., 1999, Fink et al., 2006) (Fig. 8). Confocal imaging confirms the mutually exclusive expression of Neurog1 and Pax6 in the E20 cerebellum and absence of Neurog1-immunoreactive cells in the RL (Fig. 8d – f) and EGL (Fig. 8g – i). We next examined the co-expression of Ptf1a, a bHLH factor required for the specification of all GABAergic cell types in the cerebellum (Hoshino et al., 2005b, Pascual et al., 2007). As expected, patterns of anti-Ptf1a and anti-Neurog1 immunolabeling have significant overlap at E20 (Fig. 8j – l). Quantification

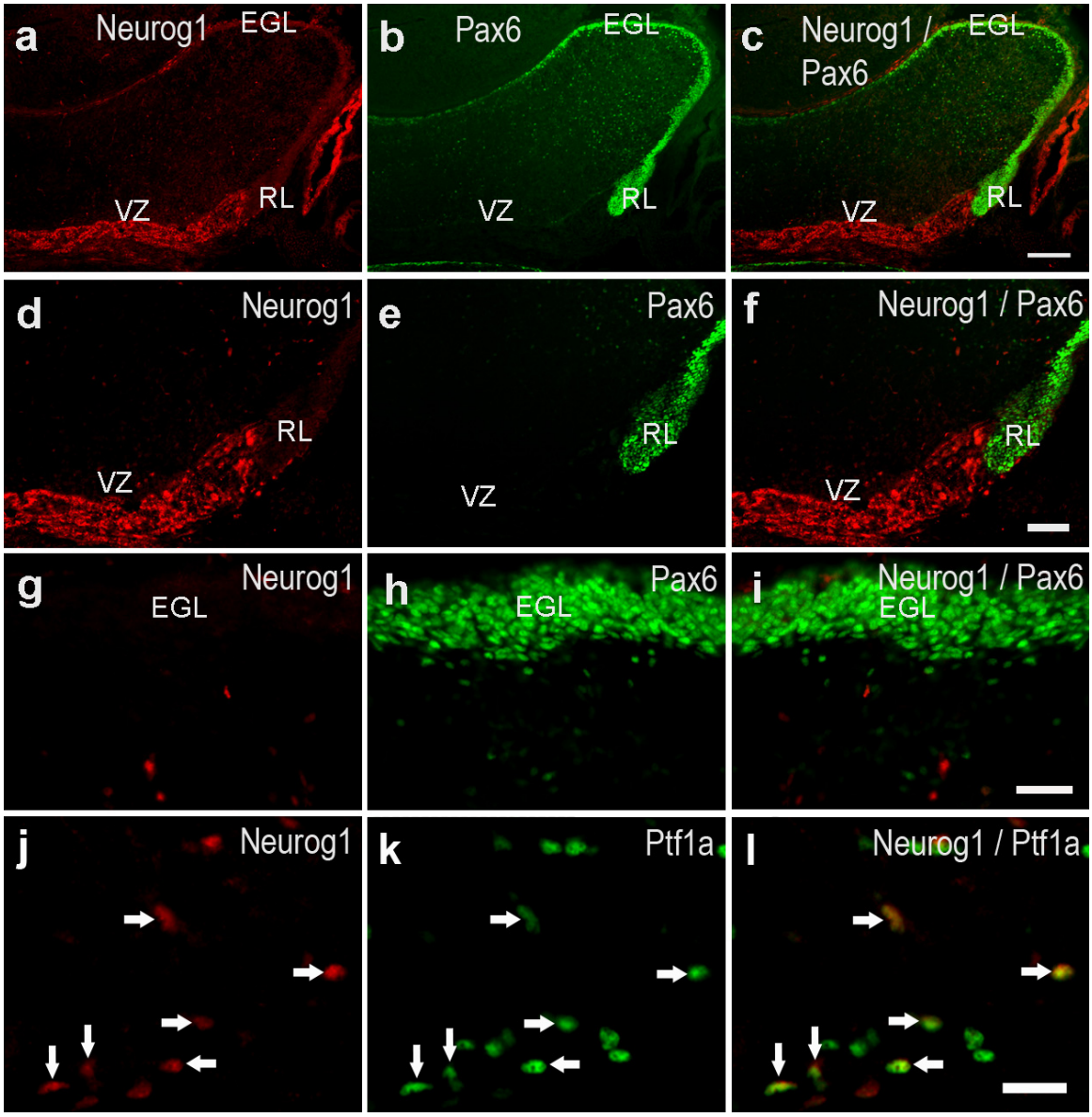

Figure 8: Neurog1 expression in early generated γ-aminobutyric acid (GABA)ergic interneurons in the cerebellum of late embryonic (embryonic day [E] 20) mice. a – l: Dual immunofluorescence labeling of coronal sections of the brain: anti-Neurog1 (a,d,g,j); anti-Pax6 (b,e,h); anti-Ptf1a (k); and overlay (c,f,i,l). **a – i**: Dual anti-Neurog1 immunolabeling with antibodies to Pax6, a marker of glutamatergic granule cells, confirms mutually exclusive expression of the transcription factors. **j – l**: Neurog1 and Ptf1a are co-expressed in E20 cerebellar cells. Cells co-immunoreactive for anti-Neurog1 and anti-Ptf1a antisera are indicated by arrows. The images are taken from the IMZ of the lateral vermis of the left cerebellum. The spatiotemporal pattern and Ptf1a-positve/Pax6-negative immunoreactivity of Neurog1-immunolabeled cells in the cerebellum of late embryonic mice suggest Neurog1 is expressed in early generated GABAergic interneurons. IMZ, intermediate zone; VZ, ventricular zone; RL, rhombic lip; EGL, external germinal layer. Scale bars = 100 µm in a – c, 50 µm in d – f, 25 µm in g – l, 10 µm in j – l.

of the proportion of Neurog1-immunoreactive cells co-immunolabeled with Ptf1a antisera reveals that 79.18 ± 6.06% cells co-express Ptf1a in the vermis. Cell counts reveal a lower proportion of 44.44 ± 1.71% Ptf1a-immunoreactive cells co-immunoreactive for Neurog1, indicating Neurog1 is expressed in a subset of Ptf1a-expressing cells in the E20 cerebellum. Combined, the spatiotemporal pattern and Ptf1a-postive/Pax6-negative immunoreactivity of Neurog1-immunoreactive cells in the E14 – E20 cerebellum point to expression in early generated GABAergic interneurons.

Neurog1 is expressed in mitotically active and migrating precursor cells in the cerebellar white matter of postnatal mice

Neurog1 ISH has been reported in the prospective WM, IGL, and ML but not DCN or glia of the postnatal cerebellum (Schuller et al., 2006). Consistent with these data, anti-Neurog1 immunohistochemistry detects Neurog1-expressing cells in the prospective WM and IGL but not the EGL of the cerebellum of young postnatal mice. Thin (one to two cells across), discontinuous streams of elongated profiles extend into each of the five primary lobules along the prospective WM in the cerebellum of P1 neonates (not shown). These cells are flanked by a scattered, heteromorphic population of elongated and globular cellular profiles along the inner aspects of the cerebellar cortex. The density of Neurog1-immunoreactive cells in the WM increases during the first postnatal week with immunoreactive cells forming a mostly continuous stream one to three cells across. Increased numbers of Neurog1-immunoreactive cells are also seen clustered (in aggregates up to five cells or more across) at the WM/IGL interface, whereas fewer immunopositive cells are observed in the upper reaches of the IGL (Fig. 9, see p. 38). Neurog1-immunoreactive cells at the WM/IGL interface have a mixture of

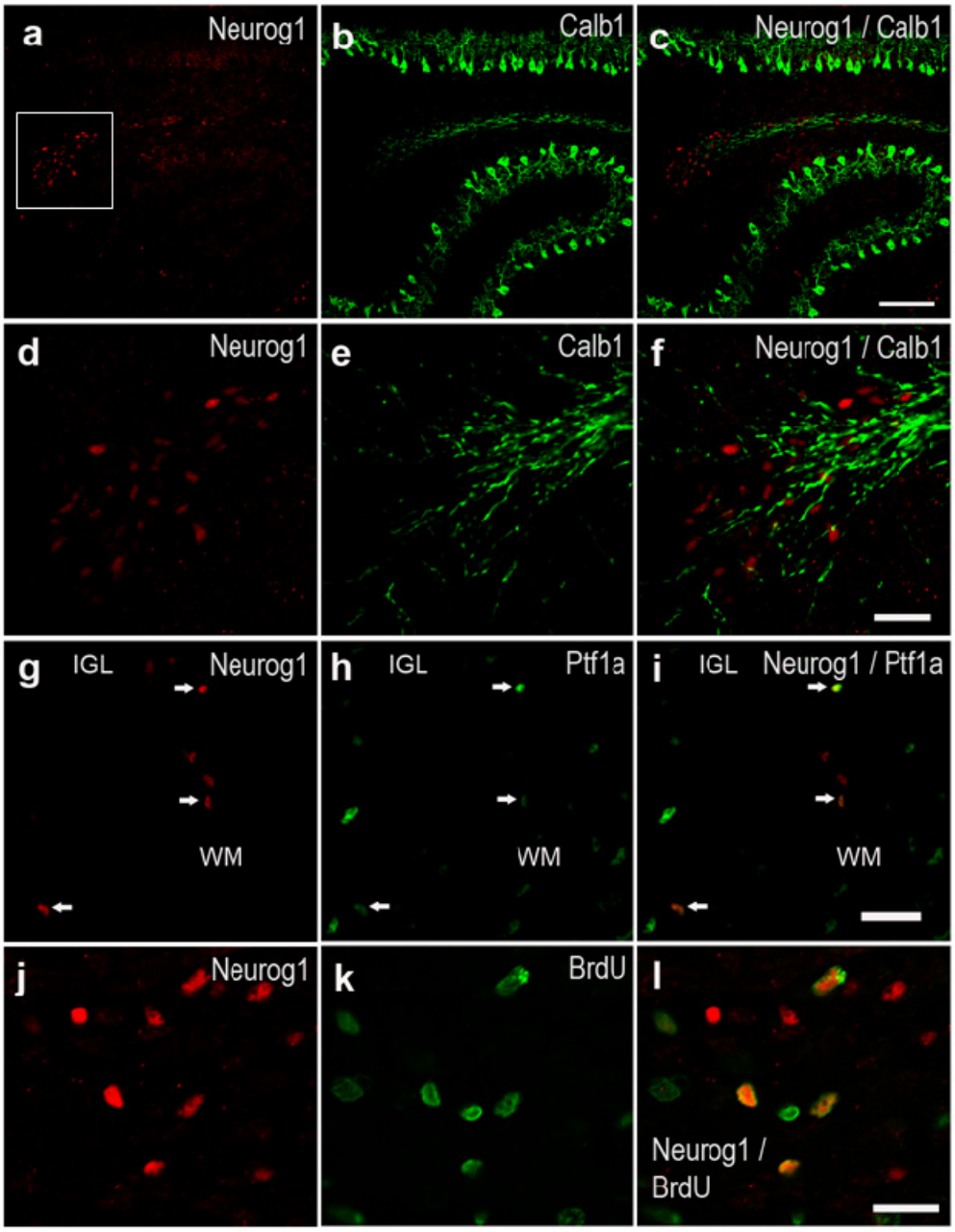

Figure 9: Neurog1 expression in γ-aminobutyric acid (GABA)ergic interneurons in the postnatal cerebellum. **a – i**: Dual immunofluorescence labeling of sagittal cerebellar sections from a postnatal day (P) 7 mouse brain: (a,d,g) anti-Neurog1; (b,e) anti-Calb1; (h) anti-Ptf1a; and (c,f,i) overlay. All images are taken from lobule VI of the vermis. **a – f**: Dual anti-Neurog1 immunolabeling with antisera to the cerebellar Purkinje cell-specific calcium-binding protein Calb1 reveals the close apposition of Neurog1-immunoreactive cells to Purkinje cell axons in the WM tracts. **a – c**: Lower magnification images showing a stream of Neurog1-immunoreactive cells in the WM and clustering of immunoreactive cells at the WM/IGL interface as the folia opens out. Boxed area of WM/IGL interface indicates area shown in higher magnification below. **d – f**: Clustered Neurog1-immunoreactive cells at the WM/IGL interface vary in morphology (globular/elongated) and orientation toward the surrounding cortex. **g – i**: Neurog1-immunoreactive cells in both the WM and IGL are co-immunoreactive to Ptf1a antisera (arrows) in support of a GABAergic identity. **j – l**: Neurog1-expressing cells include proliferating bromodeoxyuridine (BrdU)-immunopositive precursor cells. WM, prospective white matter tracts; IGL, granule cell layer. Scale bars = 100 μm in a – c, 50 μm in d – i, 20 μm in j – l.

elongated and globular profiles and are orientated in a variety of directions toward the surrounding cortex (Fig. 9d – f). In contrast, Neurog1-immunoreactive profiles located in the lower aspects (crus) of the lobules are more homogeneously elongated and orientated along the laminar axis of the cortex. We speculate that these morphologies correspond to the migratory and maturational states of Neurog1-positive cells, with elongated profiles representing cells in active migration and globular profiles representing cells undergoing later stage differentiation events. Of particular note, we did not observe Neurog1-immunoreactive cells orientated in directions toward the DCN or Neurog1-immunoreactive neurons within this structure during this period.

Migrating cells in the WM of the postnatal cerebellum are known to include mitotically active GABAergic interneuron precursors (Zhang and Goldman, 1996a, Maricich and Herrup, 1999). We examined the cell lineage and mitotic profile of postnatal Neurog1-expressing cells by anti-Ptf1a and BrdU pulse-immunolabeling. Antisera to Ptf1a reveals that Neurog1-immunoreactive cells in the WM and IGL co-express the GABAergic cerebellar cell-lineage marker in the P7 cerebellum (Fig. 9g – i). Short (2 hour) BrdU pulse-labeling of P7 mice reveals a minor fraction of Neurog1-immunoreactive cells are mitotic, with BrdU co-localization in approximately 5-10% of Neurog1-immunoreactive cells (Fig. 9j – l). Co-localization of BrdU and Neurog1 was observed in the deep WM, rarely in the WM/IGL interface and not detected in the lower IGL, consistent with globular/IGL cells undergoing postmitotic differentiation.

A decline in the frequency of Neurog1-immunoreactive profiles in the WM and IGL is detected as early as P8.5; by P11 immunoreactive profiles are sparsely scattered throughout the WM/IGL, forming an increasingly discontinuous stream of cells in the

WM (not shown). At P15, a few Neurog1-immunoreactive profiles are detected in the most distal WM regions and in the IGL (< 5 per lobule); at P18.5 no Neurog1-immunoreactive cells are observed within the cerebellum (not shown). The declining presence of Neurog1-positive cells in the second and third postnatal weeks parallels the developmental decline in stellate and basket cell production (Weisheit et al., 2006) and, combined with their spatio-temporal pattern, Ptf1a-immunoreactivity and the presence of proliferating progenitors, provide strong evidence that Neurog1 is expressed in migrating basket and stellate cell lineages as they ascend the WM tracts to final cortical destinations.

CHAPTER 4: FATE MAPPING OF NEUROGENIN1-EXPRESSING PROGENITORS

Neurogenin1 short-term reporter-gene mice reveal Neurogenin1 is expressed in interneuron cell lineages of the cerebellar cortex

The data from anti-Neurog1 immunolabeling suggest transient, sequential Neurog1 expression in developing Purkinje cell and interneuron cell lineages of the cerebellar cortex. Co-immunolabeling experiments indicate that Neurog1 expression does not overlap with cell-specific immunomarkers (although Neurog1 is co-expressed with the pan GABAergic cerebellar cell lineage marker Ptf1a). To test our hypothesis that Neurog1 is expressed in Purkinje cell and interneuron cell lineages of the cerebellar cortex but not the DCN, we examined Neurog1-positive cell fates using bacterial artificial chromosome (BAC) reporter gene mice. We used *Neurog1*$^{EGFP/+}$ mice (GENSAT project) to track short-term Neurog1-positive cell fates. The *Neurog1*$^{EGFP/+}$ line was generated using BAC RPCI-23-457E22, the same vector engineered to produce *Neurog1*^{CreER} mice used to map Neurog1 cell fates in the inner ear (Raft et al., 2007).

Neurog1$^{EGFP/+}$ mice have been used to map short-term cell fates in the developing thalamus (Vue et al., 2007) and co-immunolabeling of Neurog1 with EGFP confirms the persistence of the EGFP reporter in differentiating Neurog1-positive cerebellar cell lineages (Fig. 10, p. 42). Patterns of EGFP expression and co-immunoreactivity in embryos are consistent with Neurog1 expression in cell lineages of the cerebellar cortex and not the DCN. However, the data reveal reporter gene expression in expected GABAergic and unexpected glutamatergic cell types.

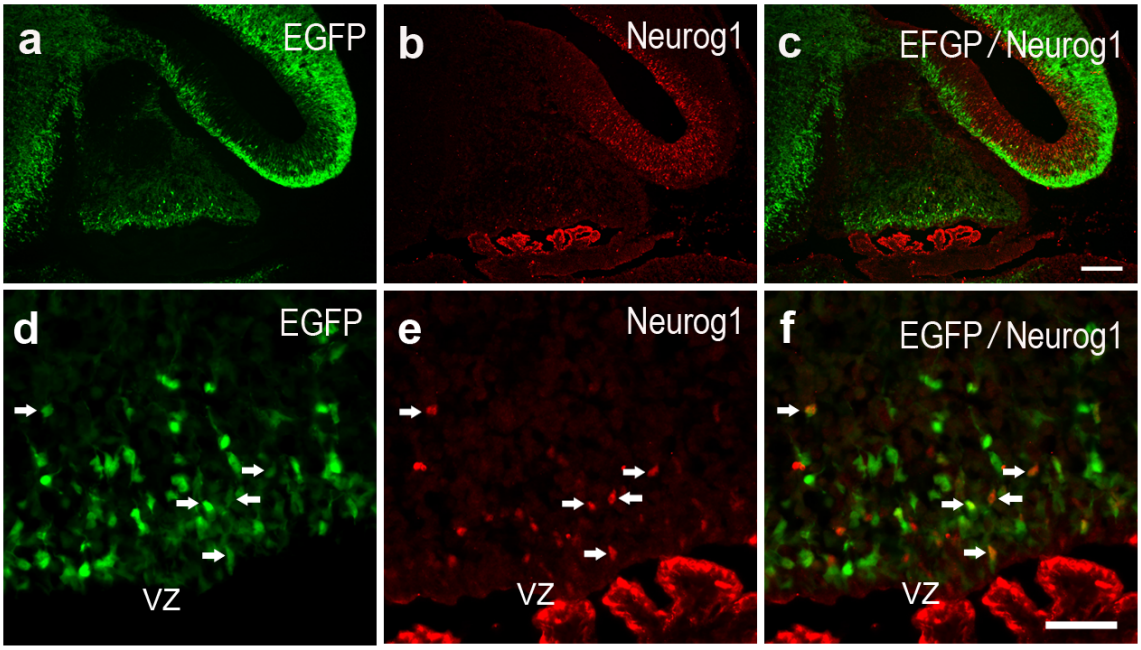

Figure 10: Neurog1$^{EGFP/+}$ mice are reliable short-term lineage tracers for Neurog1. Endogenous Neurog1 and enhanced green fluorescent protein (EGFP) reporter protein are expressed in overlapping territories in the cerebellum and tectum of embryonic Neurog1$^{EGFP/+}$ reporter gene transgenic mice. Images are taken from sagittal brain sections processed for immunofluorescence labeling of Neurog1 using polyclonal rabbit anti-Neurog1 antisera. **a – c**: Low magnification images of the cerebellum and tectum showing substantial expression of Neurog1 and EGFP reporter in these two structures. **d and e**: Higher magnification view of cerebellar anlage showing co-expression of EGFP reporter with Neurog1-immunoreactivity (arrows) in cells in the VZ and IMZ. Although Neurog1 and EGFP are co-expressed, EGFP signal is present in substantial numbers of cells that are Neurog1-immunonegative. The data indicate that EGFP reporter protein is maintained in neurons as they transition to differentiation zones in the cerebellum; as was reported to be the case in the thalamus of embryonic Neurog1$^{EGFP/+}$ mice by Vue et al. (2007). Scale bars = 100 μm in a – c, 50 μm in d and e.

Consistent with specific Neurog1 expression in cortical cell lineages, EGFP-positive cells do not co-express the early DCN lineage markers Tbr1 and Tbr2 in E14.5 mice (Fig. 11a – f, p. 44) (Englund et al., 2006, Fink et al., 2006). In *Neurog1*$^{EGFP/+}$ mice, EGFP is robustly co-expressed with the inhibitory interneuron cell marker Pax2 (Maricich and Herrup, 1999) at E20 (Fig. 11g – i) and immunolabeling with Pax6 antisera confirms that EGFP-expressing cells are absent from the emerging EGL (Fig. 11j – l). However, the Pax6 data unexpectedly reveal low numbers of cells dual positive for EGFP and Pax6 in the caudal cerebellum/RL region (Fig. 11j – l). Pax6 is a marker of glutamatergic cell lineages in the cerebellum and is expressed in early generated DCN projection neurons and later in granule cell and UBC lineages of the cerebellar cortex (Hevner et al., 2006). The presence of EGFP-positive/Pax6-positive cells in the caudal cerebellum/RL but not the EGL favors reporter gene expression in UBC rather than granule cell lineages. Accordingly, we immunolabled sections from E20 *Neurog1*$^{EGFP/+}$ mice with antisera to the transcription factor Tbr2. Tbr2 is expressed in developing UBCs throughout migration stages and into adulthood, whereas granule cells express the transcription factor only transiently as they exit the EGL (Englund et al., 2006, Hevner et al., 2006). Tbr2 immunolabeling reveals concentrated immunoreactivity in the caudal cerebellum/RL that includes a small fraction of dual Tbr2-positive/EGFP-positive cells with migratory-like morphologies (Fig. 11m – o). The presence of dual Pax6-positve/EGFP-positive and dual Tbr2-positive/EGFP-positive cells in the *Neurog1*$^{EGFP/+}$ cerebellum indicates that the *Neurog1* reporter is expressed in UBC lineages in these mice.

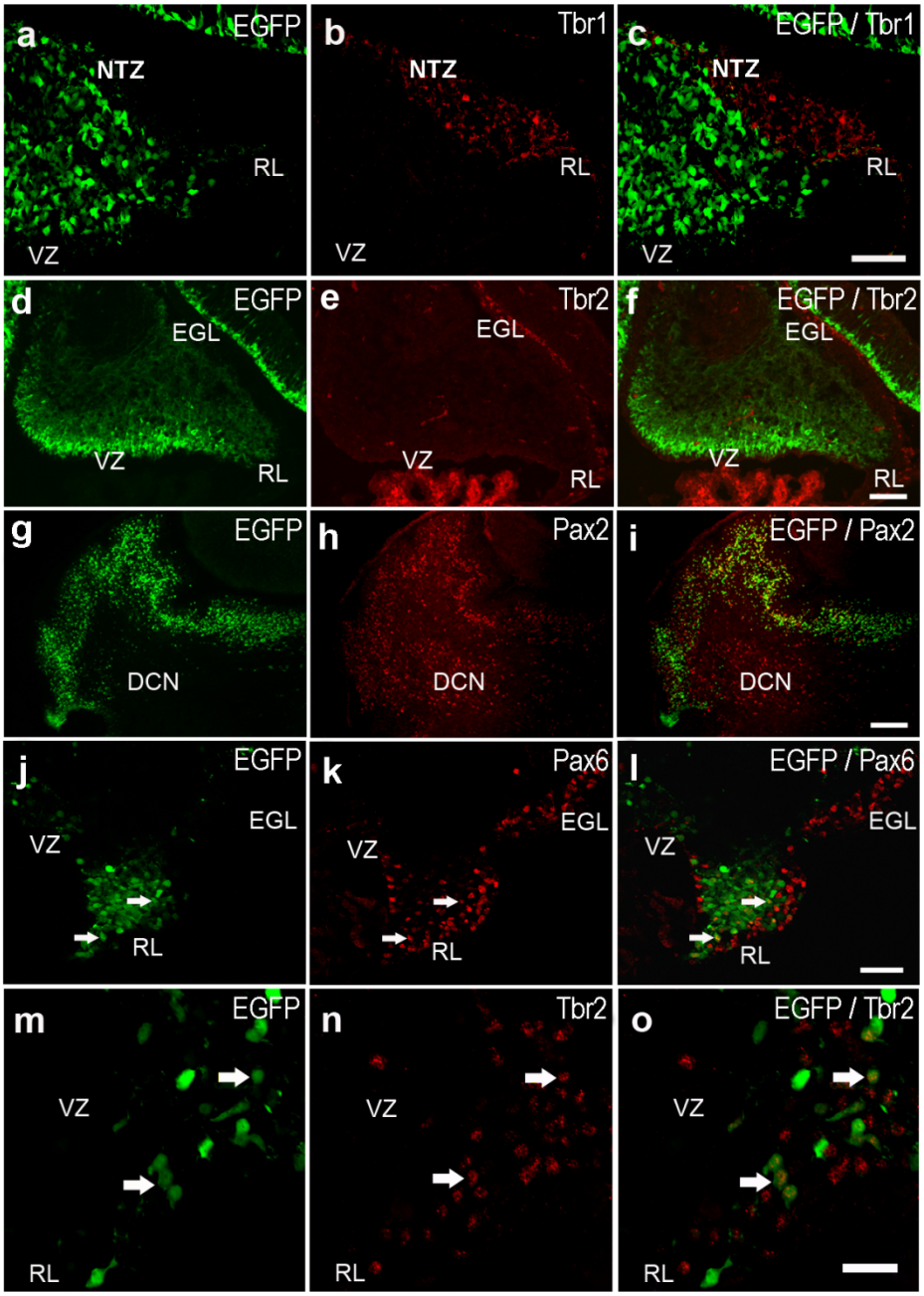

Figure 11: Short-term fate mapping using *Neurog1*$^{EGFP/+}$ mice reveals reporter gene expression in interneuronal cell lineages of the cerebellar cortex. **a – i**: Early deep cerebellar nuclei (DCN) cell lineage markers Tbr1 and Tbr2 are not co-expressed with EGFP reporter in the embryonic cerebellum. **a – e**: Images are taken from sagittal cerebellar sections of embryonic day (E) 14 *Neurog1*$^{EGFP/+}$ mice processed for: anti-Tbr1 (a – c); anti-Tbr2 immunohistochemistry (d,e). **g – i**: Immunolabeling with anti-Pax2 antibody, an inhibitory interneuron cell marker, reveals substantial co-expression with EGFP in the cerebellar cortex but not DCN of E20 mice. Images are taken from a coronal cerebellar sections of E20 *Neurog1*$^{EGFP/+}$ mice. **j – o**: Immunolabeling with antisera to Pax6 and Tbr2 indicates EGFP reporter gene is expressed in a subset of glutamatergic cerebellar cells. Images are taken from the caudal cerebellum in sagittal sections of E20 *Neurog1*$^{EGFP/+}$ mice. **j –o** : Confocal microscopy confirms the presence of dual EGFP/Pax6-positive cells (arrows) and dual EGFP/Tbr2-positive cells (arrows) in the RL and caudal cerebellum. CP, choroid plexus; DCN, deep cerebellar nuclei; EGL, external germinal layer; NTZ, nuclear transitory zone; RL, rhombic lip; VZ, ventricular zone. Scale bars = 50 μm in a – f, 100 μm in g – l, 25 μm in j – o.

During postnatal development, EGFP-expressing cells form dense migratory streams in the WM of the cerebellum. These migratory streams contain both Pax2-positive inhibitory interneuron cell lineages and Olig2-positive oligodendrocyte progenitor cells (Grimaldi et al., 2009). Immunohistochemical labeling using antibodies to Pax2 and Olig2 reveals that EGFP-expressing cells in these migratory streams are Pax2-positive and Olig2-negative (Fig. 12, p. 46). Additionally, using quantitative reverse transcriptase-polymerase chain reaction (qRT-PCR), we confirm that EGFP-expressing cells isolated from P6 – P8 *Neurog1*$^{EGFP/+}$ cerebellar tissue robustly co-express Pax2 together with the expression of Neurog1. Furthermore, analysis of a range of developmental stages (E20 – P18) indicates that EGFP-expressing cells settle first in the IGL of the cortex, then in the PCL, and lastly in the ML of the cerebellum (Fig. 13, p. 47), a pattern that is consistent with the known inside-out progression of inhibitory interneuron specification in the cerebellar cortex (Leto et al., 2006). As first reported by Grimaldi et al (2009), our anti-Olig2 data confirm additional expression of Olig2 in the DCN. No dual-positive Olig2/EGFP cells are present in this region, providing further evidence that Neurog1-positive progenitors do not contribute to deep cerebellar nuclei. These data suggest that Neurog1 contributes to GABAergic inhibitory cell lineages of the cerebellar cortex.

Many cortical cells maintain reporter gene expression in late postnatal and adult *Neurog1*$^{EGFP/+}$ mice. Co-immunofluorescence labeling of EGFP with antibodies to GABA neurotransmitter, the Golgi cell marker metabotropic glutamate receptor 2 (Grm2) (Simat et al., 2007) and the calcium binding protein parvalbumin (Pvlb), which labels stellate and basket cells, confirms that these cells are exclusively mature GABAergic

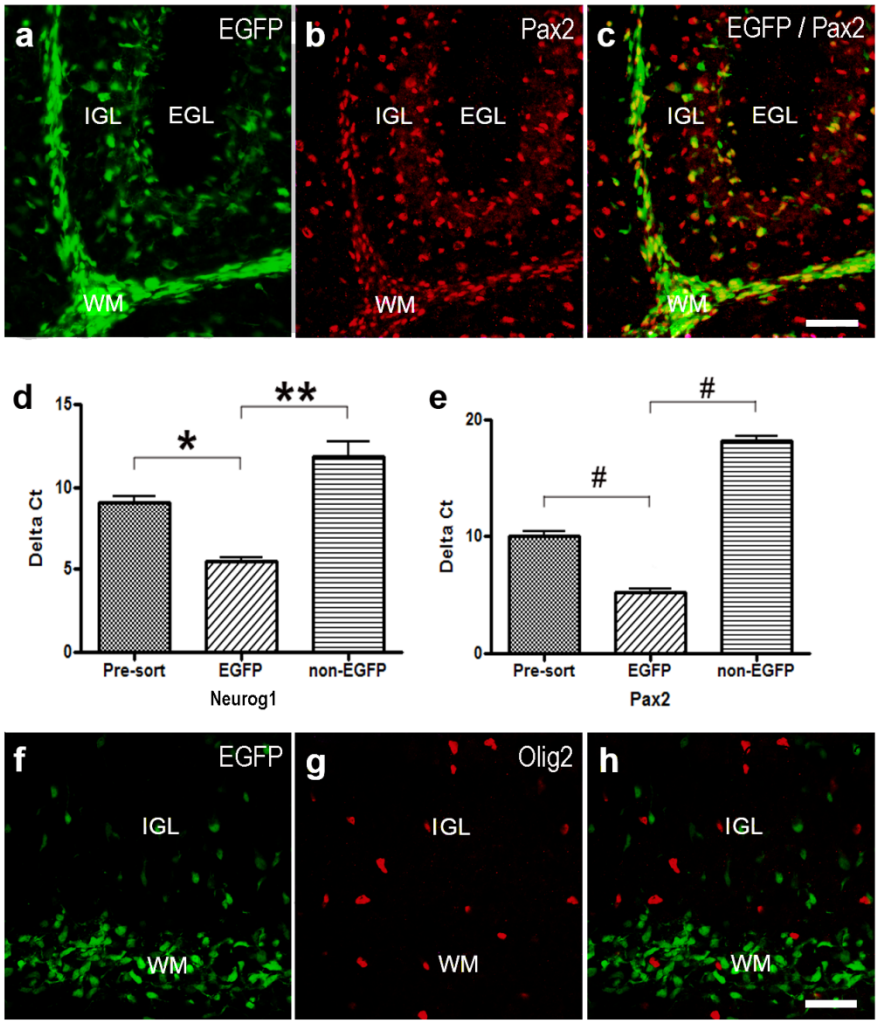

Figure 12: Short-term fate mapping using *Neurog1*$^{EGFP/+}$ mice confirms Neurog1 expression in γ-aminobutyric acid (GABA)ergic interneuron cell lineages in the cerebellar cortex but not deep cerebellar nuclei (DCN). **a – c**: EGFP-expressing cells in the white matter (WM) and cortex co-express the cerebellar GABAergic interneuron cell marker Pax2. a – c: Images are taken from lobule VI of the cerebellar vermis in sagittal sections of postnatal day (P) 7 *Neurog1*$^{EGFP/+}$ mice processed for anti-Pax2 immunofluorescence: enhanced green fluorescent protein (EGFP) epifluorescence (a); anti-Pax2 (b); overlay (c). **d,e**: Enrichment of Neurog1 and Pax2 mRNA in EGFP epifluorescent cerebellar cells in postnatal *Neurog1*$^{EGFP/+}$ reporter gene transgenic mice. Quantitative real-time reverse transcriptase-polymerase chain reaction (qRT-PCR) was used to compare Neurog1 and Pax2 expression levels following fluorescence-activated cell sorter (FACS) isolation of EGFP epifluorescent cerebellar cells from P6 to P8 *Neurog1*$^{EGFP/+}$ mice (n = 3). Cycle threshold (Ct) values for Neurog1 and Pax2 were normalized to Actb values to calculate ΔCt for comparison. Bar chart represents ΔCt values in presorted, EGFP epifluorescent (EGFP), and nonepifluorescent (non-EGFP) FACS-isolated cells. Significantly lower Neurog1 and Pax2 Δ Ct values, and thereby higher levels of transcript, are present in the FACS-isolated EGFP sample compared with presorting or non-EGFP isolates. *Neurog1 ΔCt presorting versus EGFP, $P < 0.005$; **Neurog1 ΔCt EGFP versus non-EGFP, $P < 0.001$; # Pax2 ΔCt presorting versus EGFP and Pax2 ΔCt EGFP versus non-EGFP, $P < 0.0001$ (unpaired two-tail *t*-tests). **f – h**: *Neurog1*$^{EGFP/+}$-expressing cells in the WM and cortex do not co-express the oligodendrocyte and DCN lineage marker Olig2. **f – h**: Images are taken from lobule V of the cerebellar hemisphere in sagittal sections of P7 *Neurog1*$^{EGFP/+}$ mice processed for anti-Olig2 immunofluorescence: EGFP epifluorescence (f); anti-Olig2 (g); overlay (h). EGL, external germinal layer; IGL, granule cell layer; WM, prospective white matter tracts. Scale bars = 50 μm in a – c, 25 μm in f – h.

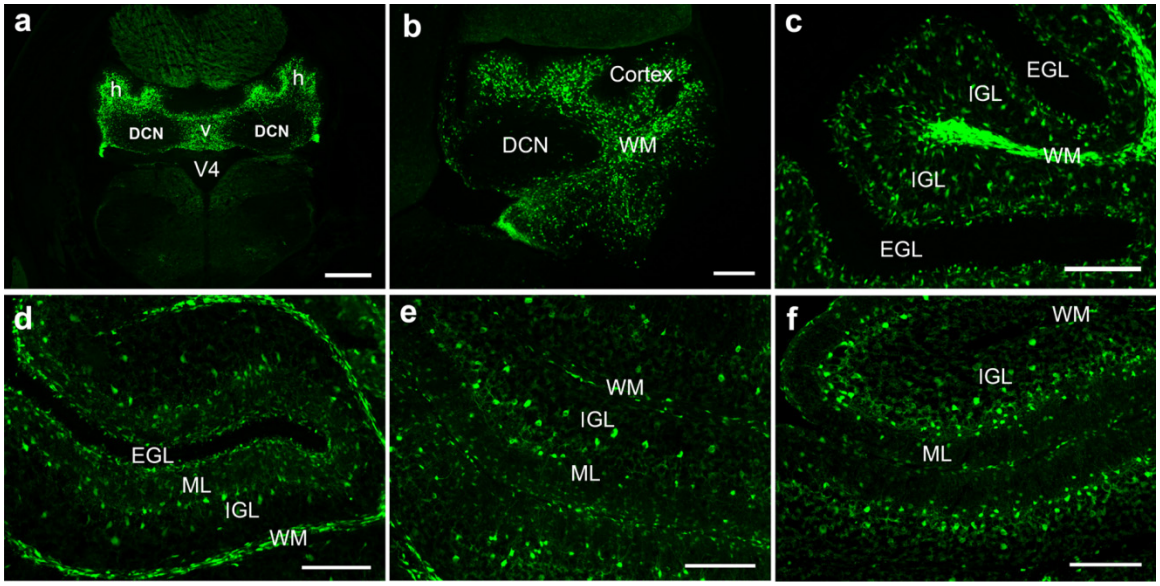

Figure 13: EGFP-expressing cells differentiate in an inside-out pattern in the developing cerebellar cortex of *Neurog1*$^{EGFP/+}$ mice. a – f: Images are taken from: embryonic day (E) 19 (a); postnatal day (P) 1 (b); P7 (c); P10 (d); P14 (e); and P18 (f) Neurog1-EGFP reporter gene mice. a–c: Upper figure panel images are captured directly from enhanced green fluorescent protein (EGFP) epifluorescence, reflecting the high expression levels of the reporter gene in the embryo and early postnatal mice. d – f: In lower figure panel images, the EGFP reporter gene signal has been enhanced by anti-GFP immunofluorescence. All images are taken from sagittal sections of the cerebellar vermis with the exception of a, which is taken from a coronal section of medial rostral-caudal location within the cerebellum. V4, fourth ventricle; v, vermis; h, hemispheres; DCN, deep cerebellar nuclei; WM, prospective white matter tracts; EGL, external germinal layer; IGL, granule cell layer; ML, molecular layer. Scale bars = 250 μm in a, 100 μm in b – f.

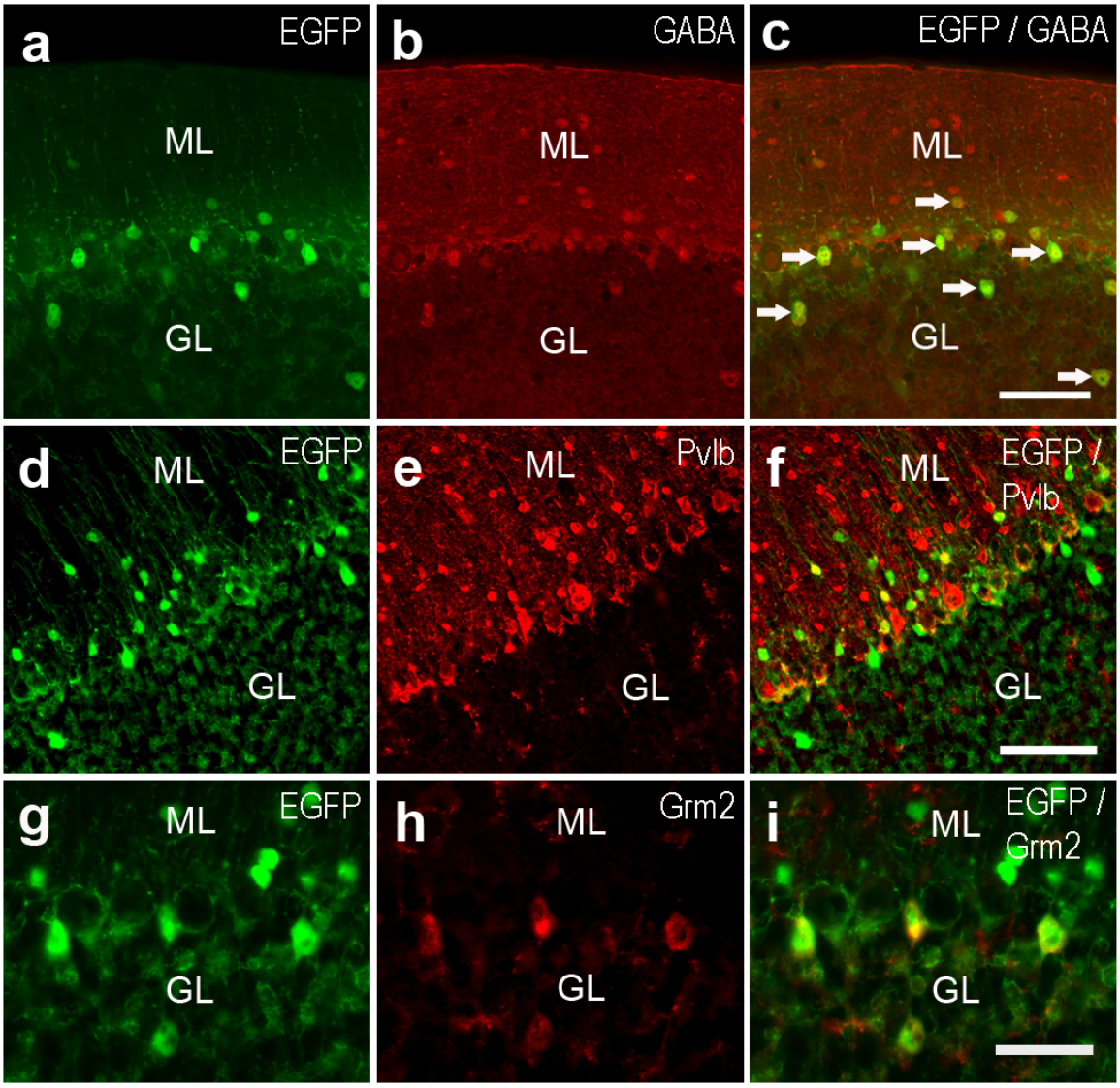

Figure 14: *Neurog1*$^{EGFP/+}$ reporter is expressed in mature γ-aminobutyric acid (GABA)ergic cell fates in the cerebellum of postnatal day (P) 30 *Neurog1*$^{EGFP/+}$ mice. **a – c**: Dual immunofluorescence labeling of *Neurog1*$^{EGFP/+}$ reporter and GABA neurotransmitter in a coronal cerebellar section. Examples of dual *Neurog1*$^{EGFP/+}$/GABA-immunofluorescent cells are indicated by arrows. **d – i**: Dual immunofluorescence labeling of *Neurog1*$^{EGFP/+}$ reporter with the ML interneuron marker parvalbumin (d – f) and the metabotropic glutamate receptor Grm2 (g – i), a marker for Golgi cell interneurons in the IGL, confirms reporter gene expression in GABAergic interneurons of both cortical layers. The images are taken from cerebellar lobules V and VI of the vermis. IGL, granule cell layer; ML, molecular layer. Scale bars = 100 µm in a – f, 50 µm in g – i.

interneurons (Fig. 14, p. 48). In summary, data from *Neurog1*$^{EGFP/+}$ mice support the hypothesis that Neurog1 is expressed in GABAergic interneuron cell lineages in the cerebellar cortex. In contrast, immunolabeling against the Purkinje cell-specific protein calbindin1 (Calb1) did not reveal cells co-expressing EGFP and Calb1 (data not shown); this, despite strong EGFP expression in known sites of Purkinje cell neurogenesis. In addition, *Neurog1*$^{EGFP/+}$ fate-mapping suggests that Neurog1 progenitors contribute to UBCs, an unexpected finding in view of the distinct origins and glutamatergic fate of these interneurons.

Neurogenin1 long-term reporter-gene mice reveal Neurogenin1 is expressed in Purkinje cell lineages of the cerebellar cortex

We hypothesized that differences in the persistence of EGFP protein between Purkinje and interneuron cell lineages might underlie our failure to identify dual EGFP /Calb1-positive cells in *Neurog1*$^{EGFP/+}$ mice. To test this hypothesis, we examined long-term Neurog1-positive cell fates in *Neurog1*$^{Cre/+}$ mice (gift of J.Johnson, UT SW Med. Ctr.) crossed with double-reporter Z/EG mice (*Neurog1*^{Cre}*;Z/EG*) (Novak et al., 2000). *Neurog1*$^{Cre/+}$ mice were generated with the same vector used to produce the *Neurog1*$^{EGFP/+}$ mice mentioned previously. Double-reporter Z/EG mice express *lacZ* under the control of the CMV enhancer/chicken actin promoter (pCAGGS). Following its expression, Cre recombinase activity removes the *lacZ* gene thereby intrinsically activating the constitutive expression of the EGFP reporter in a given cell (Novak et al., 2000). Analysis of EGFP epifluorescence in P30 *Neurog1*^{Cre}*;Z/EG* mice reveals sporadic EGFP expression in Purkinje cells of the cerebellar cortex, with greater frequency in the hemispheres compared to the vermis (Fig. 15, p. 51). No other EGFP epifluorescent cell types were present in the cerebellum, although fibers with mossy fiber-like glomeruli and

climbing fiber-like morphologies were visible by direct EGFP epifluorescence in the cerebellum. We speculated that the absence of EGFP epifluorescence signal in inhibitory interneuron cell lineages resulted from sub-detection levels of reporter gene expression in these cells. Accordingly, we amplified the EGFP signal using anti-EGFP immunohistochemistry and ABC Vectastain®. This approach did not identify additional EGFP-expressing cell types in the cerebellum (Fig. 16, p. 52) despite increased EGFP signal strength in other central nervous system (CNS) sites of Neurog1 expression such as the neocortex (not shown). In addition, anti-EGFP immunohistochemistry did not increase the frequency of EGFP-expressing Purkinje cells in the *Neurog1^{Cre};Z/EG* mouse cerebellum, suggesting "all or nothing" reporter gene expression in these cells. Analysis of P7 *Neurog1^{Cre};Z/EG* mice, a time-point at which Neurog1 is actively expressed in interneuron cell lineages in the WM, also failed to detect immunopositive interneurons by anti-GFP or anti-Cre immunohistochemistry. Indeed the EGFP signal was markedly weaker in reporter gene-expressing Purkinje cells at this age, suggesting EGFP reporter signal strength accumulates in neurons over time. To test whether variations in Z/EG reporter gene expression could contribute to the absence of EGFP signal in interneurons, we examined the pattern of lacZ expression in the cerebellum of *Neurog1^{Cre};Z/EG* mice by β-galactosidase activity. Robust β-galactosidase staining was detected in all Purkinje cells but only weakly and sporadically in other cerebellar cell types in *Neurog1^{Cre};Z/EG* and *Neurog1$^{+/+}$;Z/EG* littermates (P30, not shown). This suggests the following: (1) lower level Z/EG reporter gene expression could account for the lack of EGFP expression in non-Purkinje cell lineages; and (2) sporadic EGFP expression in *Neurog1^{Cre};Z/EG* Purkinje cells results from either variations in Cre efficiency among the Purkinje cell

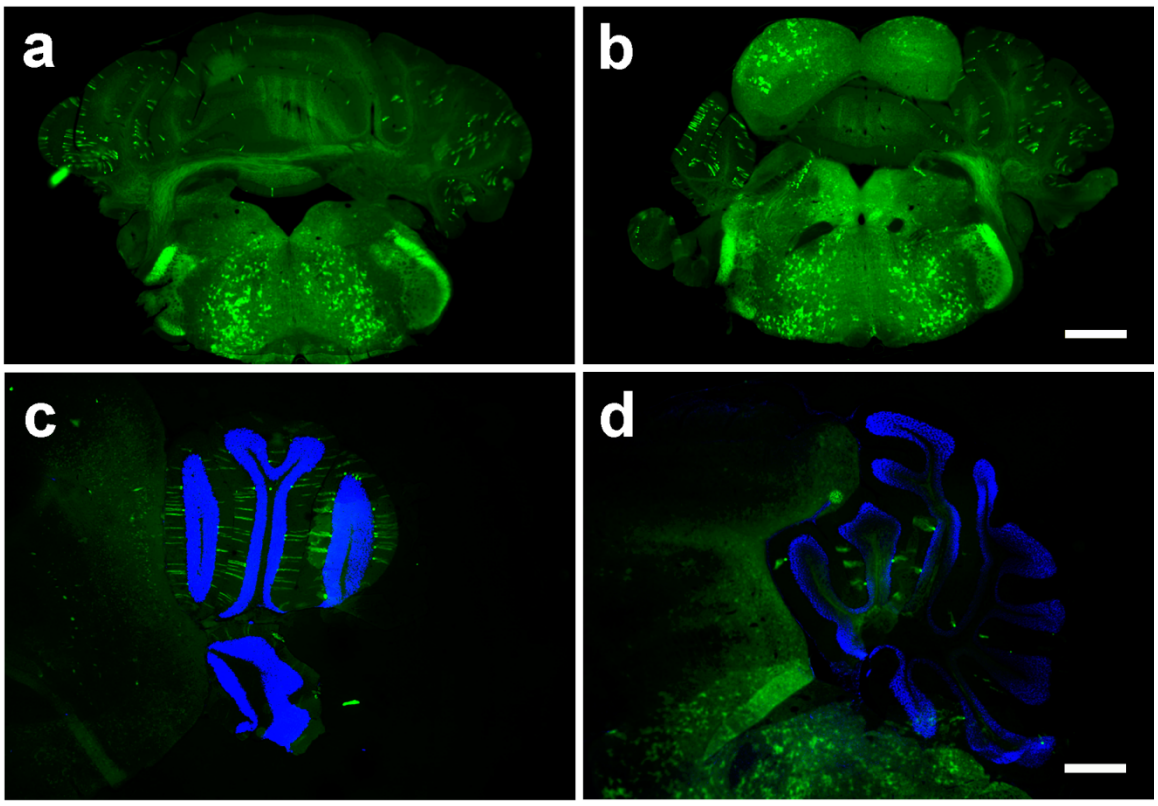

Figure 15: Distribution of EGFP-expressing Purkinje cells in the cerebellum of *Neurog1*^{Cre}*:Z/EG* mice. Coronal (a-b) and sagittal (c-d) cerebellar sections from postnatal day (P) 30 *Neurog1*^{Cre}:Z/EG mice demonstrates sporadic EGFP expression in Purkinje cells with greater frequency in the hemispheres compared to the vermis of the cerebellar cortex. **a**: Low magnification image of enhanced green fluorescent protein (EGFP) epifluorescent Purkinje cells in a coronal section of the caudal cerebellum. **b**: Low magnification image of EGFP epifluorescent Purkinje cells in a coronal section of the rostral cerebellum. **c**: Low magnification image of EGFP epifluorescent Purkinje cells in a sagittal section of the lateral cerebellum. **d:** Low magnification image of EGFP epifluorescent Purkinje cells in a sagittal section of the medial cerebellum. Sagittal sections are counterstained with DAPI (4′,6-diamidine-2-phenylidole-dihydrochloride). Note the higher density of EGFP-expressing Purkinje cells in the lateral hemispheres compared to the vermis/medial cerebellar cortex. Scale bars = 1 mm in b, 800 μm in d.

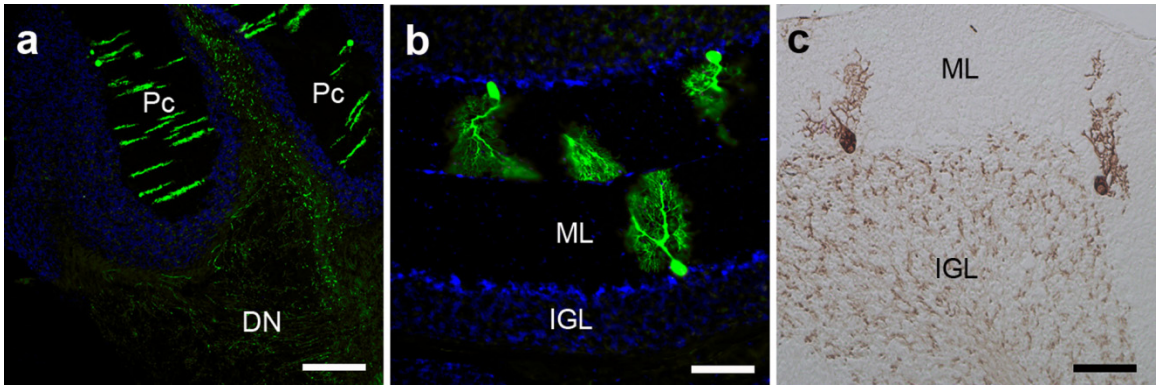

Figure 16: Long-term fate mapping using *Neurog1*^{Cre}:Z/EG mice confirms Neurog1 expression in Purkinje cell lineages. Cerebellar sections from postnatal day (P) 30 *Neurog1*^{Cre}:Z/EG mice counterstained with DAPI (4′,6-diamidine-2-phenylidole-dihydrochloride; a,b) or processed for anti-GFP immunohistochemistry (c). **a**: Low magnification image of enhanced green fluorescent protein (EGFP) epifluorescent Purkinje cells (Pc) in a coronal section. The image is taken from the right cerebellum and includes the dentate nucleus (DN) containing EGFP epifluorescent axonal fibers but not cell bodies. **b**: Higher magnification image of EGFP epifluorescent Purkinje cells taken from lobule V/VI in a sagittal cerebellar section of the vermis. Note the absence of EGFP epifluorescent interneuron cell bodies in the granule cell (IGL) and molecular (ML) layers. **c**: Anti-GFP immunohistochemistry does not reveal EGFP-expressing inhibitory interneurons in the granule cell (IGL) and molecular (ML) layers of the cerebellar cortex. The image is taken from lobules VIII/IX. The glomerular-like immunoreactive profiles in the IGL are likely mossy fiber afferents. EGFP epifluorescent climbing-fiber-like profiles also occasionally penetrate the ML (not shown). Scale bars = 200 µm in a, 100 µm in b,c.

population or from the restricted expression of Neurog1 in a subset of Purkinje cell progenitors. In conclusion, the data from *Neurog1^{Cre};Z/EG* fate mapping confirms that Neurog1-positive progenitors contribute to Purkinje cell lineages in the cerebellum. Weak Z/EG expression and/or insufficient penetrance of Cre recombinase in non-Purkinje cell cerebellar lineages means we are unable to map Neurog1-positive progenitor contributions to interneuron populations in *Neurog1^{Cre};Z/EG* mice.

Neurogenin1 long-term inducible report mice confirm cell fates of Neurogenin1-expressing precursors and reveal the temporal contribution of Neurogenin1 to neuronal lineages in the developing cerebellum

In a recent publication, Kim et. al (2011) use the *Neurog1*-CreER^{T2} (*Neurog1^{CreER}*) transgenic mouse to show expression of Neurog1 in both Purkinje cell and interneuron cell lineages of the cerebellar cortex (Kim et al., 2011). *Neurog1*-CreER^{T2} mice were generated using the BAC RPCI-23-457E22, the same vector engineered to produce the *Neurog1$^{EGFP/+}$* and *Neurog1$^{Cre/+}$* transgenic mouse lines previously mentioned. The data reported by Kim et al. (2011) confirms our combined IHC and reporter gene data documenting expression of Neurog1 by Purkinje cell and interneuron cell types in the cerebellum. Accordingly, we hypothesized that *Neurog1*-CreER^{T2} could be used to generate a complete spatiotemporal fate map of Neurog1-expressing progenitors in the cerebellum.

To test this hypothesis, we created a series of Neurog1-CreER^{T2} fate maps during critical periods of cerebellar neurogenesis. We bred Z/EG double-reporter mice (described previously) with the *Neurog1^{CreER}* mouse line (*Neurog1^{CreER};Z/EG*) that express a fusion protein of the Cre recombinase fused to a mutated estrogen receptor (ER). In the absence of tamoxifen (TMX), the fusion protein is sequestered in the cytosol

and the recombinase remains inactive. TMX binding to the ER results in the translocation of the protein to the nucleus and DNA recombination occurs (in this instance the GFP is "flipped in") (Koundakjian et al., 2007). We delivered TMX by injection at a range of developmental time points (E11.5 – P7.5) that correspond to the birthdates of the different cell types of the cerebellum, as reviewed by Carletti and Rossi (2008), as well as later stages when neurogenesis of the cerebellum is thought to be silent (P40). Our results replicate the *Neurog1*-CreER reporter gene expression in Purkinje cells reported by Kim et al. (2011) and extend their observations of reporter gene expression in inhibitory interneuron cell types. We confirm reporter gene expression in all inhibitory interneuron cell types of the cerebellar cortex. Our data provide a detailed temporal fate map that is consistent with the majority of the dogma of cerebellar cytogenesis but also challenges some assumptions. The pattern of TMX-induced EGFP expression matched the inside-out developmental sequence of GABAergic interneuron development (Schilling, 2000, Leto et al., 2006) with Golgi cells expressing EGFP upon administration of TMX at the earliest developmental time-points (E11.5 – P7), Lugaro and candelabrum cells at later developmental time-points (E14.5 – E16.5), and basket and stellate cells at the latest developmental time-points (E16.5 – P7). Surprisingly, we find that the earliest Neurog1-fated inhibitory interneurons, Golgi cells, arise during, not after the period of Purkinje cell production. Additionally, we report that EGFP epifluorescence is observed in UBC, a finding consistent with IHC and *Neurog1*$^{EGFP/+}$ data. Unexpectedly, however, we also observed EGFP epifluorescence in a small population of neurons of the DCN and a restricted number of granule cells.

Neurog1-fated cells in the E11.5 cerebellum

Analysis of EGFP expression in *Neurog1^{CreER};Z/EG* adult mice that were given TMX injections at E11.5 revealed EGFP expression in Purkinje cells, Golgi cells, and neurons of the DCN. The EGFP protein is distributed throughout the entire cell including axonal and dentritic processes, permitting cell-type identification through known morphological and cytoarchitectural characteristics. The morphological detail revealed through EGFP epifluorescence confirms expression of EGFP in Purkinje cell lineages (Fig. 17, p. 56). The pattern of EGFP-expressing Purkinje cells was sporadic with an apparent increase in frequency of EGFP-positive cells in the medial regions of the cortex compared to the lateral regions (Fig. 17c – d), a pattern nearly opposite of the pattern observed in the constitutive Cre-reporter mice (refer back to Fig. 15, p. 49).

Birthdating studies by other labs have supported the idea that neurogenesis of projection neurons in the cerebellum, such as those of the DCN and Purkinje cells, is completed prior to interneuron neurogenesis (Miale and Sidman, 1961), reviewed by Carletti and Rossi (2008). However, in mice that had been injected with TMX at E11.5 we identified EGFP epifluorecscent cells in the IGL having cell morphology characteristic of Golgi cells (Fig. 17b and e). Using anti-Grm2 antibody, a marker that labels roughly 80% of the Golgi cell population in the cerebellum (Simat et al., 2007), we observed Grm2/EGFP dual-positive cells in the granular layer of the cerebellar cortex (Fig. 17f – g). Interestingly, the vast majority of Golgi-like EGFP-positive cells at this time-point are Grm2 negative.

Our previous reports using short-term reporter mice suggest that Neurog1 is not expressed by neurons of the DNC. However, injection of TMX at E11.5 as well as all subsequent time-points, except the adult, demonstrate that Neurog1 is expressed by a

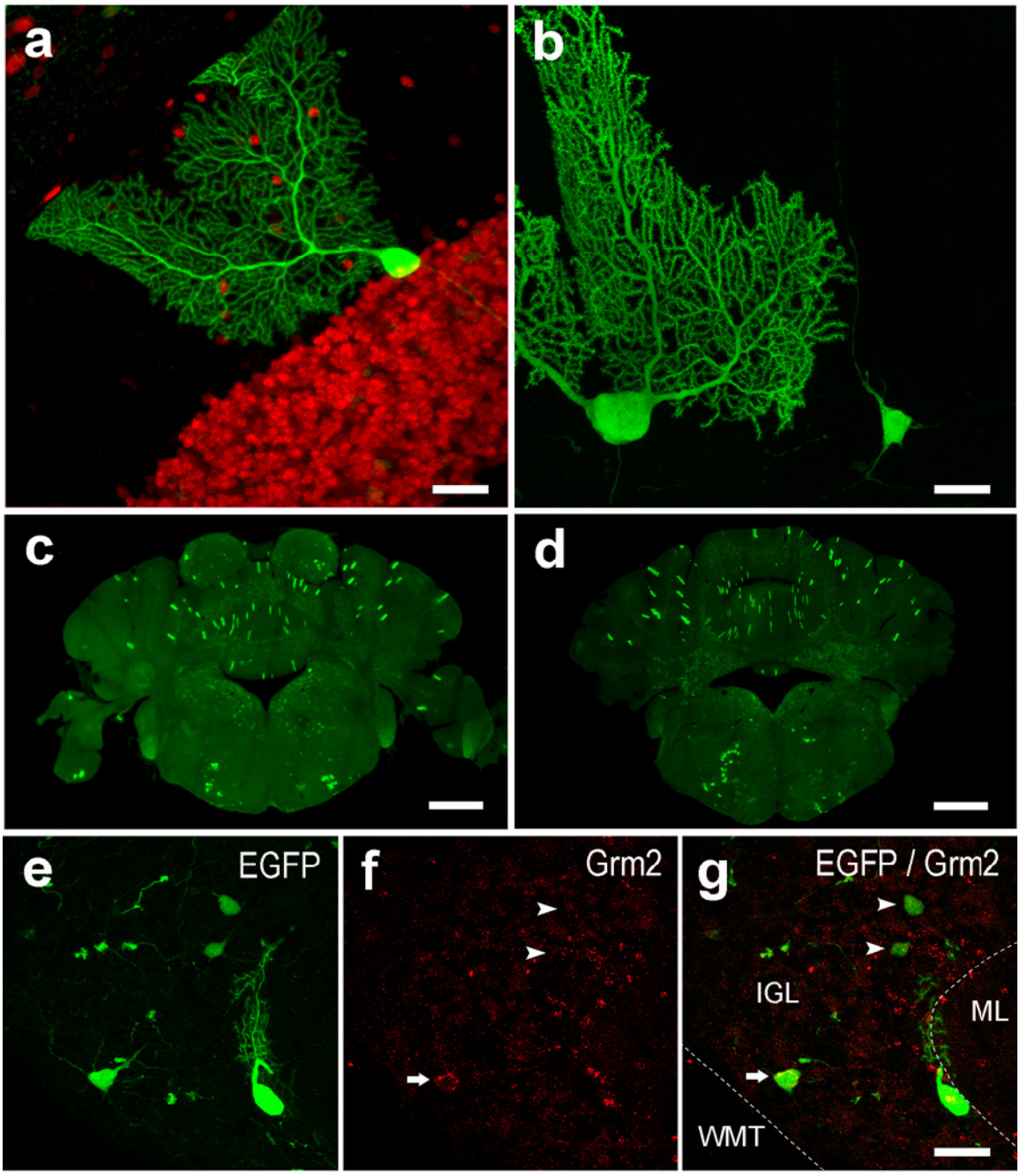

Figure 17: *Neurog1^{CreER};Z/EG* mice injected with tamoxifen (TMX) at embryonic day (E) 11.5 demonstrate Neurog1 contribution to Purkinje cell and Golgi cell lineages. All sections are enhanced with GFP antibody. **a:** Sagittal section counter-labeled with anti-NeuN (red) reveals the classic morphological details of the Purkinje cell with its elaborate dendritic arborizations extending upward from the large cell body in the Purkinje cell layer into the molecular layer (ML) toward the pial surface and a single thin axon projecting through the internal granular layer (IGL). **b:** Sagittal section reveals EGFP expression in Golgi cells coincident to expression in Purkinje cells. **c & d:** Rostral (c) and caudal (d), low magnifaction images of coronal sections enhanced with anti-GFP antiserum reveal the sporadic distribution of E11.5 Neurog1-fated Purkinje cells settling principally in medial regions of the cerebellar cortex. **e – g:** Sagittal section counter-labeled with Grm2 reveals Neurog1-fated Golgi cells are both Grm2-positive (arrows) and Grm2-negative (arrowheads). Images (f) and (g) are projections representing 10μm selected from the entire z-stack (33μm) projection.Scale bars = 50 μm in a and g, 35 μm in b, 1 mm in c & d.

very small fraction of neurons in the DCN. Co-labeling with anti-NeuN, an antibody against a neuron-restricted antigen of the cell nucleus, confirms that EGFP/NeuN dual-positive cells are found within the boundaries of the DCN. The frequency of this observation is rather low and appears to be independent of the time-point of TMX administration, only appearing in one or two cells per slice and only occurring in approximately half of the DCN-containing slices sampled (about 8 slices per time point per animal).

Additionally, we observed EFGP-positive cells in the ML. These observations were even more infrequent than the appearance of EGFP-positive neurons of the DCN (data not shown). Morphological features of these cells included small cell bodies and fine processes all restricted to the upper regions of the molecular layer.

In summary, these results indicate that Neurog1-fated cells contribute to a sporadically distrubted population of Purkinje cells found largely in the cortex. Furthermore, the data demonstrates that Neurog1-fated cells at this time-point consist primarily of a Grm2-negative subpopulation of Golgi cells. Together the data suggests that inhibitory interneurons of the cortex, specifically Golgi cells, develop concomitantly to Purkinje cell development.

Neurog1-fated cells in the E14.5 cerebellum

Analysis of EGFP expression in *Neurog1^{CreER};Z/EG* adult mice that were given TMX injections at E14.5 revealed EGFP expression in Golgi cells, Lugaro cells, candelabrum-like cells, basket cells, neurons of the DCN and an unidentified cell type of the ML. Golgi cells appear to be the dominant cell type that represent this time-point while EGFP expression in Lugaro, candelabrum, and basket cells is scarce. EGFP-

expressing cells in the IGL co-label with anti-Grm2 antibody, confirming a Golgi cell identity (Fig. 18a – c, p. 59) and NeuN immunolabeling demonstrates the appearance of EGFP-expressing neurons in the DCN (data not shown).

Parvalbumin (Pvlb) expression is known to be limited to Purkinje cells, basket cells, and stellate cells in the cerebellum (Bastianelli, 2003). Additionally, expression of NeuN in the cerebellum is limited to granule cells and an unknown cell-type found in the ML (Weyer and Schilling, 2003). The identity of Lugaro and candelabrum cells can therefore be partially determined through negative immunolabeling with anti- Pvlb and/or anti-NeuN antiserum combined with other criteria such as morphology and cytoarchitectural position. A drawback to the anti-Pvlb antibody is poor penetration, which, in our experiments, only penetrated approximately 10 μm on either side of free-floating sections. Thus, we only considered EGFP-expressing cells that were located within the range of penetration of the antibody. EGFP-positive/Pvlb-negative cells were identified with cell bodies located just beneath the PCL and cell processes extending laterally along the PCL-IGL border (Fig. 18d – f, and g,), characteristics suggesting a Lugaro cell identity. Additionally, we identified EGFP-expressing cells similar in morphology and cortical loaction to the one in Figure 18d that are anti-NeuN-negative; however, we are unable to identify Lugaro-like cells that are dual-positive for EGFP and calretinin (Calb2), a protein that, in the IGL, is expressed by UBCs and Lugaro cells (Geurts et al., 2001), as well as Golgi cells and granule cells (Simat et al., 2007). These results indicate that E14.5 Neurog1- expressing precursor cells contribute to a subpopulation of Lugaro cells that are Calb2-negative.

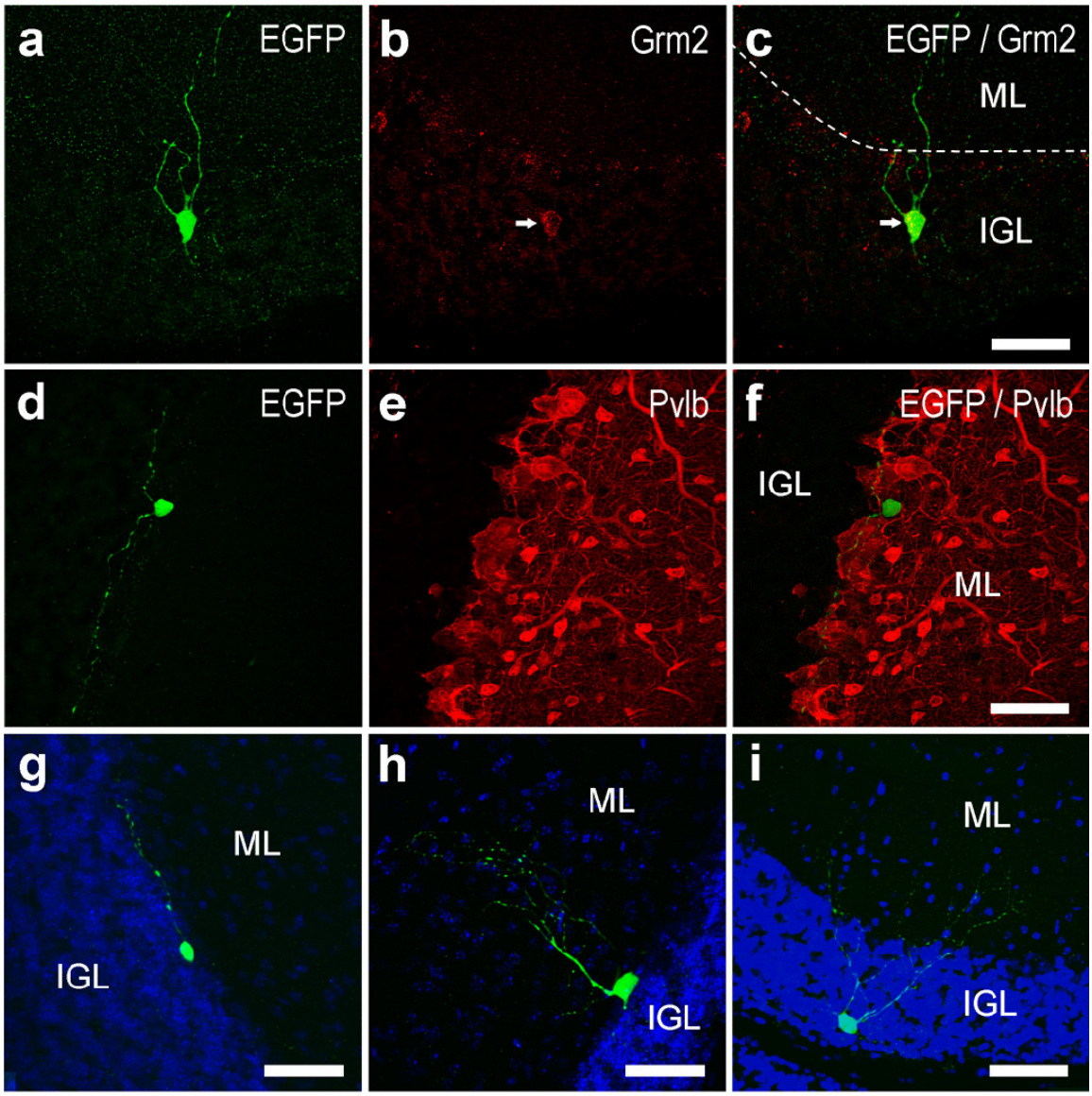

Figure 18: Confocal z-stack projection images of *Neurog1*^{CreER}*;Z/EG* mice injected with tamoxifen (TMX) at embryonic day (E) 14.5 demonstrate Neurog1 contribution to Golgi, Lugaro, and candelabrum cell lineages. **a - c:** A sagittal section of the cerebellum dual-labeled with antibodies against GFP and Grm2 confirm a Golgi cell phenotype. Arrows indicate dual-labeled cell. **d – f:** A sagittal section of the cerebellum enhanced with GFP antibody reveals the morphological details of the Lugaro cell with its processes extending laterally along the Purkinje cell layer (PCL) and counter-labeling with anti-Pvlb (red) demonstrates it is Pvlb-negative. **g - i:** Lugaro cell (g), candelabrum cell (h), and Golgi cell (i) counterstained with DAPI. Key: ML (molecular layer); IGL (internal granular layer); Scale bars = 50 µm in c,f,g, and I; 85 µm in h.

Identification of EGFP-expressing candelabrum cells proved to be difficult because there are no known cell-specific molecular markers (Schilling et al., 2008). However, we observed EGFP expression in cells with cell bodies in the PCL and dendritic processes extending upward toward the pial surface (Fig. 18h), characteristics suggesting a candelabrum cell phenotype. We were unable to further establish this phenotype with negative anti-Pvlb immunolabeling because the infrequency of EGFP expression in this cell type did not yield an EGFP-positive candelabrum-like cell within the range of anti-Pvlb antibody penetration. Therefore, conclusions at this time-point are based largely on morphological and topographical characteristics of candelabrum cells. While there are no known molecular markers available to distinguish between basket cells and stellate cells, the lower one-third of the ML is a region of the cerebellar cortex where basket cells generally reside (Sultan and Bower, 1998). Although few in number, we did identify EGFP-expressing cells in the lower regions of the ML. None of these cells exhibited the more classical characteristics of basket cells, such as processes extending into the PCL and wrapping around the cell body of multiple Purkinje cells, however, most of these cells were found to be Pvlb-positive and NeuN-negative suggesting a basket cell phenotype (Fig. 19, p. 61). Additionally, an absence of Pvlb/EGFP dual-positive cells in the upper two-thirds of the molecular layer, a region where stellate cells generally reside (Sultan and Bower, 1998), is consistent with previous reports that basket and stellate cells differentiate independently of one another, with basket cells initiating differentiation prior to the onset of stellate cell neurogenesis (Altman, 1969, Rakic, 1973).

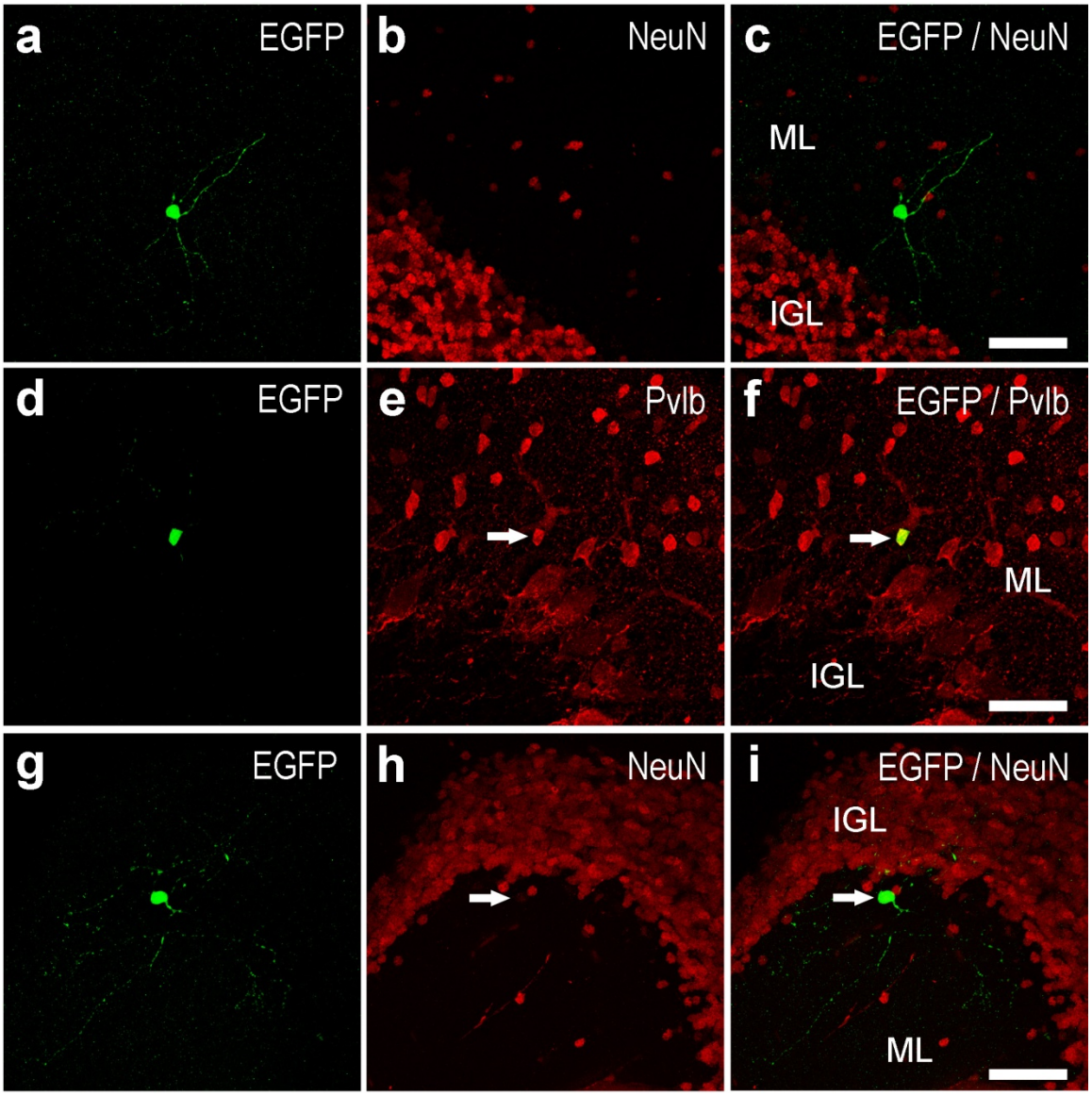

Figure 19: Confocal z-stack images of sagittal cerebellar sections from *Neurog1*^{CreER}*;Z/EG* mice injected with tamoxifen (TMX) at embryonic day (E) 14.5 demonstrate Neurog1 contribution to basket cells and an unidentified NeuN-positive cell type. **a - c:** Immunolabeling with GFP (green) and NeuN (red) reveals an EGFP-positive/NeuN-negative cell in the lower regions of the molecular layer (ML) indicating a basket cell phenotype. **d - f** Immunolabeling with GFP (green) and Pvlb (red) reveals an EGFP-positive/Pvlb-positive cell in the lower regions of the ML, an unidentified cell type. **g - i:** Immunolabeling with GFP (green) and NeuN (red) reveals an EGFP-positive/NeuN-positive cell in the lower regions of the ML, an unidentified cell type. Key: ML (molecular layer), IGL (internal granular layer); Arrows indicate position of double-positive cells. Scale bars = 50 μm.

Interestingly, confocal imaging reveals an extremely small number of EGFP-positive cells, also in the lower ML, that co-label with NeuN antiserum (Fig. 19g – i). These characteristics are indicative of an unidentified cell type previously described by Weyer et. al (2003). As revealed by EGFP-epifluorescence these cells have an intermediate sized cell body with one major dendritic process sprouting from the cell body toward the pial surface that immediately bifurcates into two major branches, each branch having a number of smaller branches. The axon appears to leave the cell body opposite the dendrites and projects into the PCL.

In summary, these results support the finding that at E14.5 Neurog1 is expressed by cerebellar progenitor cells fated to become primarily Golgi cells but also by Lugaro cells, candelabrum cells, basket cells, and an unidentified NeuN-positive cell-type. Additionally, the data suggest that Neurog1-expressing progenitors continue to contribute to the neurogenesis of a small number of neurons found in the DCN of the E14.5 cerebellum.

Neurog1-fated cells in the E16.5 cerebellum

Analysis of EGFP expression in *Neurog1^{CreER};Z/EG* adult mice that were given TMX injections at E16.5 revealed EGFP expression in neurons of the DCN, Golgi cells, Lugaro cells, candelabrum cells, basket cells, UBCs, and granule cells. EGFP continues to be expressed in Golgi cell populations at E16.5 (Fig 20 a – c, p. 62) and remains the dominant cell type of this time-point. It is also continues to be expressed in basket cells

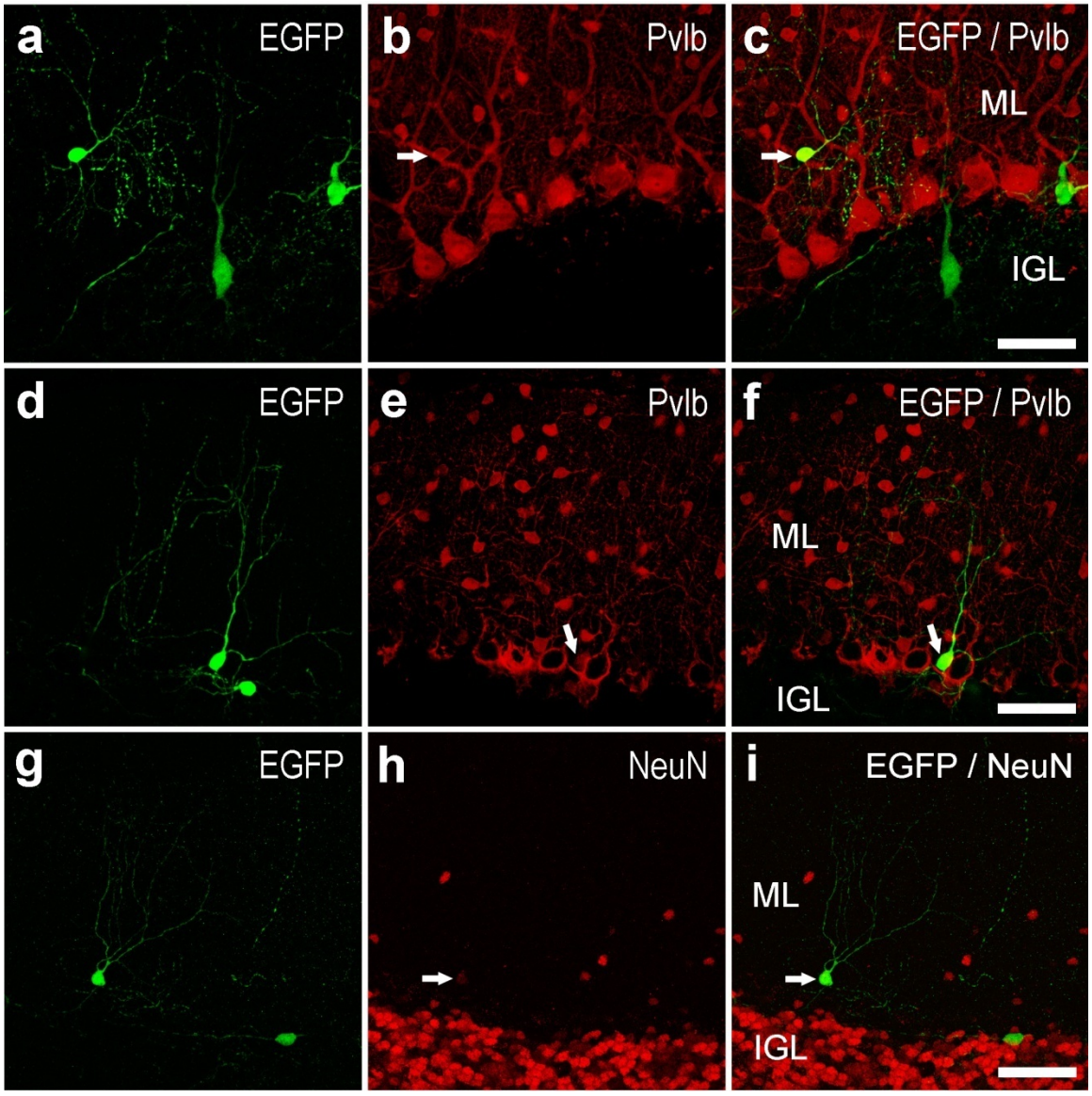

Figure 20: Confocal z-stack images of sagittal cerebellar sections from *Neurog1*^{CreER}*;Z/EG* mice injected with tamoxifen (TMX) at embryonic day (E) 16.5 demonstrate Neurog1 contribution to Golgi, basket, Lugaro, and candelabrum cells and an unidentified NeuN-positive cell type. **a - c:** Immunolabeling with GFP (green) and NeuN (red) reveals an EGFP-positive/NeuN-negative cell in the lower regions of the molecular layer (ML) indicating a basket cell phenotype. Also shown in the IGL and PCL are Golgi cells. **d - f** Immunolabeling with GFP (green) and Pvlb (red) reveals an EGFP-positive/Pvlb-positive cell in the PCL. The morphology and position of the cell suggests a candelabrum cell identity, however Pvlb-positive immunolabeling has not previously been demonstrated in candelabrum cells. Figure 20d is the projection image of 20 z-stack images, each with an optical thickness of one micrometer. Figure 20e and 20f are projection images from the same series of images shown in figure 20d but only include the eight images that show the Pvlb immunopositive candelabrum cell. **g - i:** Immunolabeling with GFP (green) and NeuN (red) reveals an EGFP-positive/NeuN-positive cell in the lower regions of the ML, an unidentified cell type. Also shown in the bottom right of the image is a Lugaro cell with its NeuN-negative cell body bordering the IGL and PCL. Key: ML (molecular layer), IGL (internal granular layer); Arrows indicate position of double-positive cells. Scale bars = 50 µm.

as shown by EGFP/Pvlb dual-positive cells in the lower ML (Fig 20a – c). EGFP-postive stellate cells remain absent in mice injected with TMX at this time-point.

Neurog1 continues to contribute to candelabrum-like cells. Figure 20d – f shows the pear-shaped cell body wedged between Purkinje cell bodies (outlined with Pvlb immunolabeling), classical characteristics of candelabrum cells (Crook et al., 2006). The cell body of this cell was found at the extreme limits of Pvlb penetration, however, analysis of a 1 μm thick confocal image from the 20 μm z-stack series reveals complete overlap of EGFP and Pvlb immunolabeling in the cell body (Fig 20d – f). These observations suggest that some candelabrum cells likely express Pvlb, an observation not previously reported. Neurog1 also contributes to an unidentified NeuN-positive cell type, which was explained previously. The cell shown in Figure 20g – i demonstrates more dramatically the morphology of the processes, with the dendritic trunk abruptly dividing into two major stems and each stem having multiple branching points. Also shown in the same image is an EGFP-positive/NeuN-negative cell, which not not only suggests that the Alexa Fluor 555 (red) signal is not due to bleed-through from Alexa Fluor 488 fluorescence emission (Fig 20g – i), but also, based on NeuN-negative immunolabeling and morphology, demonstrates the contribution of Neurgo1 to a population of Lugaro cells at this time-point. In addition to NeuN-negative immunolabeling, Calb2-immunolabeling has been reported to identify Lugaro cells. Interstingly, we report that none of the Calb2-labeled tissue slices gave any indication that Neurog1-fated Lugaro cells express calretinin (Fig 21, p. 64). This new finding suggests that Neurog1-expressing precursors are primarily restricted to Calb2-negative Lugaro cells at this time-point.

As predicted by our *Neurog1* short-term reporter gene analysis, inducible EGFP reporter gene expression revealed that Neurog1 is also expressed by UBC lineages. Using the *Neurog1*^{CreER}*;Z/EG* reporter mice we were able to confirm EGFP expression in UBCs by a combination of morphological and immunohistochemical analysis. UBCs are located in the IGL and, in general, have a thick dendritic trunk that abruptly branches into dendrioles giving it a stocky brush-like appearance. Their axons often project across the IGL and terminate in a small network of branches that appear as rosettes (Nunzi et al., 2001, Schilling et al., 2008). Enhancement of EGFP signal with anti-GFP antibody reveals morphological details that are characteristic of UBCs (Fig 21a,d, and g, p. 65). UBCs like many cell types of the cerebellum are a heterogenous population of cells. Calretinin (Calb2) is expressed by a large subpopulation of UBCs of the mouse cerebellum(Nunzi et al., 2002b). Immunolableing with anti-Calb2 antibodies revealed that the majority of EGFP-positve UBCs are Calb2-negative (Fig 21a – f). Additionally, confocal imaging of these cells immunolabled with anti-NeuN antibody demonstrates co-immunolabeling with EGFP (Fig 21g – i). This result suggests that in addition to a NeuN-negative population of UBCs, as reported by Weyer et. al (2003), the cerebellum has a subpopulation of NeuN-positive UBCs. Populations of these EGFP-expressing cells are found largely in lobule X of the cerebellum (Fig 21, p.64), which corresponds to the primary location of UBCs (Mugnaini et al., 1997, Dino et al., 1999, Englund et al., 2006). Combined with our previous experiments using short-term fate mapping, these results strongly suggest that Neurog1 is expressed by a population of cells fated to become UBCs.

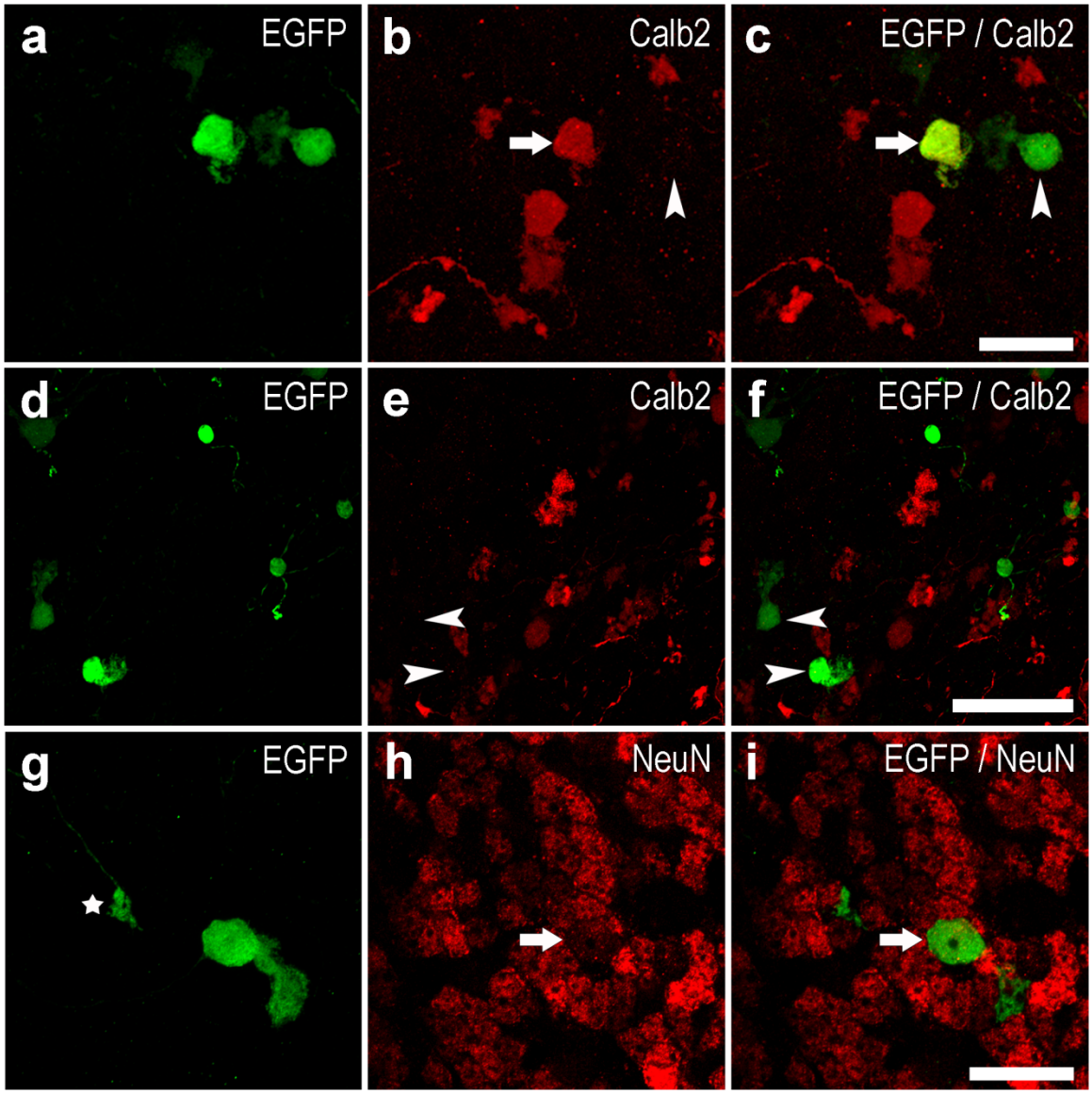

Figure 21: Confocal z-stack images of sagittal cerebellar sections from *Neurog1*^{CreER}*;Z/EG* mice injected with tamoxifen (TMX) at embryonic day (E) 16.5 demonstrate Neurog1 contribution to unipolar brush cell (UBC) lineages. **a, d, g:** Immuno-enhanced EGFP (green) images of UBCs demonstrating their classical morphology. Also in image (g) is the rosette-like terminal (star) of an axon projection likely coming from another UBC. **a – c:** Co-immunolabeling with immunoserum against calretinin (Calb2) demonstrates a mixture of EGFP-positive/Calb2-positive UBCs (arrows) and EGFP-positive/Calb2-negative UBCs (arrowheads). **d – f:** Co-immunolabeling with antiserum against Calb2 demonstrates the abundance of EGFP-positive/Calb2-negative UBCs (arrowheads). **g – h:** Image (g) is a 15 µm thick z-stack projection of a UBC. Images (h) and (i) are 2 µm thick z-stack projections taken from figure (g) showing an EGFP-positive/NeuN-positive UBC. Arrows indicate position of double-positive cell while arrowheads indicate position of EGFP-positive/Calb2-negative cells. Scale bars: c = 25 µm, f = 50 µm i = 20 µm,.

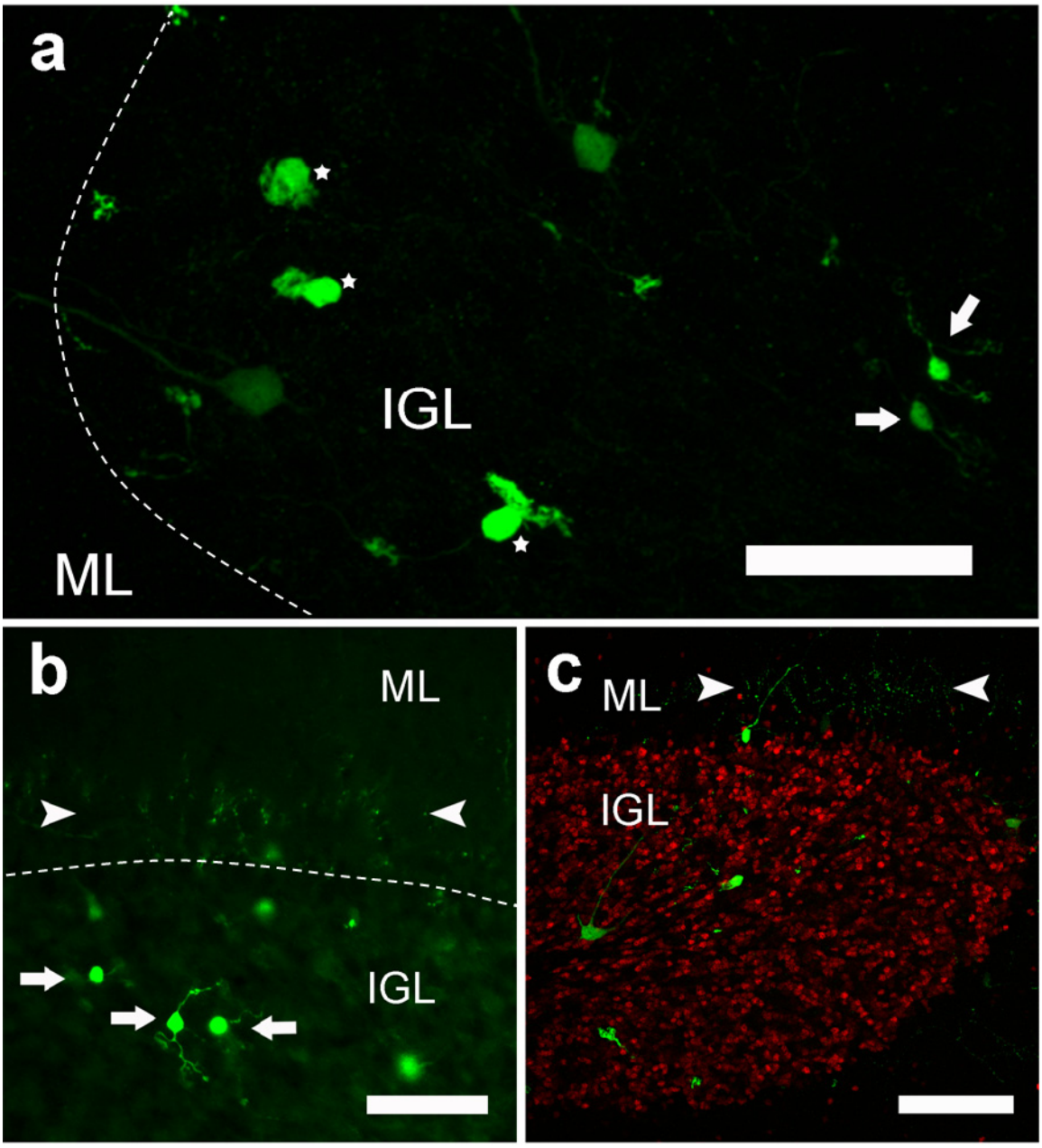

Figure 22: Sagittal images of lobule X of the cerebellum taken from sections of *Neurog1*^{CreER}*;Z/EG* mice that were injected with tamoxifen (TMX) at embryonic day (E) 16.5 demonstrate Neurog1 contribution to unipolar brush cell (UBC) and granule cell lineages. **a:** A 20 µm thick confocal z-stack projection image of immuno-enhanced EGFP (green) cells showing UBCs (stars) and granule cells (arrows) in the internal granular layer (IGL) of lobule X of the cerebellum. **b:** An image of immuno-enhanced EGFP (green) granule cells (arrows) demonstrating a region of EGFP-positive parallel fibers (between arrowheads) in the molecular layer (ML). **c:** A 20 µm thick confocal z-stack projection image of Immuno-enhanced EGFP (green) and NeuN (red) channels reveals the absence of granule cells and the persistence of parallel fibers (region between arrowheads). Scale bars = 50 in a; 25 in b; 100 in c.

Although granule cells are primarily generated during postnatal development in the mouse (Altman and Bayer, 1997) we observed that TMX injection at E16.5 labeled a minor population of EGFP epifluorescent granule cells restricted primarily to lobule X of the cerebellum. Granule cells have a few short dendritic processes extending from its small granular cell body. Granule cells that are generated earlier in development settle at lower regions of the IGL and correspondingly have axons that form parallel fibers at lower levels of the ML (Altman and Bayer, 1997, Espinosa and Luo, 2008). Our results demonstrate expression of EGFP in small granular-like cells of the IGL with dendritic processes that resemble those of granule cells (Figure 22a – b, p. 66). These EGFP-positive cells are typically found in the middle to lower regions of the IGL of lobule X. We also observed the appearance of EGFP epifluorescent "speckles" in the lower regions of the ML directly above the EGFP-expressing granule cells. This observation was restricted to the ML of lobule X and may represent the sagittal view of the parallel fibers (axonal processes) which run perpendicular to the sagittal plane. We continue to see this speckling in sections of lobule X even when there are no apparent granule cells present (Fig 22c). This observation demonstrates the great length that parallel fibers extend, which is on average 5 mm or 2.5 mm from the point of bifurcation (Harvey and Napper, 1991). Furthermore, besides a population of unidentified cells of the ML, UBCs and granule cells are the only other cell type in the cortex of the cerebellum to express the neuronal marker NeuN (Weyer and Schilling, 2003). Immunolabeling with anti-NeuN antibody reveals that these cells are indeed positive for NeuN (data not shown). These results suggest that Neurog1 contributes to a small population of early-generated granule cells primarily restricted to lobule X of the cerebellum.

In summary, at E16.5 Neurog1 contributes to basket cell lineages and a minor population of UBCs and granule cells found preferentially in lobule X. Furthermore, Neurog1 continues to contribute to Golgi and Lugaro cells of the IGL, candelabrum cells of the PCL, an unidentified population of NeuN-positive cells in the ML, and neurons of the DCN. The spatio-temporal pattern of Neurog1-fated cells corresponds to the sequential and overlapping pattern of cytogenesis in the cerebellar cortex.

Neurog1-fated cells in the P0 cerebellum

Analysis of EGFP expression in *Neurog1^{CreER};Z/EG* adult mice that were given TMX injections at P0 revealed EGFP expression in neurons of the DCN, granule cells, Golgi cells, basket cells, and stellate cells. As previously mentioned, stellate cells subsequently differentiate to basket cells. We labeled sections with anti-Pvlb antibody and identified Pvlb/EGFP dual-positive cells in both the lower and upper regions of the ML (Fig 23, p 69). We also noted that the frequency of EGFP-positive basket and stellate cells was greatest when TMX was administered at this early postnatal time-point. These results are consistent with other studies that demonstrate the emergence of stellate cells following the onset of basket cell neurogenesis and suggest that Neurog1 contribution to these cell types peaks around P0 in the developing mouse cerebellum.

We were unable to identify the presence of Pvlb-negative/EGFP-positive cells in the PCL or ML, indicating that Neurog1 no longer contributes to Lugaro and candelabrum cell types at P0. We also did not identify cells with UBC-like characteristics suggesting that Neurog1 contribution to UBC cell lineages also stops before birth. However, Neurog1 continues to be expressed by cells fated to become Golgi cells, granule cells, and neurons of the DCN.

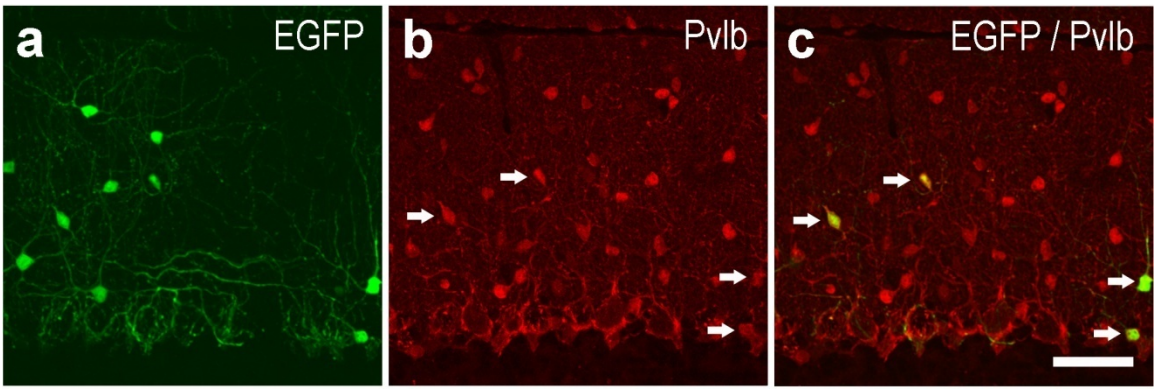

Figure 23: Sagittal section of the cerebellum taken from a *Neurog1*^{CreER}*;Z/EG* mouse that was injected with tamoxifen (TMX) at postnatal day (P) 0 demonstrates Neurog1 contribution to basket and stellate cell lineages. **a:** A 40 µm thick confocal z-stack projection image of immuno-enhanced EGFP (green) cells showing the morphological and spatial details of EGFP-expressing cells. **b – c:** Projection images taken from the series of z-stack images used to create figure a and equaling a total of 6 µm. (a) Pvlb immunolabing (red). Arrows indicate the position of dual immunopositive cells. (c) Both red (Pvlb) and green (EGFP) channels show all EGFP-positive cells are Pvlb-positive. Arrows indicate dual immunopositive cells. Scale bar = 50 µm.

Neurog1-fated cells in the P7 cerebellum

Analysis of EGFP expression in *Neurog1CreER;Z/EG* adult mice that were given TMX injections at P7 revealed EGFP expression in neurons of the DCN, granule cells, Golgi cells, basket cells, and stellate cells. Our data show a higher frequency of EGFP-positive stellate cells compared to EGFP-positive basket cells (Fig 24a – c, p. 70). We confirmed the presence of these cell types through immunolabeling with Pvlb (Fig 24d – f), as described previously. Analysis of NeuN immunolabeling does not reveal any EGFP/NeuN dual positive cells for this time-point, suggesting that Neurog1 contribution to molecular layer cell types continues to be restricted postnatally to basket and stellate cell lineages. These results are also consistent with the inside-out pattern of development of GABAergic interneurons. Additionally, we observed EGFP expression in neurons of the DCN, Golgi cells, and a very limited number of granule cells, suggesting Neurog1 continues to contribute to the neurogenesis of these cell types.

Neurog1-fated cells in the adult cerebellum

Injection of a single dose of BrdU in P40 WT mice labels a small population of cells distributed throughout the cerebellar cortex (data not shown). Therefore we speculated that analysis of EGFP expression in *Neurog1CreER;Z/EG* mice that were given TMX injections at P40 (adult) would reveal EGFP expression in a limited number of cell types. In our analysis we observed a relatively small number of EGFP-expressing cells (average of 1-2 per 40µm thick sagittal section) principally in the ML of the cerebellum (Fig 25, p. 71). The majority of these EGFP-positive cell types co-label with anti-Pvlb antibody suggesting basket and stellate cell types. These cells were found in both the PCL and ML but not the IGL or DCN and have the appearance of candelabrum,

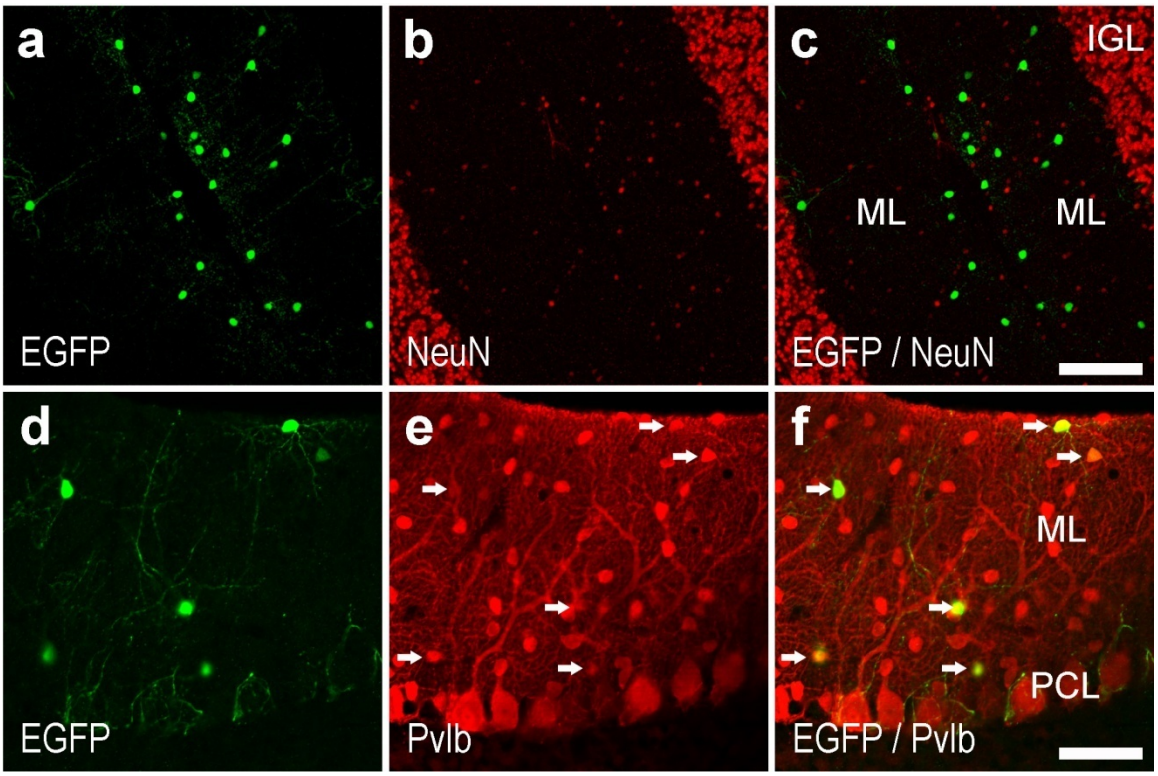

Figure 24: Sagittal sections of the cerebellum taken from a *Neurog1*^{CreER}*;Z/EG* mouse that was injected with tamoxifen (TMX) at postnatal day (P) 7 demonstrates Neurog1 contributes primarily to stellate cell lineages and secondarily to basket cell lineages. **a – c:** A confocal z-stack projection image of immuno-enhanced EGFP (green) cells showing the distribution of EGFP-expressing cells. All EGFP-positive cells are NeuN (red)-negative. **d – f:** Immuno-enhanced EGFP (green) cells and Pvlb immunolabing (red) demonstrates all EGFP-positive cells are also immune-positive for Pvlb. Arrows indicate the position of dual immunopositive cells. Scale bar = 100 μm in c; 50 μm in f.

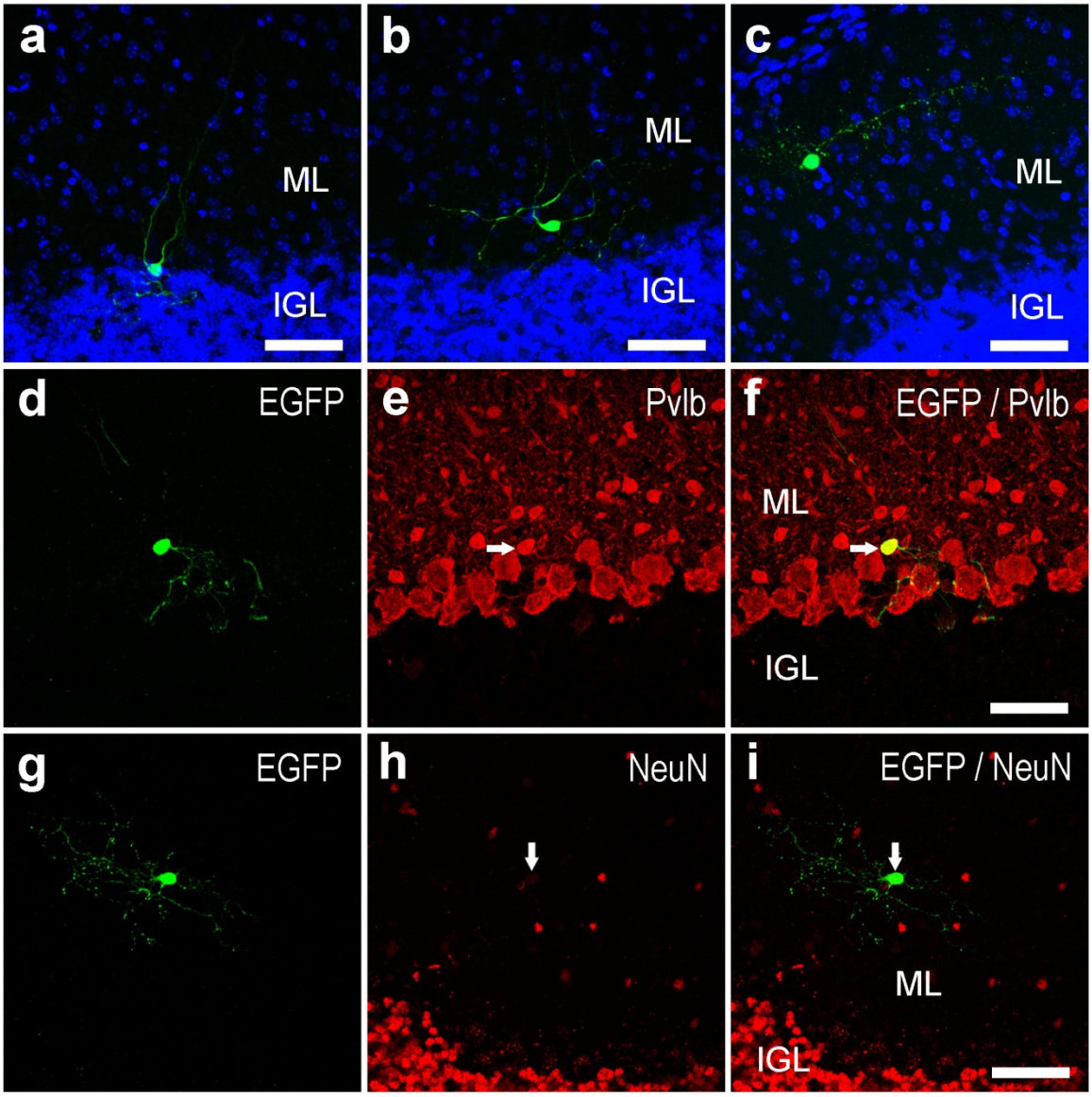

Figure 25: Confocal z-stack projection images of sagittal sections of the cerebellum taken from *Neurog1*^{CreER}*;Z/EG* mice that were injected with tamoxifen (TMX) at postnatal day (P) 40 provides evidence for Neurog1-fated neurons in the cerebellum and identifies multiple cell types that are derived from Neurog1-expressing cells. **a:** DAPI (blue) counterstaining reveals an immuno-enhanced EGFP (green) cell body between the molecular layer (ML) and internal granular layer (IGL) with two major processes extending toward the pial surface suggesting a candelarbrum cell identity. **b:** Immuno-enhanced EGFP-positive cell body is found in the lower ML with processes projecting toward the IGL suggesting a basket cell identity. **c:** Immuno-enhanced EGFP cell body found in the upper ML typical of stellate cells. **d – f:** Immuno-enhanced EGFP cell found in the lower ML co-labels with Pvlb antisera (red) confirming a basket cell identity. Arrows indicate the position of dual immunopositive cells. **g – h:** Immuno-enhanced EGFP cell found in the ML co-immunolabels with NeuN antisera confirming the cell type is an unknown cell type identified by Weyer et. al (2003). Arrows indicate the position of dual immunopositive cells. Scale bars = 50 µm.

Lugaro, basket, and stellate cells. The location of these cells is consistent with the results for cerebellar neurogenesis in the rabbit (Sotelo, 2011). Our results indicate that Neurog1 continues to contribute to inhibitory interneurons in the PCL and ML of the cerebellum throughout adulthood.

In summary, the data we have collected in our analysis of EGFP expression in *Neurog1^{CreER};Z/EG* mice suggest that Neurog1 is expressed in all GABAergic interneuron cell lineages of the cerebellar cortex. The pattern of TMX-induced EGFP expression matched the inside-out developmental sequence of GABAergic interneuron development (Schilling, 2000, Leto et al., 2006) with Golgi cells expressing EGFP upon administration of TMX at the earliest developmental time-points (E11.5 – P7), Lugaro and candelabrum cells at later developmental time-points (E14.5 – E16.5), and basket and stellate cells at the latest developmental time-points (E16.5 – P7). Additionally, EGFP expression in UBCs confirms our previous studies that indicate that Neurog1-expressing progenitors contribute to UBC lineages. Interestingly, we demonstrate that Neurog1-expressing progenitors contribute to Golgi cell lineages concurrently with Purkinje cells during early cerebellar neurogenesis and that Neurog1 expression is maintained in Golgi cell progenitors throughout embryonic development. Surprisingly, we discovered that EGFP is expressed by a limited population of granule cells and neurons of the DCN. Finally, we provide evidence for Neurog1-fated neurons in the adult cerebellum of the rodent and identify the specific cell types that are generated during adult cerebellar neurogenesis, namely, candelabrum cells, Lugaro cells, basket cells, stellate cells, and an unidentified NeuN-positive cell type of the ML.

CHAPTER 5: EFFECT OF LOSS OF FUNCTION OF NEUROGENIN1 ON CEREBELLAR DEVELOPMENT

The cellular mechanisms through which Neurogenin1 regulates neurogenesis in the cerebellum are poorly understood. A common method for determining the function of a protein is to block its synthesis and investigate the cellular and molecular changes that occur. In this study we use a mouse model that has a targeted mutation where the single exon of *Neurog1* is replaced by *neo*, a bacterial gene that confers neomycin resistance, thereby abolishing transcription and subsequent translation of the gene (Ma et al., 1998). Unfortunately, this mutation results in neonatal lethality, likely due to the loss of cranial sensory ganglia that may interfere with the suckling reflex (Ma et al., 1998). Therefore our investigation of *Neurog1* loss-of-function is limited to embryonic and P0 mice.

Our previous analyses using immunohistochemical and fate mapping strategies have revealed two major periods when Neurog1-expressing progenitors appear: an early developmental period of the cerebellum (E11 – E13) that generates primarily Purkinje cells and a later developmental period (E16 – P0) that generates primarily inhibitory interneurons. Therefore we directed our examination of Neurog1 function toward these two periods of neurogenesis.

Neurogenin1 is required to maintain the Lhx1/5-positive progenitor population

LIM-homeodomain proteins Lhx1 and Lhx5 (Lhx1/5) are expressed by postmitotic Purkinje cell progenitors during early stages (E11 – E14) of cerebellar development (Zhao et al., 2007). Accordingly, Lhx1/5 expression provides an ideal marker for quantifying early generated Purkinje cells.

Our Lhx1/5-Neurog1 immunolabeling experiments suggest that Neurog1 is expressed in cells of the VZ as they exit the cell cycle and before they transition to Lhx1/5-expressing cells (Lundell et al., 2009). We hypothesized that if Neurog1 is functionally relevant to the development of Purkinje cells we would be able to measure a significant ($p < 0.05$) difference in the Lhx1/5 population of the developing cerebellum in Neurog1 loss-of-function (KO) mice compared to wild-type (WT) mice. In a double-blinded comparative analysis of E13.5 Neurog1 WT and KO littermates we sampled approximately seven sections per animal and counted all Lhx1/5-positive cells that were found within the boundaries of the cerebellar anlage. A total of three animals were used for each group (KO and WT). This analysis revealed that loss of Neurog1 function results in a 22% reduction in Lhx1/5-positive cells ($p = 0.0276$, two-tailed t-test) (Fig 26, p. 77).

Neurogenin1 is required to maintain the Pax2-positive progenitor population

Inhibitory interneurons of the cerebellum are primarily generated during later stages of cerebellar development (Zhang and Goldman, 1996b). Pax2 is a paired box transcription factor expressed by all GABAergic interneurons of the cerebellum during late stages of cerebellar development (Maricich and Herrup, 1999). We measured the effect of Neurog1 loss-of-function on inhibitory interneuron neurogenesis of the cerebellar cortex by quantifying the Pax2-positive cell population at P0, the latest viable developmental stage in Neurog1 deficient mice. Analysis was performed using standard stereological methods as described previously. The results show that there is a significant decrease in the Pax2-positive population in the cerebellum of Neurog1 KO mice compared to WT mice ($p = 0.0497$, one-tailed t-test) (Fig 27, p.77)

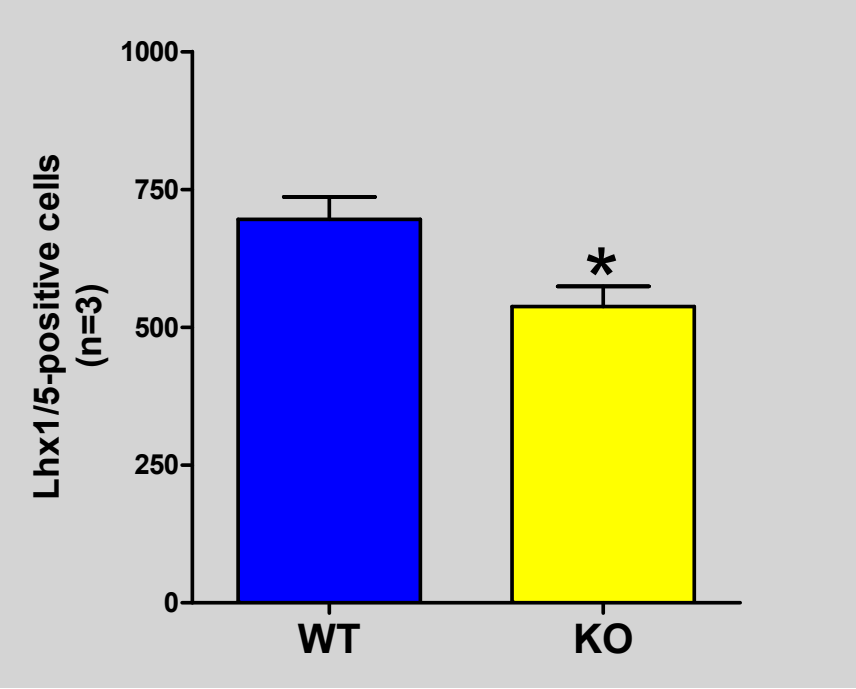

Figure 26: Lhx1/5-positive cell population is reduced in E13.5 *Neurog1 null* (KO) mice. Double-blinded quantification of sagittal sections of the cerebellum of Neurog1 WT and KO mice (n = 3) demonstrates a decrease of the Lhx1/5-positive population due to loss-of-function of Neurog1 ($p < 0.05$)

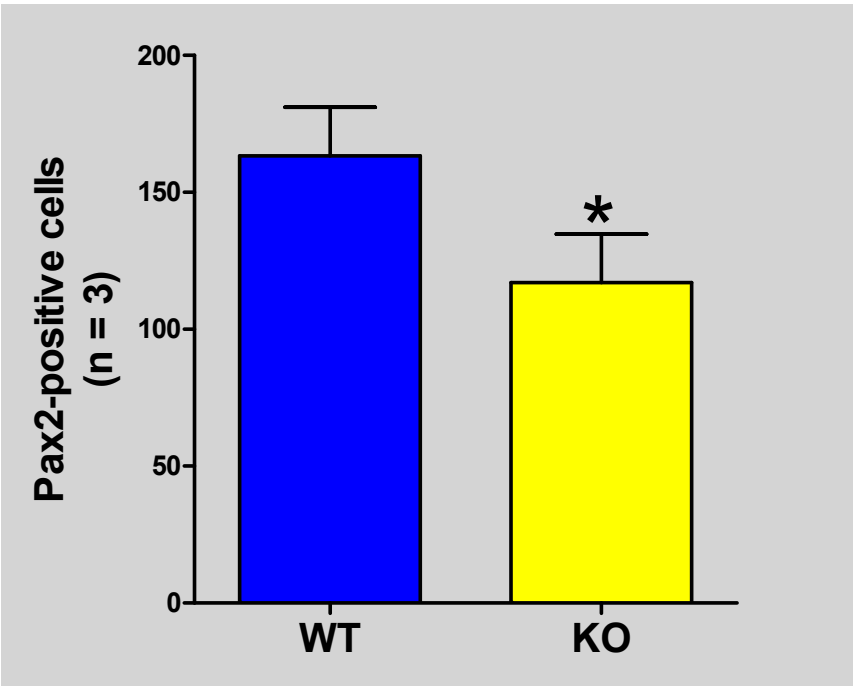

Figure 27: Pax2-positive population is reduced in P0 *Neurog1 null* (KO) mice. Stereological quantification of the cerebellum of Neurog1 WT and KO mice (n = 3) demonstrates a trending decrease of the Pax2-positive population due to loss-of-function of Neurog1. Results are taken from the raw data (total markers counted).

Examination of Cell Cycle Dynamics in the *Neurog1 null* cerebellum

Several studies have demonstrated the critical function of bHLH transcription factors in the initiation of neuronal differentiation (Casarosa et al., 1999, Fode et al., 2000, Nieto et al., 2001). Considering that Neurog1 has been shown to induce neurogenesis in progenitors (Sun et al., 2001) and is expressed prior to the expression of Lhx1/5, we hypothesized that the reduction in the Lhx1/5 population seen in Neurog1 KO mice is caused by a delay in exit from the cell cycle. Similar mechanisms may also be playing a role in the reduction of the Pax2 population. Therefore, we examined the status of three different features of development that could potentially reduce the Lhx1/5 and/or Pax2 populations: Apoptosis, cell-cycle exit, and G2/M-phase.

Apoptosis in the E12.5 and P0 cerebellum

Apoptosis or programmed cell death is a mechanism used in development to eliminate the over abundance of cells that are initially generated (Kerr et al., 1972, Martin, 2001, Cheng et al., 2011). The peak period of apoptosis in the cerebellum occurs during postnatal development (Cheng et al., 2011), however, in order to rule out apoptosis as a contributing factor in the depletion of Lhx1/5 and Pax2 populations we used cleaved caspase-3 antiserum to analyze the apoptotic status of cells at these two time-points. The caspase proteins are central components in the apoptotic pathway (Martin and Green, 1995, Alnemri et al., 1996, Zimmermann et al., 2001). The activated form of caspase-3, cleaved caspase-3, has been identified as a reliable marker of apoptosis and is widely used to determine the occurrence of programmed cell death in the

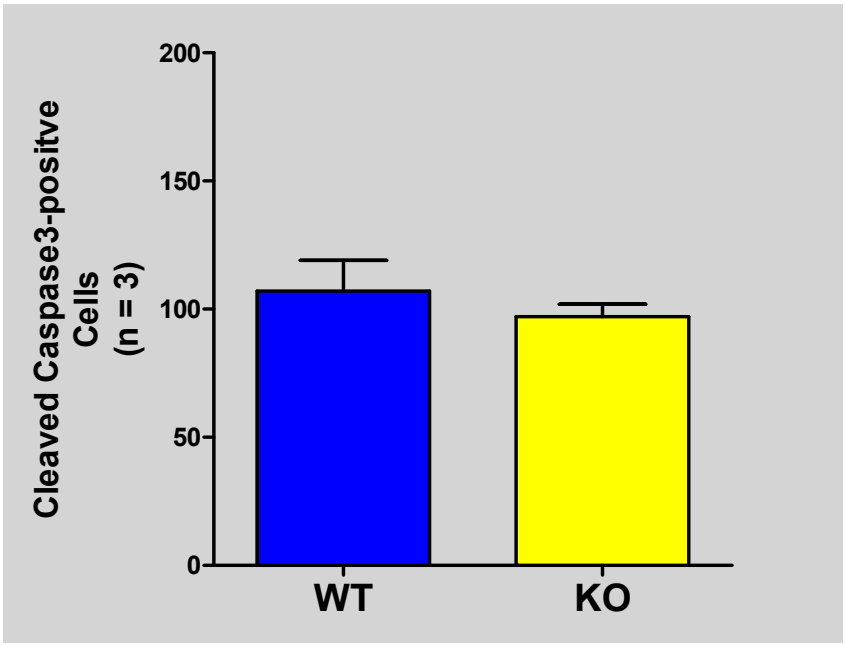

Figure 28: Measurement of apoptosis in the E12.5 cerebellum of *Neurog1 null* (KO) and wild-type (WT) mice. Quanitification of cleaved caspase-3 immunolabeled cells reveals no significant difference between WT and KO mice in E12.5

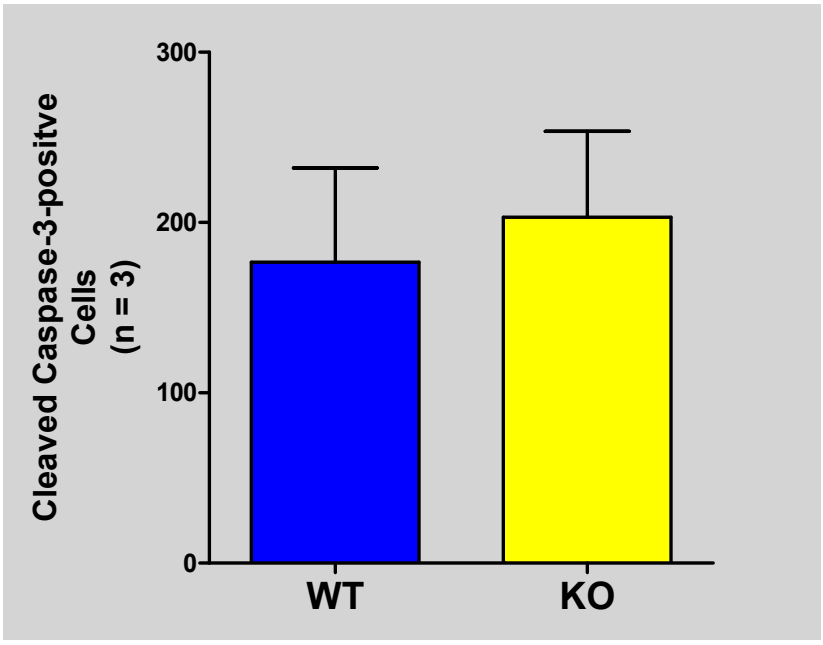

Figure 29: Measurement of apoptosis in the P0 cerebellum of *Neurog1 null* (KO) and wild-type (WT) mice. Quantification of cleaved caspase-3 immunolabeled cells reveals no significant difference between WT and KO mice in apoptosis P0 cerebellum

nervous system (Srinivasan et al., 1998, Urase et al., 1998). In a blinded comparative analysis we demonstrate that there is no significant difference in the number of cleaved caspase3-expressing cells in the E12.5 (n = 3) or P0 (n = 3) cerebellum (Fig 28 - 29, p.79).

Cell-cycle exit in the E12.5 and E18.5 cerebellum

As mentioned previously, Neurog1 is involved in inducing neuronal differentiation of progenitor cells. Changes in cell populations that result from loss of *Neurog1* may be due to its involvement in cell cycle progression. The cell cycle can be divided into four distinct phases: gap1(G1), synthesis (S), gap 2 (G2), and mitosis (M) (Quastler and Sherman, 1959). Cells may exit the cell cycle following mitosis and enter the resting (G_0) phase where they can either re-enter the cell cycle or continue on toward terminal differentiation. Ki67 is a protein that is expressed during all phases of the cell cycle but is not expressed in the resting phase following cell cycle exit (Gerdes et al., 1983, Gerdes et al., 1984). Therefore, we can determine the number of cells that exit the cell cycle during a predetermined period of time by injecting timed-pregnant mice with bromo-deoxyuridine (BrdU), a thymidine analog that is incorporated into DNA during the S-phase of the cell cycle, and subsequently co-immunolabel prepared tissue samples with antibodies against BrdU and Ki67. Cells that are BrdU-positive and Ki67-negative represent cells that were in the S-phase of the cell cycle at the time of injection and have since exited the cell cycle.

In the ventricular zone of the E12 mouse cerebrum the length of the cell cycle has been measured to be on average 10.2 hours with the G1-phase lasting an average of 3.3 hours, the S-phase 4.9 hours, and the G2/M-phase 2.0 hours (Takahashi et al., 1995).

Therefore we injected *Neurog1*$^{+/-}$ time-mated females at 12.5 days post coitum with three doses of BrdU each spaced two hours apart and harvested the embryos 6 hours following the last injection. Using a comparative analysis approach we counted the number of BrdU-positive/Ki67-negative cells in Neurog1 WT (M = 367.0, SD = 391.2) and KO (M = 258.0, SD = 182.9) mice. Statistical analysis using the student's t-test revealed no significant difference in the number of cells exiting the cell cycle at this time-point (n = 3, p = 0.5956; Fig 30, p.82).

We also investigated cell cycle exit in the cerebellum of E18.5 under the same injection and incubation schedule as the E12.5 embryos. Using stereological methods, quantification of BrdU-positive/Ki67-negative cells revealed a very low number of cells that had exited the cell cycle in both Neurog1 WT (M = 16.00, SD = 14.18) and KO (M = 7.00, SD = 7.550) mice. Statistical analysis using the student's t-test revealed no significant difference in cells exiting the cell cycle of KO mice compared to WT mice at this later developmental time-point (n = 3, p = 0.1885; Fig 31, p. 82).

In summary, although there appears to be a trend in the data with a decrease in cells that exit the cell cycle in Neurog1 KO mice, the effect is rather small and does not reach statistical significance at an "n" value of three. Therefore, the data suggest that Neurog1 has little to no effect on cell cycle exit during E12.5 or E18.5 cerebellar development.

G2/M-phase in E12.5 and E18.5 cerebellum

To further investigate the function of Neurog1 we looked at its effect within the cell cycle. As stated previously a small fraction of Neurog1-expressing cells, in both

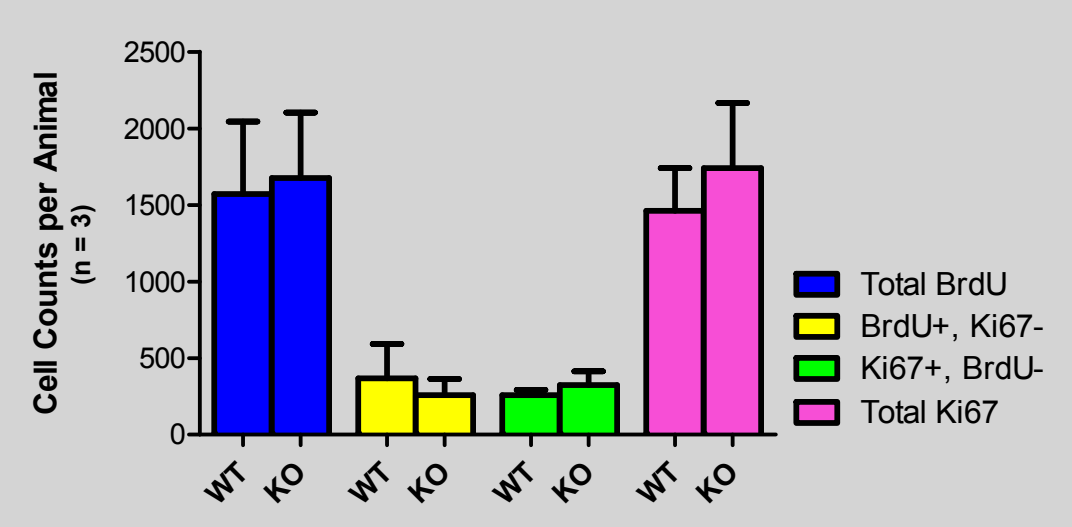

Figure 30: Analysis of cell cycle exit in embryonic day (E) 12.5 mice. Pregnant mice were injected with three doses of BrdU each spaced two hours apart at 12.5 days post coitum. Six hours later pups were harvested. Tissue was co-immunolabeled with anti-BrdU antiserum and anti-Ki67 antiserum. Cells in the cerebellum of wild-type (WT) and knockout (KO) littermates were quantified using a comparative analysis approach. Comparison of WT and *Neurog1* KO cell counts reveal no significat difference in cells exiting the cell cycle (Yellow).

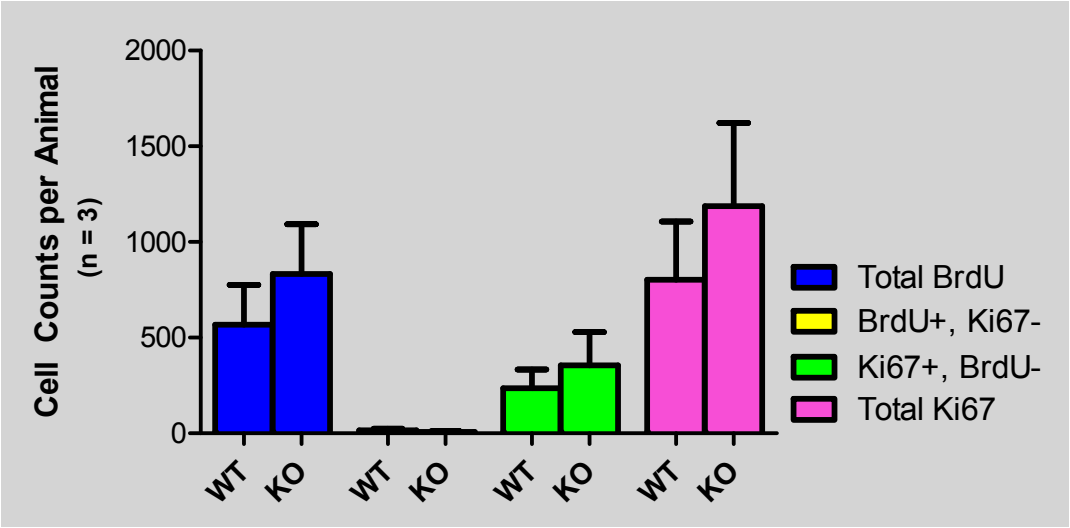

Figure 31: Analysis of cell cycle exit in embryonic day (E) 18.5 mice. Pregnant mice were injected with three doses of BrdU each spaced two hours apart at 18.5 days post coitum. Six hours later pups were harvested. Tissue was co-immunolabeled with anti-BrdU antiserum and anti-Ki67 antiserum. Cells in the cerebellum of wild-type (WT) and knockout (KO) littermates were quantified using stereological techniques. Comparison of WT and *Neurog1* KO cell counts reveal no significat difference in cells exiting the cell cycle (Yellow).

early and late stages of cerebellar development, co-immunolabel with antibody against BrdU after two-hours from a single injection, indicating that Neurog1 is likely expressed at some point between the S-phase and neuronal differentiation. We hypothesized that a more pronounced effect might be observed if we looked at the individual phases of the cell cycle, particularly at the G2/M-phase, which is the final phase of the cell cycle before cells begin to exit. We used antibodies against the phosphorylated form of histone H3 (PHH3), a protein that becomes phosphorylated during the late G2-phase and throughout chromosome condensation of the M-phase (prophase – metaphase) of the cell cycle (Hendzel et al., 1997). The S-phase is between 4 – 5 hours while the G2/M-phase is about 2 hours (Takahashi et al., 1995). Therefore, we injected *Neurog1*$^{+/-}$ timed-mated mice at 12.5 days post coitum with three doses of BrdU each spaced two hours apart and harvested the embryos three hours after the last injection. Using a comparative analysis approach we counted the number of BrdU-positive/PHH3-negative cells in Neurog1 WT and KO mice. Statistical analysis using the student's t-test revealed no significant difference in the number of cells that had exited the G2/M-phase at this time-point (n = 3, p = 0.0526 (WT: M = 593.3, SD = 183.2.2; KO: M = 503.3, SD = 157.7.9); Fig. 32, p.84).

We also investigated G2/M-phase status in E18.5 under the same injection and incubation schedule described for the E12.5 analysis. Using stereoligcal methods we quantified the BrdU-positive/PHH3-negative cells. Statistical analysis using the student's t-test revealed a significant difference in BrdU-positive/PHH3-negative cells compared to WT mice at this later developmental time-point (n = 3, p = 0.0221 (WT: M = 415.0, SD = 66.3; KO: M = 323.3, SD = 42.91); Fig. 33, p. 84).

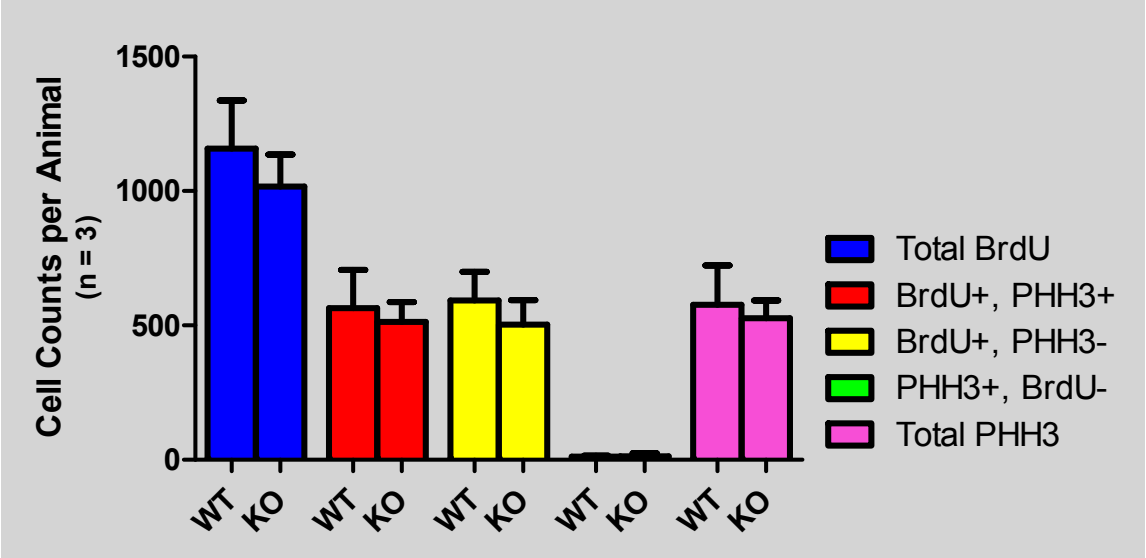

Figure 32: Comparative analysis of G2/M-phase in the E12.5 cerebellum. Pregnant mice were injected with three doses of BrdU each spaced two hours apart at 12.5 days post coitum. Three hours later pups were harvested. Tissue was co-immunolabeled with anti-BrdU antiserum and anti-PHH3 antiserum. Cells in the cerebellum of wild-type (WT) and knockout (KO) littermates were quantified using a comparative analysis approach. Comparison of WT and *Neurog1* KO cell counts reveal no significant difference in cells that are in the G2/M-phase, have exited the G2/M-phase or have not yet entered the G2/M-phase (Yellow).

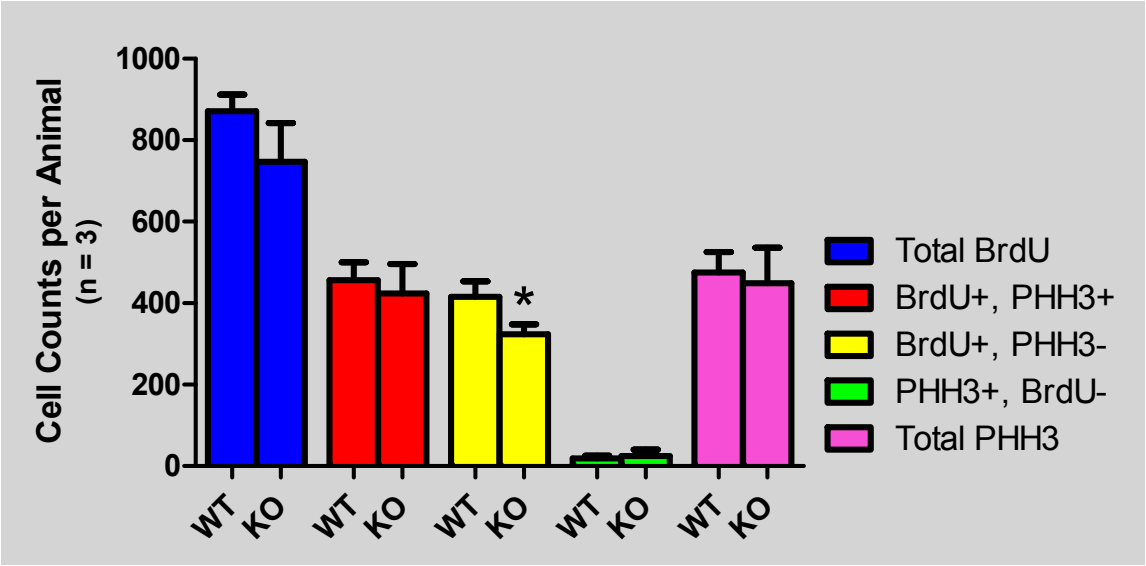

Figure 33: Stereological analysis of the G2/M-phase in the E18.5 cerebellum. Pregnant mice were injected with three doses of BrdU each spaced two hours apart at 18.5 days post coitum. Three hours later pups were harvested. Tissue was co-immunolabeled with anti-BrdU antiserum and anti-PHH3 antiserum. Cells in the cerebellum of wild-type (WT) and knockout (KO) littermates were quantified using stereological techniques. Comparison of WT and *Neurog1* KO cell counts reveal a significant difference ($p < 0.05$) in cells that have either exited the G2/M-phase or have not entered the G2/M-phase (Yellow)

To summarize the results from our analysis of Neurog1 KO mice, we observed significant decreases in the Lhx1/5-expressing and Pax2-expressing populations in the E13.5 and P0 cerebellum, respectively. These deficiencies can be attributed to loss of Neurog1 function. We did not observe any changes in apoptosis at these two time-points. We did observe a trending decrease in cells that exited the cell cycle due to loss of Neurog1 function at both E12.5 and P0 time-points, however, the results were not significant. Analysis of the G2/M-phase revealed a significant decrease in the number of cells that were BrdU-positive/PHH3-negative at E18.5. A similar trend was observed in E12.5 mice though not significant. BrdU-positive/PHH3 negative cells are either cells that have remained in the S-phase or exited the G2/M-phase from the time-point that they were labeled with BrdU, therefore a decrease in this population of cells suggests either a shortening of the S-phase and/or a lengthened G2/M-phase.

CHAPTER 6: DISCUSSION

In this study we have examined the expression and function of the pro-neural bHLH transcription factor Neurog1 in the developing mouse cerebellum and the fates of Neurog1-positive progenitors. One of the first studies to indicate a possible link between Neurog1 and cerebellar development was an investigation on expression of bHLH factors in medulloblastoma; primitive neuroectodermal tumors of the cerebellum (Rostomily et al., 1997). Several years later a group of medulloblastoma researchers identified *Neurog1* mRNA transcripts restricted to regions of the ventricular zone and overlapping regions of Ki67 expression in the E12.5 mouse cerebellum (Salsano et al., 2007). Further investigation by the same group suggested a possible role for Neurog1 in specifying GABAergic neurons of the cerebellum (Zordan et al., 2008). These studies led to our hypothesis that Neurog1 is expressed by GABAergic neurons of the cerebellum. Expression patterns and known functions of bHLH proteins led us to further hypothesize that Neurog1 it is involved in regulating exit from the cell cycle.

Our results indicate that Neurog1 is expressed in the cerebellum during embryonic and early postnatal phases of development. Spatio-temporal expression patterns, Neurog1-positive co-immunoreactivity, and cell fates are all consistent with the expression of Neurog1 in GABAergic cell lineages of the cerebellar cortex. Surprisingly, IHC and fate mapping studies suggest that Neurog1 is also expressed by a small population of granule cells and UBCs, which are excitatory interneurons of the cerebellar cortex. Neurog1 is prominently expressed during two distinct phases of GABAergic neurogenesis in the cerebellum: (1) in early specified neurons, including Purkinje cells, in the embryonic cerebellar primordium; and (2) in GABAergic interneurons as they

migrate to final cortical destinations in the cerebellum of late embryonic and early postnatal mice. In contrast to the widespread expression of Neurog1 in multiple neuronal cell types of the cerebellar cortex, we find that its expression in the DCN is restricted to a very small and diffuse population of neurons.

Quantitative analysis of cell populations following loss of *Neurog1* demonstrated depletion of early specified precursors (Purkinje cells) and late-embryonic/early-postnatal specified precursors (GABAergic interneurons) of the cerebellum, indicating Neurog1 has a functional role in the processes employed to maintain these two precursor populations. An evaluation of cell cycle progression in cerebellar progenitor cells in Neurog1-deficient mice demonstrated that Neurog1 is involved in regulating the dynamics between the S-phase and G2/M-phase of the cell cycle.

Neurog1 is expressed in Purkinje cell lineages

In their recent publication Zordan et. al (2008) reported three key results regarding the expression of *Neurog1* in the E12.5 cerebellum: One, it is expressed caudally within larger Ascl1, Ptf1a, and Neurog2 expression territories; two, it is distinct from Pax2 ISH signal; and three, it overlaps the Lhx1/5 expression territory (Zordan et al., 2008). Similar to Zordan et al., we detected Neurog1 expression in two distinct territories in the E13.5 cerebellar primordium: a rostral, isthmic territory that is continuous with Neurog1-immunoreactivity in the ventricular neuroepithelium of the pons; and a non-continuous territory in the caudal VZ and IMZ of the cerebellar anlage proper that is rostral of the RL. Although the exact topographical cell fate of caudal VZ progenitors in the Neurog1 territory has not been defined, this pattern is consistent with Neurog1 expression in newly generated Purkinje cells (Altman and Bayer, 1997).

In support of this hypothesis, Neurog1 ISH signal is reported to overlap with Lhx1/5 ISH territory (Zordan et al., 2008). Lhx1/5 is restricted to expression in post-mitotic Purkinje cells and is required for the normal development of these neurons (Zhao et al., 2007). Our analysis of *Neurog1 null* mice reveals that KO of Neurog1 results in a depletion of the Lhx1/5-expressing cells at E12.5, suggesting that Neurog1 is expressed by precursors for Purkinje cell lineages and is required for their normal transition to post-mitotic/Lhx1/5-expressing Purkinje cell neurons

Interestingly, although anti-Lhx1/5 immunolabeling reveals topographically similar immunoreactive territories in the isthmus and cerebellar anlage at E13.5, high magnification imaging using confocal microscopy reveals that anti-Neurog1 and anti-Lhx1/5 immunosignals are mutally exclusive suggesting that Lhx1/5 is expressed following Neurog1 expression. Our interpretation that this pattern reflected sequential Neurog1 and Lhx1/5 expression in Purkinje cells (rather than Neurog1 and Lhx1/5 expression in distinct cell lineages) was supported by Cre-flox fate mapping studies (Cre and CreER) that confirmed *Neurog1* expression in Purkinje cell lineages (Kim et al., 2011). Furthermore computational genome-wide predictions of Neurogenin/NeuroD target genes identifies *Lhx5* as one of 347 putative direct E-box targets of the bHLH factors (Seo et al., 2007), which is consistent with the hypothesis that the LIM homeobox gene is a downstream target of Neurog1 regulated bHLH factor cascades. Although targeted inactivation of *Lhx5* and *Lhx1* results in severe restrictions in Purkinje cell differentiation and survival, targeting of either gene alone does not affect cerebellar development (Zhao et al., 2007). It is therefore tempting to speculate that the functional

redundancy of *Lhx1* and *Lhx5* observed by these authors represents compensatory Lhx1 activity following the disruption of normal Lhx5-mediated events initiated by Neurog1.

Neurog1 is expressed in GABAergic interneuron cell lineages of the cortex

In agreement with ISH studies showing declining Neurog1 expression from E12.5 to E13.5 (Zordan et al., 2008), we observed a reduction in Neurog1-immunolabeling in E14 WT mice. Lower levels of Neurog1-immunoreactivity in the VZ and IMZ were maintained throughout the remaining period of embryonic development in the cerebellum in WT mice. In support of this dynamic pattern of Neurog1 expression our results, as well as results from Kim et. al (2011), have shown that expression of Neurog1 in Purkinje cell precursors peaks at E11.5 in *Neurog1CreER;Z/EG* mice (Kim et al., 2011). Additionally, we also saw a decrease in strength of EGFP signal in *Neurog1CreER;Z/EG* mice injected at E14 and E16. This latter period of embryonic development marks the first phase of inhibitory interneuron neurogenesis in the cerebellar VZ with the production of DCN, Golgi and Lugaro cell interneurons (Carletti and Rossi, 2008). Accordingly, a majority of these Neurog1-expressing cells that co-expressed Ptf1a, a bHLH transcription factor necessary for the development of all GABAergic cerebellar neurons, are absent from the RL and EGL, and do not co-express markers of cerebellar glutamatergic cells.

As the cortex of the cerebellum expands and develops into its characteristic laminar and lobulated postnatal form, clustered Neurog1 immunoreactive cells were detected in the nascent WM tracts. This pattern of Neurog1 expression suggests specific expression of the bHLH factor in migrating inhibitory interneurons in the postnatal cerebellum. Retroviral lineage-tracing has revealed that dividing WM precursor cells generate the full spectrum of GABAergic interneurons in the cerebellar cortex (Zhang

and Goldman, 1996b). Consistent with these observations we also observed EGFP expression in all GABAergic interneuron cell types of the cerebellar cortex in *Neurog1CreER;Z/EG* mice.

Neurog1 is expressed in glutamatergic interneuron cell lineages of the cortex

In the cerebral cortex Neurog1 is predominantly expressed by precursors destined to glutamateric cell fates (Kim et al., 2011). The few studies that have looked at expression of Neurog1 in the cerebellum have demonstrated that, unlike its expression in the cerebral cortex, Neurog1 is expressed principally in GABAergic cell lineages (Zordan et al., 2008, Kim et al., 2011). Our short-term fate mapping analysis showed that a small population of Neurog1-fated cells co-labeled with Tbr2, a marker for glutamatergic interneurons (Englund et al., 2006, Fink et al., 2006). Further examination of Neurog1 cell fates in *Neurog1^{CreER};Z/EG* mice revealed Neurog1 expression in UBC and granule cell lineages. Interestingly, Neurog1 has been identified in an invasive form of medulloblastoma (Rostomily et al., 1997, Salsano et al., 2007), however, despite evidence that the majority of these tumors originate from granule cell precursors (Salsano et al., 2004) there have been no studies to date that support expression of Neurog1 in glutamatergic cell linages of the cerebellum. Thus, our observations are the first to indicate a role for Neurogenin1 in glutamatergic neurogenesis of the cerebellum and provides new avenues for medulloblastoma research.

UBCs are born during late embryonic development (Englund et al., 2006); they are found primarily in lobules IX and X and the majority of them co-label with the calcium binding protein calretinin (Nunzi et al., 2002a). Expression of Neurog1 in UBC precursors was supported by the temporal and spatial appearance of EGFP reporter

following TMX administration. Although a few Neurog1-fated UBCs co-labeled with calretinin we observed that they were primarily calretinin-immunonegative. Therefore, in the latter case the morphological and histological features of these UBCs were used as an exclusive indicator of cell type. Interestingly, we also observed that these neurons expressed low levels of NeuN. In a detailed analysis of NeuN expression in the cerebellum it was shown that NeuN expression levels are dependent upon the physiological status of the cell (Weyer and Schilling, 2003). The absence of calretinin combined with low-level expression of NeuN in these UBC subtypes suggests they are physiologically distinct from calretinin-positive/NeuN negative UBCs. In support of this theory one of the well documented functions of calretinin is modulation of neuronal excitability (Schiffmann et al., 1999, Camp and Wijesinghe, 2009). Although the report by Weyer et al (2003) also suggested that NeuN expression in the cerebellum is restricted to granule cells and an uncharacterized cell type of the ML (Weyer and Schilling, 2003), the lack of other markers for calretinin-negative/NeuN-positive UBCs might explain why other NeuN-positve cell types were not identified in this study. Our analysis extends these observations to include calretinin-negative UBCs as a third population of NeuN expressing neurons of the cerebellar cortex. These results are the first to suggest that Neurog1 is expressed by glutamatergic interneuron precursors of the cerebellum.

Neurog1 is expressed in adult-generated neurons of the cerebellar cortex

Neurogenesis in the cerebellum is generally considered to cease during the third postnatal week and only one study has reported active mitosis and neurogenesis in the adult cerebellum of the mammalian brain (Ponti et al., 2008). Furthermore, previous studies of Neurog1 expression report that it is either not expressed or not expressed at

sufficient levels in the adult brain to be detected by northern blot analysis (Ma et al., 1996, McCormick et al., 1996). However, in our analysis of inducible reporter mice we found that Neurog1 continues to contribute to neuronal populations in the adult cerebellum. Furthermore, these Cre reporter-expressing, adult-generated neurons were confined to regions of the ML and PCL and appear to be exclusively GABAergic. These observations correspond to the report by Ponti et.al (2008) where adult generated neurons expressed Pax2, a marker for GABAergic interneurons, and were also restricted to the ML and PCL (Ponti et al., 2008).

Neurog1 is expressed by neurons of the deep cerebellar nucleus

Several reports have suggested that Neurog1 expression in the cerebellum is restricted to neurons fated to reside in the cerebellar cortex. Moreover, analysis of Neurog1 expression using the same *Neurog1*^{CreER} transgenic mouse with a different reporter system (*R26R*^{LacZ}), which expresses β-galactosidase in response to Cre activity, also failed to identify Neurog1 expression in the DCN. However, contrary to these reports we demonstrated that Neurog1 is expressed in neurons destined to the DCN, albeit very small in number. According to our data Neurog1 was expressed by DCN precursors at all time-points investigated except for the adult. This is supported by other reports that have shown neurons of the DCN are specified throughout all phases of cerebellar development until P15 of the mouse (Maricich and Herrup, 1999, Fink et al., 2006).

The DCN contains glutamatergic projection neurons and GABAergic interneurons (Miale and Sidman, 1961, Maricich and Herrup, 1999). In view of our recent findings suggesting multiple Neurog1-specified cell fates, it is feasible that glutamatergic and/or

GABAergic neurons of the DCN are Neurog1-fated. Although there was no indication from our earlier studies of Neurog1 expression in either of these cell types, it is important to note that just as glutamatergic and GABAergic precursors of the cerebellar cortex express the transcription factors Pax6 and Pax2, respectively, so do those of the DCN (Maricich and Herrup, 1999, Fink et al., 2006). Furthermore, Tbr2 is expressed by all UBCs and neurons of the DCN (Englund et al., 2006, Fink et al., 2006). Therefore, it is possible that these cells were difficult to identify due to similarities in the spatial and temporal expression of their fate-specific markers and the relatively low number of Neurog1-fated DCN neurons combined with the short-term expression of the EGFP reporter.

Differential transgene expression in the cerebellum of *Neurog1*$^{EGFP/+}$, *Neurog1*$^{Cre/+}$, and, *Neurog1*$^{CreER/+}$ BAC transgenic mice

Our Neurog1 fate mapping studies confirm Neurog1 precursors contribute to Purkinje cells (*Neurog1*^{Cre}-fated) and inhibitory interneuron (*Neurog1*$^{EGFP/+}$-fated) cell lineages of the cerebellar cortex. Curiously, *Neurog1*$^{EGFP/+}$ and *Neurog1*^{Cre} fate mapping marked mutually exclusive cell lineages in the cerebellum, despite the fact that both lines were generated using modified BAC BAC RPCI-23-457E22. Although a lack of co-expression of Purkinje cell markers with EGFP in *Neurog1*$^{EGFP/+}$mice can be explained by downregulation of the reporter gene in committed Purkinje cells, the absence of reporter gene expression in *Neurog1*$^{Cre/+}$; Z/EG inhibitory interneurons was less expected. Our evidence from β-galactosidase staining indicates low level Z/EG expression in non-Purkinje cell cerebellar lineages is one possible explanation. However, *Neurog1*$^{Cre/+}$;Rosa26LacZ mice similarly mark only Purkinje cell lineages in the cerebellum (J.E. Johnson personal communication), casting doubt that low level Z/EG

reporter gene expression is a major contributory factor. Interestingly our studies using inducible *Neurog1*^{CreER};*Z/EG* mice marks excitatory and inhibitory interneurons in addition to Purkinje cells. *Neurog1*^{CreER};*Z/EG* mice were engineered using the same BAC BAC RPCI-23-457E22 vector adapted to generate *Neurog1*$^{Cre/+}$ mice. More extensive fate mapping in the inducible (*Neurog1*^{CreER}) compared to the consititutive (*Neurog1*^{Cre}) Cre recombinase line is unexpected as Cre penetrance is usually reduced by the addition of the ER element. However, it would appear that lower Cre penetrance in the *Neurog1*^{Cre} line accounts for the lack of Purkinje cell fate-mapping. In view of the fact both Cre lines were generated from the same BAC, the most likely explanation for the different fate-maps is lower BAC copy number in the *Neurog1*^{Cre} compared to *Neurog1*^{CreER} mice. This could be confirmed by Southern blot or qPCR and is a reminder of the difficulties in attempting to determine the full repertoire of precursor cell fates using Cre-flox systems.

Neurog1 inducible fate-mapping introduces a novel view of the temporal specification pattern of cerebellar neurogenesis

Although our fate-mapping studies are largely supported by the current model for the sequence of neurogenesis in the cerebellum (reviewed by Carletti, 2008) there are several differences that should be highlighted. The first notable difference is the timing of onset of Neurog1 expression in Golgi cells relative to the disappearance of Neurog1 expression in Purkinje cell lineages. Birthdating studies have demonstrated that all cortical interneurons are born following the birth of all Purkinje cells (Miale and Sidman, 1961, Altman and Bayer, 1997). However, our results indicated that the onset of Golgi cell neurogenesis overlaps with Purkinje cell neurogenesis. This relationship suggests that Purkinje and Golgi cells may derive from a common progenitor from E11.5 – E13.5, the time frame of Purkinje cell neurogenesis. Interestingly, Corl2, a transcriptional co-

repressor, is expressed exclusively by Purkinje cells immediately following cell cycle exit, similar to the expression of Neurog1 (Minaki et al., 2008). However, unlike Neurog1 its expression is not transient and persists in the adult cerebellum indicating that Corl2 may be required for divergence of these cells types if they are indeed from a common progenitor. Unfortunately, our specultations cannot be substantiated without a better understanding of the relationship between Corl2 and Neurog1.

Second, basket and stellate precursors express Neurog1 earlier than expected. Birthdating studies have demonstrated that basket and stellate cells are born postnatally and sequentially to one another with basket cells being the first to appear followed by stellate cells (Miale and Sidman, 1961, Yamanaka et al., 2004). Although our results were consistent with the sequence of basket and stellate cell neurogenesis we observed that basket cell neurogenesis is initiated as early as E16.5. Although E17.5 – E19.5 time-points were not investigated it is reasonable to suspect that Neurog1-fated stellate cells may appear at some point during these late embryonic time points.

There are a few assumptions that should be considered in relation to this new model of the temporal sequence of cerebellar neurogenesis. Perhaps most significant is that it is our perspective is biased to the timing of *Neurog1* activation. Our analyses of BrdU incorporation and Neurog1 expression have indicated that activation of Neurog1 and exit from the cell cycle are closely linked. The difference in time from beginning of the S-phase, the period of the cell cycle when BrdU is incorporated into the cell, to cell cycle exit is approxiamately seven hours (Takahashi et al., 1995). This small difference in time between BrdU-labeling and Neurog1 expression supports the assumption that reported birthdates of cerebellar cell types should closely match that of *Neurog1*

activation. In support of this we found that fate mapping of Neurog1-expression in Purkinje cells as well as several other cell types of the cerebellum correspond precisely with their birthdates as reported in the literature. Therefore, we can assume that the timing of the reporter system is accurate. A likely explanation for the discrepancy between our time sequence of cerebellar development and what has been reported is simply due to the numbers of cells that are generated. Our reporting system is more sensitive to small populations of cells because EGFP signal accumulated over time compared to BrdU signal which is diminished during subsequent cell divisions. Furthermore, as Neurog1 is expressed in cells as they exit their final mitotic division and transition to neuronal differentiation, it is a more precise birthdating approach for neurogenesis than BrdU which is incorporated in all precursor cells in the S-phase of the cell cycle.

Neurog1 is expressed by an uncharacterized cell type of the molecular layer

We have identified that a subpopulation of uncharacterized, NeuN-expressing neurons of the ML are Neurog1-fated. NeuN is a nuclear protein that is expressed by a very limited number of cerebellar neuronal cell types, and its expression levels are dependent upon the physiological status of the cell (Weyer and Schilling, 2003). Consistent with what is known about NeuN expression in the cerebellum we observed that these Neurog1-fated cells predominantly, if not exclusively, expressed low levels of NeuN, indicating that Neurog1 is expressed by a physiologically distinct class of NeuN-expressing cells in the ML. These cells were first detected in the E11.5 cerebellum and through E16.5, they reappeared during adult neurogenesis. Interesting they do not appear to follow the inside out pattern of development that characterizes the inhibitory

interneurons of the cerebellar cortex. Unfortunately, despite the relative abundance of NeuN-positve cells in the ML little is known concerning their neurochemical phenotype. Our results are the first to demonstrate the temporal sequence of neurogenesis of these cell types and will provide a useful tool for future characterization.

Neurog1 maintains pools of GABAergic cortical precursors of the cerebellar cortex through mechanisms that regulate dynamics between S-phase and G2/M-phases of the cell cycle

Early embryonic development

The distribution of Neurog1-positive cells in the E13.5 VZ and IMZ suggests that Neurog1 is expressed in Purkinje cells as they transition from proliferative precursors to committed Purkinje cells. In line with this, BrdU pulse-labeling experiments revealed that the majority of Neurog1-positive cells were BrdU-negative while Neurog1 was detected in a small population of BrdU-positive cells in dorsal rather than ventral regions of the caudal cerebellum. This suggests that Neurog1 is expressed in only a minor fraction of cycling progenitor cells and that these progenitors are likely undergoing late cell divisions. Although there is evidence of dynamic bHLH expression in cycling neocortical progenitors (Britz et al., 2006) that could also account for the low frequency of Neurog1/BrdU dual positive cells in the cerebellar VZ, the relatively high proportion of Neurog1-positive/BrdU-negative cells in dorsal differentiation regions (IMZ) favors our interpretation that the bHLH factor is expressed in newly-committed Purkinje cells as they move away from the VZ.

In our cumulative BrdU-labeling analysis using Ki67 as a co-marker we demonstrated that loss of function of Neurog1 did not result in any significant changes in cell cycle dynamics at E12.5. Though no significant differences between WT and KO

mice were observed it should be noted that there was a trending decrease in cell cycle exit with a corresponding increase in total Ki67-positive cells in *Neurog1 null* mice. Additionally, further analysis of the cell cycle demonstrated a decrease in BrdU-positive/PHH3-negative cells. This shift could be interpreted as either a lengthening of the S-phase or a shortening of the G2/M-phase since both instances would produce a decrease in BrdU-positive/PHH3-negative population. However, shortening of the G2/M-phase does not fit other observations that indicated a delay in cell cycle exit as a result of loss of Neurog1 function. Therefore, it is more likely that loss of Neurog1 results in delayed entry into the G2/M-phase (prolonged S-phase).

Late embryonic/early postnatal development

The use of Pax2 expression to track GABAergic interneuron maturation in the cerebellum confirms the presence of mitotically active and post-mitotic precursors in the WM (Maricich and Herrup, 1999, Weisheit et al., 2006). Consistent with this, BrdU pulse-labeling revealed that a small fraction of Neurog1-expressing cells proliferate in the WM of young postnatal mice. We observed Neurog1 expression in cell clusters along the entire WM lengths, with concentrated immunoreactivity in cells exiting the WM for final cortical destinations. Although Neurog1 expression was detected in cells in the surrounding IGL, these cells were primarily located in regions bordering the WM suggesting Neurog1 is downregulated in cells as they penetrate the cortex. Overall, the pattern of Neurog1 immunolabeling indicates the bHLH factor is transiently and dynamically expressed in precursors as they migrate in the WM and rapidly downregulated in cells as they invade the surrounding cortex.

In the neocortex, Neurog2-mediated cortical neurogenesis has been shown to involve the initiation of migration through activation of the small GTP-binding protein Rnd2 (Heng et al., 2008). Our data indicates the possibility of analogous Neurog1 function in cerebellar interneuron migration (via the activation of as yet unknown targets). The fact that we detect Neurog1 expression in relatively low numbers of cells in the WM argues against the maintenance of Neurog1 expression throughout migratory stages. Therefore, it would appear that Neurog1 is transiently expressed in precursors transitioning to interneuron cell fates. Furthermore, genes involved in axon guidance and migration are turned on and/or upregulated in the cerebellar primordium of *Neurog1 null* mice (Dalgard et al., 2011).

In our cumulative BrdU-labeling analysis of later embryonic/early postnatal periods we saw changes in BrdU/Ki67 labeling and BrdU/PHH3 labeling that paralleled those observed in our early embryonic analysis. We reported a significant reduction in BrdU-positive/PHH3-negative cells. The difference in statistical significance between the two time-points likely represents the wide-spread expression of Neurog1 among numerous cell types in later stages of cerebellar development compared to early time-points where Neurog1 is primarily expressed by one cell type lineage, Purkinje cells.

It should be noted that we saw little to no difference in cell cycle exit between WT and KO mice. This is likely reflective of the fact that over the span of development the cell cycle length increases due to a continuously increasing length of the G1-phase. For example, in the VZ of the E11 mouse cerebral cortex the G1 phase lasts on average 3.2 hours for a total average length of 8.1 hours; comparatively, in the E16 VZ the G1 phase lasts approximately 12.4 hours for a total of 18.4 hours (Takahashi et al., 1995).

Therefore, in view of the differences in cell cycle length at older ages of development it is necessary to repeat the experiment with a longer time-period between final BrdU injection and harvesting of tissue.

Neurogenesis in the postnatal cerebellum is ongoing, in fact Neurog1 contributes significantly to basket and stellate cell populations following birth. A major limitation to our study of Neurog1 function in the cerebellum is that conventional knockout of *Neurog1* is postnatally lethal (Ma et al., 1998). Therefore to circumvent this problem we plan to use a floxed Neurog1 conditional KO mouse model to limit Neurog1 deletion to the postnatal cerebellum.

Concluding remarks

In this study, we reveal the expression of the pro-neural bHLH transcription factor Neurogenin1 (Neurog1) in the developing cerebellum of embryonic and postnatal mice. We show that Neurog1 is expressed in proliferating precursors as they transition primarily to committed GABAergic cell lineages of the cerebellar cortex. We also demonstrate that Neurog1 is expressed in glutamatergic cell lineages. Many studies of bHLH factors have highlighted the combinatorial nature of these proteins in their specification of neuronal subtypes. Our demonstration of the expression of Neurog1 in GABAergic as well as glutamatergic cell lineages within the cerebellum underscores the complexity of the transcriptional codes employed in the execution of neuronal determination and differentiation.

Although our studies have greatly expanded our knowledge of the diverse cell types specified by Neurog1, its anomalous expression has been implicated in disease

processes of the cerebellum (Salsano et al., 2007, Ho et al., 2008). Therefore, continued investigation to understand its function in postnatal and adult neurogenesis is essential.

REFERENCES

Alnemri ES, Livingston DJ, Nicholson DW, Salvesen G, Thornberry NA, Wong WW, Yuan J (1996) Human ICE/CED-3 protease nomenclature. Cell 87:171.

Altman J (1969) Autoradiographic and histological studies of postnatal neurogenesis. 3. Dating the time of production and onset of differentiation of cerebellar microneurons in rats. J Comp Neurol 136:269-293.

Altman J, Bayer SA (1997) Development of the cerebellar system in relation to its evolution, structure, and function. Boca Raton, FL: CRC Press.

Amos B (2000) Lessons from the history of light microscopy. Nat Cell Biol 2:E151-152.

Aoki E, Semba R, Kashiwamata S (1986) New candidates for GABAergic neurons in the rat cerebellum: an immunocytochemical study with anti-GABA antibody. Neurosci Lett 68:267-271.

Bastianelli E (2003) Distribution of calcium-binding proteins in the cerebellum. Cerebellum 2:242-262.

Ben-Arie N, Bellen HJ, Armstrong DL, McCall AE, Gordadze PR, Guo Q, Matzuk MM, Zoghbi HY (1997) Math1 is essential for genesis of cerebellar granule neurons. Nature 390:169-172.

Bertrand N, Castro DS, Guillemot F (2002) Proneural genes and the specification of neural cell types. Nat Rev Neurosci 3:517-530.

Britz O, Mattar P, Nguyen L, Langevin LM, Zimmer C, Alam S, Guillemot F, Schuurmans C (2006) A role for proneural genes in the maturation of cortical progenitor cells. Cereb Cortex 16 Suppl 1:i138-151.

Bullock TH, Bennett MV, Johnston D, Josephson R, Marder E, Fields RD (2005) Neuroscience. The neuron doctrine, redux. Science 310:791-793.

Camp AJ, Wijesinghe R (2009) Calretinin: modulator of neuronal excitability. Int J Biochem Cell Biol 41:2118-2121.

Carletti B, Rossi F (2008) Neurogenesis in the cerebellum. Neuroscientist 14:91-100.

Casarosa S, Fode C, Guillemot F (1999) Mash1 regulates neurogenesis in the ventral telencephalon. Development 126:525-534.

Cheng XS, Li MS, Du J, Jiang QY, Wang L, Yan SY, Yu DM, Deng JB (2011) Neuronal apoptosis in the developing cerebellum. Anat Histol Embryol 40:21-27.

Crook J, Hendrickson A, Robinson FR (2006) Co-localization of glycine and gaba immunoreactivity in interneurons in Macaca monkey cerebellar cortex. Neuroscience 141:1951-1959.

Dalgard CL, Zhou Q, Lundell TG, Doughty ML (2011) Altered gene expression in the emerging cerebellar primordium of Neurog1-/- mice. Brain Res 1388:12-21.

De Carlos JA, Borrell J (2007) A historical reflection of the contributions of Cajal and Golgi to the foundations of neuroscience. Brain Res Rev 55:8-16.

de Castro F, Lopez-Mascaraque L, De Carlos JA (2007) Cajal: lessons on brain development. Brain Res Rev 55:481-489.

De Smet HJ, Baillieux H, De Deyn PP, Marien P, Paquier P (2007) The cerebellum and language: the story so far. Folia Phoniatr Logop 59:165-170.

Dino MR, Willard FH, Mugnaini E (1999) Distribution of unipolar brush cells and other calretinin immunoreactive components in the mammalian cerebellar cortex. J Neurocytol 28:99-123.

Engelkamp D, Rashbass P, Seawright A, van Heyningen V (1999) Role of Pax6 in development of the cerebellar system. Development 126:3585-3596.

Englund C, Kowalczyk T, Daza RA, Dagan A, Lau C, Rose MF, Hevner RF (2006) Unipolar brush cells of the cerebellum are produced in the rhombic lip and migrate through developing white matter. J Neurosci 26:9184-9195.

Espinosa JS, Luo L (2008) Timing neurogenesis and differentiation: insights from quantitative clonal analyses of cerebellar granule cells. J Neurosci 28:2301-2312.

Fink AJ, Englund C, Daza RA, Pham D, Lau C, Nivison M, Kowalczyk T, Hevner RF (2006) Development of the deep cerebellar nuclei: transcription factors and cell migration from the rhombic lip. J Neurosci 26:3066-3076.

Fode C, Ma Q, Casarosa S, Ang SL, Anderson DJ, Guillemot F (2000) A role for neural determination genes in specifying the dorsoventral identity of telencephalic neurons. Genes Dev 14:67-80.

Frampton M (2008) Embodiments of Will: Anatomical and Physiological Theories of Voluntary Animal Motion from Greek Antiquity to the Latin Middle Ages, 400 B.C.–A.D. 1300

Fukuda S, Taga T (2005) Cell fate determination regulated by a transcriptional signal network in the developing mouse brain. Anat Sci Int 80:12-18.

Gerdes J, Lemke H, Baisch H, Wacker HH, Schwab U, Stein H (1984) Cell cycle analysis of a cell proliferation-associated human nuclear antigen defined by the monoclonal antibody Ki-67. J Immunol 133:1710-1715.

Gerdes J, Schwab U, Lemke H, Stein H (1983) Production of a mouse monoclonal antibody reactive with a human nuclear antigen associated with cell proliferation. Int J Cancer 31:13-20.

Gest H (2005) The remarkable vision of Robert Hooke (1635-1703): first observer of the microbial world. Perspect Biol Med 48:266-272.

Geurts FJ, Timmermans J, Shigemoto R, De Schutter E (2001) Morphological and neurochemical differentiation of large granular layer interneurons in the adult rat cerebellum. Neuroscience 104:499-512.

Gilbertson RJ, Ellison DW (2008) The Origins of Medulloblastoma Subtypes. Annu Rev Pathol 3:341-365.

Glickstein M, Strata P, Voogd J (2009) Cerebellum: history. Neuroscience 162:549-559.

Gong S, Zheng C, Doughty ML, Losos K, Didkovsky N, Schambra UB, Nowak NJ, Joyner A, Leblanc G, Hatten ME, Heintz N (2003) A gene expression atlas of the central nervous system based on bacterial artificial chromosomes. Nature 425:917-925.

Gowan K, Helms AW, Hunsaker TL, Collisson T, Ebert PJ, Odom R, Johnson JE (2001) Crossinhibitory activities of Ngn1 and Math1 allow specification of distinct dorsal interneurons. Neuron 31:219-232.

Grimaldi P, Parras C, Guillemot F, Rossi F, Wassef M (2009) Origins and control of the differentiation of inhibitory interneurons and glia in the cerebellum. Dev Biol 328:422-433.

Harvey RJ, Napper RM (1991) Quantitative studies on the mammalian cerebellum. Prog Neurobiol 36:437-463.

Hendzel MJ, Wei Y, Mancini MA, Van Hooser A, Ranalli T, Brinkley BR, Bazett-Jones DP, Allis CD (1997) Mitosis-specific phosphorylation of histone H3 initiates primarily within pericentromeric heterochromatin during G2 and spreads in an ordered fashion coincident with mitotic chromosome condensation. Chromosoma 106:348-360.

Heng JI, Nguyen L, Castro DS, Zimmer C, Wildner H, Armant O, Skowronska-Krawczyk D, Bedogni F, Matter JM, Hevner R, Guillemot F (2008) Neurogenin 2 controls cortical neuron migration through regulation of Rnd2. Nature.

Henke RM, Savage TK, Meredith DM, Glasgow SM, Hori K, Dumas J, MacDonald RJ, Johnson JE (2009) Neurog2 is a direct downstream target of the Ptf1a-Rbpj transcription complex in dorsal spinal cord. Development 136:2945-2954.

Hevner RF, Hodge RD, Daza RA, Englund C (2006) Transcription factors in glutamatergic neurogenesis: conserved programs in neocortex, cerebellum, and adult hippocampus. Neurosci Res 55:223-233.

Ho BC, Epping E, Wang K, Andreasen NC, Librant A, Wassink TH (2008) Basic helix-loop-helix transcription factor NEUROG1 and schizophrenia: effects on illness susceptibility, MRI brain morphometry and cognitive abilities. Schizophr Res 106:192-199.

Hoshino M, Nakamura S, Mori K, Kawauchi T, Terao M, Nishimura YV, Fukuda A, Fuse T, Matsuo N, Sone M, Watanabe M, Bito H, Terashima T, Wright CV, Kawaguchi Y, Nakao K, Nabeshima Y (2005a) Ptf1a, a bHLH transcriptional gene, defines GABAergic neuronal fates in cerebellum. Neuron 47:201-213.

Hoshino M, Nakamura S, Mori K, Kawauchi T, Terao M, Nishimura YV, Fukuda A, Fuse T, Matsuo N, Sone M, Watanabe M, Bito H, Terashima T, Wright CVE, Kawaguchi Y, Nakao K, Nabeshima Y-i (2005b) Ptf1a, a bHLH Transcriptional Gene, Defines GABAergic Neuronal Fates in Cerebellum. Neuron 47:201-213.

Ito M (2006) Cerebellar circuitry as a neuronal machine. Prog Neurobiol 78:272-303.

Kerr JF, Wyllie AH, Currie AR (1972) Apoptosis: a basic biological phenomenon with wide-ranging implications in tissue kinetics. Br J Cancer 26:239-257.

Kim EJ, Battiste J, Nakagawa Y, Johnson JE (2008) Ascl1 (Mash1) lineage cells contribute to discrete cell populations in CNS architecture. Mol Cell Neurosci 38:595-606.

Kim EJ, Hori K, Wyckoff A, Dickel LK, Koundakjian EJ, Goodrich LV, Johnson JE (2011) Spatiotemporal fate map of neurogenin1 (Neurog1) lineages in the mouse central nervous system. J Comp Neurol 519:1355-1370.

Koundakjian EJ, Appler JL, Goodrich LV (2007) Auditory neurons make stereotyped wiring decisions before maturation of their targets. J Neurosci 27:14078-14088.

Laine J, Axelrad H (1994) The candelabrum cell: a new interneuron in the cerebellar cortex. J Comp Neurol 339:159-173.

Laine J, Axelrad H (2002) Extending the cerebellar Lugaro cell class. Neuroscience 115:363-374.

Leto K, Bartolini A, Yanagawa Y, Obata K, Magrassi L, Schilling K, Rossi F (2009) Laminar fate and phenotype specification of cerebellar GABAergic interneurons. J Neurosci 29:7079-7091.

Leto K, Carletti B, Williams IM, Magrassi L, Rossi F (2006) Different types of cerebellar GABAergic interneurons originate from a common pool of multipotent progenitor cells. J Neurosci 26:11682-11694.

Lin JC, Cai L, Cepko CL (2001) The external granule layer of the developing chick cerebellum generates granule cells and cells of the isthmus and rostral hindbrain. J Neurosci 21:159-168.

Lundell TG, Zhou Q, Doughty ML (2009) Neurogenin1 expression in cell lineages of the cerebellar cortex in embryonic and postnatal mice. Dev Dyn 238:3310-3325.

Ma Q, Chen Z, del Barco Barrantes I, de la Pompa JL, Anderson DJ (1998) neurogenin1 is essential for the determination of neuronal precursors for proximal cranial sensory ganglia. Neuron 20:469-482.

Ma Q, Kintner C, Anderson DJ (1996) Identification of neurogenin, a vertebrate neuronal determination gene. Cell 87:43-52.

Machold R, Fishell G (2005) Math1 is expressed in temporally discrete pools of cerebellar rhombic-lip neural progenitors. Neuron 48:17-24.

Maricich SM, Herrup K (1999) Pax-2 expression defines a subset of GABAergic interneurons and their precursors in the developing murine cerebellum. J Neurobiol 41:281-294.

Martin LJ (2001) Neuronal cell death in nervous system development, disease, and injury (Review). Int J Mol Med 7:455-478.

Martin SJ, Green DR (1995) Protease activation during apoptosis: death by a thousand cuts? Cell 82:349-352.

Martins e Silva J (2009) From the discovery of the circulation of the blood to the first steps in hemorheology: part 2. Rev Port Cardiol 28:1405-1439.

Mason C (2009) The development of developmental neuroscience. J Neurosci 29:12735-12747.

McCormick MB, Tamimi RM, Snider L, Asakura A, Bergstrom D, Tapscott SJ (1996) NeuroD2 and neuroD3: distinct expression patterns and transcriptional activation potentials within the neuroD gene family. Mol Cell Biol 16:5792-5800.

McHenry Jr. LC (ed.) (1969) Garrison's History of Neurology: Charles C Thomas Pub Ltd.

Meyer A (1967) Marcello Malpighi and the dawn of neurohistology. J Neurol Sci 4:185-193.

Miale IL, Sidman RL (1961) An autoradiographic analysis of histogenesis in the mouse cerebellum. Exp Neurol 4:277-296.

Minaki Y, Nakatani T, Mizuhara E, Inoue T, Ono Y (2008) Identification of a novel transcriptional corepressor, Corl2, as a cerebellar Purkinje cell-selective marker. Gene Expr Patterns 8:418-423.

Miyata T, Maeda T, Lee JE (1999) NeuroD is required for differentiation of the granule cells in the cerebellum and hippocampus. Genes Dev 13:1647-1652.

Mugnaini E, Dino MR, Jaarsma D (1997) The unipolar brush cells of the mammalian cerebellum and cochlear nucleus: cytology and microcircuitry. Prog Brain Res 114:131-150.

Nieto M, Schuurmans C, Britz O, Guillemot F (2001) Neural bHLH genes control the neuronal versus glial fate decision in cortical progenitors. Neuron 29:401-413.

Novak A, Guo C, Yang W, Nagy A, Lobe CG (2000) Z/EG, a double reporter mouse line that expresses enhanced green fluorescent protein upon Cre-mediated excision. Genesis 28:147-155.

Nunzi M-G, Shigemoto R, Mugnaini E (2002a) Differential expression of calretinin and metabotropic glutamate receptor mGluR1? defines subsets of unipolar brush cells in mouse cerebellum. The Journal of Comparative Neurology 451:189-199.

Nunzi MG, Birnstiel S, Bhattacharyya BJ, Slater NT, Mugnaini E (2001) Unipolar brush cells form a glutamatergic projection system within the mouse cerebellar cortex. J Comp Neurol 434:329-341.

Nunzi MG, Shigemoto R, Mugnaini E (2002b) Differential expression of calretinin and metabotropic glutamate receptor mGluR1alpha defines subsets of unipolar brush cells in mouse cerebellum. J Comp Neurol 451:189-199.

Ota M, Ito K (2003) Induction of neurogenin-1 expression by sonic hedgehog: Its role in development of trigeminal sensory neurons. Dev Dyn 227:544-551.

Pascual M, Abasolo I, Mingorance-Le Meur A, Martinez A, Del Rio JA, Wright CV, Real FX, Soriano E (2007) Cerebellar GABAergic progenitors adopt an external granule cell-like phenotype in the absence of Ptf1a transcription factor expression. Proc Natl Acad Sci U S A 104:5193-5198.

Ponti G, Peretto P, Bonfanti L (2008) Genesis of neuronal and glial progenitors in the cerebellar cortex of peripuberal and adult rabbits. PLoS One 3:e2366.

Quastler H, Sherman FG (1959) Cell population kinetics in the intestinal epithelium of the mouse. Exp Cell Res 17:420-438.

Raft S, Koundakjian EJ, Quinones H, Jayasena CS, Goodrich LV, Johnson JE, Segil N, Groves AK (2007) Cross-regulation of Ngn1 and Math1 coordinates the production of neurons and sensory hair cells during inner ear development. Development 134:4405-4415.

Rakic P (1973) Kinetics of proliferation and latency between final cell division and onset of differentiation of cerebellar stellate and basket neurons. J Comp Neurol 147:523-546.

Rostomily RC, Bermingham-McDonogh O, Berger MS, Tapscott SJ, Reh TA, Olson JM (1997) Expression of neurogenic basic helix-loop-helix genes in primitive neuroectodermal tumors. Cancer Res 57:3526-3531.

Sahin M, Hockfield S (1990) Molecular identification of the Lugaro cell in the cat cerebellar cortex. J Comp Neurol 301:575-584.

Salsano E, Croci L, Maderna E, Lupo L, Pollo B, Giordana MT, Consalez GG, Finocchiaro G (2007) Expression of the neurogenic basic helix-loop-helix transcription factor NEUROG1 identifies a subgroup of medulloblastomas not expressing ATOH1. Neuro Oncol 9:298-307.

Salsano E, Pollo B, Eoli M, Giordana MT, Finocchiaro G (2004) Expression of MATH1, a marker of cerebellar granule cell progenitors, identifies different medulloblastoma sub-types. Neurosci Lett 370:180-185.

Sarrazin AF, Villablanca EJ, Nunez VA, Sandoval PC, Ghysen A, Allende ML (2006) Proneural gene requirement for hair cell differentiation in the zebrafish lateral line. Dev Biol 295:534-545.

Schiffmann SN, Cheron G, Lohof A, d'Alcantara P, Meyer M, Parmentier M, Schurmans S (1999) Impaired motor coordination and Purkinje cell excitability in mice lacking calretinin. Proc Natl Acad Sci U S A 96:5257-5262.

Schilling K (2000) Lineage, development and morphogenesis of cerebellar interneurons. Prog Brain Res 124:51-68.

Schilling K, Oberdick J, Rossi F, Baader SL (2008) Besides Purkinje cells and granule neurons: an appraisal of the cell biology of the interneurons of the cerebellar cortex. Histochemistry and Cell Biology 130:601-615.

Schuller U, Kho AT, Zhao Q, Ma Q, Rowitch DH (2006) Cerebellar 'transcriptome' reveals cell-type and stage-specific expression during postnatal development and tumorigenesis. Mol Cell Neurosci 33:247-259.

Sellick GS, Barker KT, Stolte-Dijkstra I, Fleischmann C, Coleman RJ, Garrett C, Gloyn AL, Edghill EL, Hattersley AT, Wellauer PK, Goodwin G, Houlston RS (2004) Mutations in PTF1A cause pancreatic and cerebellar agenesis. Nat Genet 36:1301-1305.

Seo S, Lim JW, Yellajoshyula D, Chang LW, Kroll KL (2007) Neurogenin and NeuroD direct transcriptional targets and their regulatory enhancers. EMBO J 26:5093-5108.

Sillitoe RV, Joyner AL (2007) Morphology, Molecular Codes, and Circuitry Produce the Three-Dimensional Complexity of the Cerebellum. Annu Rev Cell Dev Biol.

Simat M, Parpan F, Fritschy JM (2007) Heterogeneity of glycinergic and gabaergic interneurons in the granule cell layer of mouse cerebellum. J Comp Neurol 500:71-83.

Sotelo C (2004) Cellular and genetic regulation of the development of the cerebellar system. Prog Neurobiol 72:295-339.

Sotelo C (2011) Camillo Golgi and Santiago Ramon y Cajal: The anatomical organization of the cortex of the cerebellum. Can the neuron doctrine still support our actual knowledge on the cerebellar structural arrangement? Brain Research Reviews 66:16-34.

Srinivasan A, Roth KA, Sayers RO, Shindler KS, Wong AM, Fritz LC, Tomaselli KJ (1998) In situ immunodetection of activated caspase-3 in apoptotic neurons in the developing nervous system. Cell Death Differ 5:1004-1016.

Strick PL, Dum RP, Fiez JA (2009) Cerebellum and nonmotor function. Annu Rev Neurosci 32:413-434.

Sultan F, Bower JM (1998) Quantitative Golgi study of the rat cerebellar molecular layer interneurons using principal component analysis. J Comp Neurol 393:353-373.

Sun Y, Nadal-Vicens M, Misono S, Lin MZ, Zubiaga A, Hua X, Fan G, Greenberg ME (2001) Neurogenin promotes neurogenesis and inhibits glial differentiation by independent mechanisms. Cell 104:365-376.

Takahashi T, Nowakowski RS, Caviness VS, Jr. (1995) The cell cycle of the pseudostratified ventricular epithelium of the embryonic murine cerebral wall. J Neurosci 15:6046-6057.

Ten Donkelaar HJ, Lammens M (2009) Development of the human cerebellum and its disorders. Clin Perinatol 36:513-530.

Uluc K, Kujoth GC, Baskaya MK (2009) Operating microscopes: past, present, and future. Neurosurg Focus 27:E4.

Urase K, Fujita E, Miho Y, Kouroku Y, Mukasa T, Yagi Y, Momoi MY, Momoi T (1998) Detection of activated caspase-3 (CPP32) in the vertebrate nervous system during development by a cleavage site-directed antiserum. Brain Res Dev Brain Res 111:77-87.

Vue TY, Aaker J, Taniguchi A, Kazemzadeh C, Skidmore JM, Martin DM, Martin JF, Treier M, Nakagawa Y (2007) Characterization of progenitor domains in the developing mouse thalamus. J Comp Neurol 505:73-91.

Wang VY, Rose MF, Zoghbi HY (2005) Math1 expression redefines the rhombic lip derivatives and reveals novel lineages within the brainstem and cerebellum. Neuron 48:31-43.

Weisheit G, Gliem M, Endl E, Pfeffer PL, Busslinger M, Schilling K (2006) Postnatal development of the murine cerebellar cortex: formation and early dispersal of basket, stellate and Golgi neurons. Eur J Neurosci 24:466-478.

Weyer A, Schilling K (2003) Developmental and cell type-specific expression of the neuronal marker NeuN in the murine cerebellum. J Neurosci Res 73:400-409.

Wolpert L (1995) Evolution of the cell theory. Philos Trans R Soc Lond B Biol Sci 349:227-233.

Yamanaka H, Yanagawa Y, Obata K (2004) Development of stellate and basket cells and their apoptosis in mouse cerebellar cortex. Neurosci Res 50:13-22.

Zhang L, Goldman JE (1996a) Developmental fates and migratory pathways of dividing progenitors in the postnatal rat cerebellum. J Comp Neurol 370:536-550.

Zhang L, Goldman JE (1996b) Generation of cerebellar interneurons from dividing progenitors in white matter. Neuron 16:47-54.

Zhao Y, Kwan KM, Mailloux CM, Lee WK, Grinberg A, Wurst W, Behringer RR, Westphal H (2007) LIM-homeodomain proteins Lhx1 and Lhx5, and their cofactor Ldb1, control Purkinje cell differentiation in the developing cerebellum. Proc Natl Acad Sci U S A 104:13182-13186.

Zimmermann KC, Bonzon C, Green DR (2001) The machinery of programmed cell death. Pharmacol Ther 92:57-70.

Zordan P, Croci L, Hawkes R, Consalez GG (2008) Comparative analysis of proneural gene expression in the embryonic cerebellum. Dev Dyn 237:1726-1735.